Leandro Giacobelli Cosmo

Como a coevolução em redes de mutualismo molda a aptidão e a persistência de espécies?

How does coevolution in mutualistic networks shape the fitness and persistence of species?

São Paulo

2023

Leandro Giacobelli Cosmo

Como a coevolução em redes de mutualismo molda a aptidão e a persistência de espécies?

How does coevolution in mutualistic networks shape the fitness and persistence of species?

Tese apresentada ao Instituto de Biociências da Universidade de São Paulo, para a obtenção de Título de Doutor em Ecologia, na Área de Ecologia de Populações, Comunidades e Ecossistemas.

Orientador(a):

Prof. Dr. Paulo Roberto Guimarães Jr.

São Paulo

2023

Giacobelli Cosmo, Leandro

Como a coevolução em redes de mutualismo molda a aptidão e a persistência de espécies?

127 páginas

Tese (Doutorado) - Instituto de Biociências da Universidade de São Paulo. Departamento de Ecologia.

1. Coevolução 2. Mutualismos 3. Redes Ecológicas

I. Universidade de São Paulo. Instituto de Biociências. Departamento de Ecologia.

Comissão Julgadora:

_____	_____
Prof(a). Dr.(a).	Prof(a). Dr.(a).
_____	_____
Prof(a). Dr.(a).	Prof. Dr. Paulo Roberto Guimarães Jr. Orientador

"Nature uses only the longest threads to weave her patterns, so each small piece of her fabric reveals the organization of the entire tapestry. "

Richard P. Feynman

The Character of Physical Law

Agradecimentos

Agradeço à Coordenação de Aperfeiçoamento de Pessoal de Nível Superior (CAPES), código de financiamento 001, e à Fundação de Amparo à Pesquisa do Estado de São Paulo (FAPESP, processos 2018/14809-0, 2019/22146-3 e 2022/07939-0), pelo financiamento deste trabalho.

Agradeço ao Instituto de Biociências e ao Programa de Pós-graduação em Ecologia da Universidade de São Paulo que permitiram a realização deste trabalho. Em especial, agradeço à Vera e à Erica por estarem sempre disponíveis e rapidamente responderem a qualquer dúvida e resolverem qualquer problema.

Agradeço ao meu orientador Paulo Roberto Guimarães Jr. (Miúdo) por todo o tempo dedicado a este trabalho e minha formação. O doutorado foi uma das melhores partes da minha vida e nossas interações praticamente diárias foram uma grande parte disso. Não tenho palavras para descrever o quanto você foi importante ao longo desses cinco anos que nos conhecemos. Do fundo do coração, muito obrigado!

Agradeço aos membros do meu comitê de acompanhamento, Rodrigo Cogni e Marcus A. M. de Aguiar, que acompanharam o desenvolvimento desta tese desde o seu início. Rodrigo, muito obrigado pelas sugestões e discussões e, Marcus, muito obrigado por toda a ajuda e por me ensinar tanto sobre modelos matemáticos. Aqui também deixo meu agradecimento para os membros do comitê de avaliação do meu exame de qualificação, Marco Mello, Carolina Montoya e Mayra Vidal, pelos comentários no manuscrito que constituem o capítulo 1 desta tese.

Agradeço a todos que participaram do desenvolvimento desta tese, em especial ao Mathias Pires e à Ana Paula Assis (Paulinha). Mathias, muito obrigado por compartilhar dos meus devaneios científicos e ideias mirabolantes! Nossas discussões sobre ciência foram fundamentais para esta tese. Paulinha, muito obrigado pela paciência e por ter me ensinado tanto sobre evolução ao longo dos cinco anos que estamos interagindo. Sua ajuda foi essencial para a minha formação e para este trabalho.

Agradeço também aos colaboradores ao redor do mundo com os quais tive o imenso prazer de poder trabalhar, Jordi Bascompte, John Thompson, Pedro Jordano e Alfredo Valido. Jordi, thank you so much for hosting me twice in your laboratory at Universität Zurich (UZH). I had the time of my life during my stay at UZH, all thanks to your mentoring and excitement with science. As you would say, voce é sangue bom, abraços com saudades! John, thank you so much for all your help, patience and for teaching me so much about coevolution and writing. Pedro and Alfredo, thank you for all the lessons about mutualisms and invasive species. I could not feel more fortunate for the opportunity to work with all of you!

Agradeço a todos os membros do Guimarães lab que compartilharam ideias e discussões comigo ao longo do desenvolvimento desta tese, Lucas Camacho, Lucas Nascimento, Lucas Medeiros, Andrés Arguelles, Elvira D'Bastiani Andrés Rojas, Pamela Santana, Pamela Friedman, Kate Maia, Carol Dracxler, Daniela Coelho, Bruno Melati, Debora Rother. Pessoal, vocês são sensacionais, muito obrigado por tudo!

Agradeço a todos os membros do Bascompte lab que me receberam ao longo da minha estadia em Zurique. Thank you, Rodrigo Leret, Fernando Pedraza, Klementyna Gawecka, Miguel Román, June Lorenzo, Bernat Espluga, Alessandro Vindigni and Gisela Collazo. You all made my stay much more enjoyable and productive!

Agradeço à minha mãe, Mara e ao meu irmão, Alexandre, por sempre me apoiarem e terem a paciência de me escutar falar sobre ecologia e ciência praticamente todos os dias! Muito obrigado, amo vocês.

Agradeço à Juliana Rink por ser minha companheira perfeita e sempre estar ao meu lado. Nada vale a pena sem você.

Sumário

Resumo

Interações ecológicas positivas – mutualismos - são uma das principais forças que sustentam os ecossistemas mais ricos da Terra. No entanto, entender como mutualismos sustentam a biodiversidade da Terra é desafiador por três motivos principais. Primeiro, na natureza, dezenas a milhares de espécies interagem formando redes mutualísticas. Em segundo, essas interações mutualísticas podem dar origem a pressões seletivas recíprocas entre as espécies envolvidas, resultando em mudanças evolutivas recíprocas – i.e. coevolução. A coevolução é um processo chave que molda os atributos de espécies, os quais, por sua vez, mediam como mutualismos influenciam a principal medida biológica que determina a persistência das espécies: a *aptidão média* de seus indivíduos, i.e, a capacidade de sobrevivência e se reprodução dos indivíduos de uma espécie. Terceiro, os efeitos da coevolução na aptidão média e persistência das espécies podem se manifestar em diferentes escalas espaciais. Nesta tese, abordamos esses desafios para entendermos como a coevolução em redes mutualísticas molda a *aptidão média* e a persistência das espécies em diferentes escalas espaciais. Primeiro, mostramos que, em redes mutualísticas locais, os efeitos evolutivos diretos entre as espécies podem se propagar e influenciar indiretamente outras espécies na rede. Esses efeitos evolutivos indiretos dificultam a capacidade das espécies de se adaptar tanto aos seus parceiros mutualísticos quanto a outras fontes de pressões seletivas no ambiente, moldando a *aptidão média* das espécies. Em seguida, integramos a coevolução mutualística em escala local com a dinâmica de colonização e extinção de metacomunidades em uma escala regional. Nossos resultados mostram que a coevolução mutualística local pode homogeneizar os atributos das espécies através da paisagem, facilitando colonizações, expandindo a distribuição, e aumentando a persistência mesmo quando as espécies estão mal adaptadas ao ambiente abiótico local. Juntos, nossos resultados mostram que a coevolução em redes mutualísticas é uma grande força que molda o a *aptidão média* e a persistência das espécies através de diferentes escalas espaciais.

Abstract

Mutualistic interactions - ecological interactions with a net positive effect to both interacting species - are one of the major forces that sustains many of Earth's richest ecosystems. Yet, understanding how does mutualistic interactions shape Earth's biodiversity is challenging for three main reasons. First, in mutualistic communities from dozen to thousands of species interact forming mutualistic networks. Second, these mutualistic interactions can give rise to reciprocal selective pressures between interacting species, resulting in reciprocal evolutionary changes - coevolution. Coevolution is a key process that drive species traits that, ultimately, mediate the net effect of mutualistic interactions on the main biological currency that determines the persistence of species: the fitness of its individuals, i.e. the ability of the individuals of a given species to survive and reproduce. Third, the effects of coevolution on the average fitness and persistence of species can manifest across different ecological scales, for instance, across different spatial scales. Here, we tackle these challenges to understand how coevolution in mutualistic networks shape the average fitness and persistence of species across different spatial scales. We first show that in local mutualistic networks the direct evolutionary effects between species can cascade and indirectly affect other species in the network. These indirect effects hinder the ability of species to adapt to both mutualistic partners and other sources of selective pressures in the environment, shaping species average fitness. Then, we proceeded to integrate mutualistic coevolution at a local scale, with the colonization and extinction dynamics of metacommunities at a regional scale. Our results show that local mutualistic coevolution can homogenize species traits across landscapes, facilitating colonization, range expansions and persistence even when species are maldapted to the local abiotic environment. Together, our results show that coevolution in mutualistic networks can be a major force that shape the average fitness and persistence of species across different spatial scales.

Introdução Geral

Na natureza nenhum organismo vive isolado de outros organismos. De micro-organismos, como bactérias que são parasitadas por vírus, até plantas cujos frutos são consumidos e sementes dispersadas por vertebrados como aves ou mamíferos, indivíduos de inúmeras espécies diferentes interagem. Essas interações ecológicas estão entre as principais forças que moldam a capacidade de sobrevivência e reprodução de indivíduos de uma dada espécie, i.e. a *aptidão* ou *fitness* desses indivíduos. A *aptidão* de um dado indivíduo pode reduzir ou aumentar como saldo final de interações ecológicas com indivíduos de outras espécies. Interações que aumentam a *aptidão* – definidas como mutualismos – são particularmente intrigantes porque sustentam diversos ecossistemas e moldam a biodiversidade da Terra (Bronstein 1994, 2015). Por exemplo, as fundações de recifes de corais, um dos ecossistemas mais diversos na natureza, são construídas pela simbiose entre corais e algas unicelulares, cuja fotossíntese provem até 95% do carbono e acelera a calcificação e o crescimento dos corais (Hay *et al.* 2004). Da mesma forma, ecossistemas terrestres são sustentados por como diversos animais polinizam as flores e dispersam as sementes de plantas; ou como fungos micorrízicos que estabelecem relações simbiontes com as raízes de plantas aumentam a absorção de nutrientes e a biomassa vegetal (Wilson *et al.* 2009). Entretanto, compreender os processos pelos quais mutualismos sustentam esses ecossistemas e moldam a biodiversidade da Terra é um grande desafio por três principais motivos.

Em primeiro, interações mutualísticas raramente ocorrem apenas entre duas ou poucas espécies: em comunidades ecológicas, dezenas e até milhares de espécies podem interagir simultaneamente (Thompson 2006, 2009; Bascompte & Jordano 2007; Bascompte 2009). Mesmo em uma rápida caminhada em ambientes urbanos é comum observarmos diferentes espécies de aves que dispersam sementes consumindo os frutos de diferentes plantas. Ainda, borboletas, abelhas, moscas e outros insetos são facilmente avistados visitando as flores de múltiplas espécies de plantas. Essas

interações multiespecíficas formam redes que podem apresentar diferentes padrões de interação e topologias. Nas últimas décadas, um grande esforço tem sido dedicado a descrição dessas diferentes topologias de redes de interação mutualísticas (Bascompte & Jordano 2007). Entre os padrões detectados destacam-se o aninhamento, em que as interações de espécies com um ou poucos parceiros (i.e., especialistas) consistem em um subconjunto das interações de espécies com múltiplos parceiros (i.e., generalistas); a modularidade, em que as interações estão concentradas em subgrupos ou módulos, contendo espécies com muitas interações entre si, mas com poucas interações com espécies pertencentes a outros módulos; ou ainda a topologia de centro e periferia, em que as redes contém dois subgrupos: um subgrupo coeso com espécies altamente interconectadas – o centro - e um outro subgrupo – a periferia – contendo espécies que interagem apenas com o centro da rede (Bascompte *et al.* 2003; Guimarães *et al.* 2007; Olesen *et al.* 2007; Lee 2016). As diferentes topologias de interação que são observadas na natureza, por sua vez, podem influenciar o saldo final de interações mutualísticas para populações de uma dada espécie (Bascompte & Jordano 2007; Bastolla *et al.* 2009; Poisot *et al.* 2016). Nesse sentido, um primeiro grande desafio consiste em quantificar como redes de interação podem influenciar populações de mutualistas ao longo do tempo.

Na teoria ecológica, esse desafio tem sido abordado de dois modos distintos. Por um lado, a variação do tamanho populacional de espécies ao longo do tempo – ou a dinâmica ecológica - pode ser favorecido diretamente por como as interações entre mutualistas beneficiam a *aptidão* de indivíduos. Nesse caso, a teoria vigente prediz que a dinâmica ecológica em redes mutualísticas que são predominantemente aninhadas favorece a viabilidade, estabilidade e biodiversidade em comunidades de mutualistas (Bastolla *et al.* 2009; Rohr *et al.* 2014; Bascompte & Scheffer 2022). Em última instância, porém, o efeito de interações mutualísticas na *aptidão* dos indivíduos depende de seus atributos, por exemplo, quando o comprimento da probóscide de uma borboleta ou mariposa se encaixa ao comprimento do tubo floral de uma planta e facilita tanto a aquisição de néctar pelo inseto quanto a polinização da planta (Garibaldi *et al.* 2015;

Peralta *et al.* 2020). Consequentemente, valores de atributos que permitem uma interação mais funcional e beneficiam os mutualistas envolvidos podem ser favorecidos pela seleção natural, o que causa mudanças evolutivas recíprocas nas populações desses mutualistas ao longo do tempo. Essas mudanças evolutivas reciprocas são definidas como coevolução (Janzen 1980; Thompson 2005).

Em mutualismos, a coevolução é reconhecida como uma das principais forças que potencialmente moldam os atributos das espécies (Thompson 2005; Bronstein 2015). Para mutualistas que interagem em pares isolados há um sólido corpo teórico sobre como a coevolução pode moldar os atributos de espécies. De modo geral, a teoria vigente prevê que a dinâmica coevolutiva favorece a complementaridade de atributos, resultando em um maior acoplamento nos atributos do par de mutualistas que coevoluem (Nuismer *et al.* 1999; Nuismer 2017). Em comunidades ecológicas, porém, múltiplas espécies interagem e historicamente essas interações têm sido consideradas "difusas" e com consequências imprevisíveis para a coevolução (Thompson 2005). Apenas recentemente passamos a compreender que a coevolução multiespecífica pode resultar em padrões que podem ser previstos a partir das diferentes topologias observadas em redes mutualísticas. Por exemplo, redes aninhadas ou com uma estrutura de centro e periferia são caracterizadas pela presença de espécies supergeneralistas, i.e. que interagem com uma grande proporção das demais espécies da rede. A coevolução na presença desses supergeneralistas aumenta a complementaridade entre os atributos de múltiplas espécies, o que pode resultar na convergência fenotípica em comunidades mutualísticas (Guimarães *et al.* 2011; Birskis-Barros *et al.* 2021). A convergência fenotípica emerge por como os efeitos coevolutivos entre espécies que interagem diretamente podem se propagar para outras espécies na rede (Guimarães *et al.* 2011). De fato, redes que são predominantemente aninhadas favorecem esses efeitos evolutivos entre espécies que não interagem diretamente – i.e. efeitos evolutivos indiretos – e moldam a dinâmica coevolutiva em redes mutualísticas (Guimarães *et al.* 2017). Isso desafia a visão de que em redes mutualísticas a coevolução ocorre de modo "difuso". Pelo contrário, em redes mutualísticas uma combinação de

efeitos evolutivos diretos e cascatas de efeitos indiretos que se propagam através dos inúmeros caminhos que conectam espécies em redes determinam o resultado da dinâmica coevolutiva.

Esses resultados da dinâmica coevolutiva nos atributos das espécies, por sua vez, podem retroalimentar os efeitos de interações mutualísticas na *aptidão* dos indivíduos de uma dada população e, portanto, na *aptidão* média de uma dada espécie (nesta tese referida como *aptidão* da espécie). Portanto, em redes mutualísticas a *aptidão* das espécies pode ser moldada por uma combinação de seleção recíproca entre espécies que interagem diretamente e pressões seletivas entre espécies que indiretamente estão conectadas. Essencialmente, a *aptidão* de uma espécie é a medida fundamental que determina a direção e resultado da dinâmica evolutiva, a taxa de crescimento intrínseca de populações, e consequentemente a ecologia e evolução de espécies (Lande 1976, 1982; Rice 2005; Orr 2009; Hendry *et al.* 2018). Nesse sentido, quantificarmos e mapearmos como cascatas de efeitos evolutivos em redes mutualísticas retroalimentam a *aptidão* e a persistência de espécies constitui um segundo grande desafio para compreendermos como mutualismos sustentam a biodiversidade da Terra.

Os efeitos da coevolução para a persistência de espécies, porém, podem se manifestar através de escalas ecológicas diferentes: na natureza, os padrões em uma dada escala podem emergir como resultado de mecanismos que atuam em uma escala diferente ou através de múltiplas escalas (Levin 1992; Schneider 2001; Chave 2013; Estes *et al.* 2018). Entre as diferentes escalas, a escala espacial é reconhecida como uma das principais determinantes de inúmeros processos e padrões emergentes na ecologia e evolução (Wiens 1989; Levin 1992; Estes *et al.* 2018). De fato, na teoria coevolutiva vigente, a combinação entre processos que atuam em escalas espaciais mais refinadas (i.e. localmente) e mais amplas (i.e. regionalmente) é um fator chave para a explicação de padrões fenotípicos observados através de paisagens inteiras (Thompson 2005). Por exemplo, um dos resultados mais influentes na teoria coevolutiva, o *mosaico geográfico da coevolução*, prevê que os efeitos da coevolução em populações de espécies diferentes

que interagem em sítios locais podem se manifestar na escala da paisagem por meio do fluxo gênico entre populações (Thompson 2005). Nesse caso, o fluxo gênico conecta os regimes de seleção locais e acopla as dinâmicas coevolutivas das populações no espaço. Como consequência padrões fenotípicos diferentes do que seria esperado apenas pelos regimes coevolutivos locais se manifestam no espaço (Nuismer *et al.* 1999, 2000; Gomulkiewicz *et al.* 2000; Lemos-Costa *et al.* 2017; Medeiros *et al.* 2018; Fernandes *et al.* 2019). Assim, o terceiro grande desafio consiste em compreendermos como os efeitos da coevolução local se mapeiam na *aptidão* e persistência de espécies através de paisagens inteiras.

Nesta tese, dividida em dois capítulos, abordamos esses desafios e estudamos como a coevolução em comunidades mutualísticas, em que múltiplas espécies interagem e formam redes de interação, pode moldar a *aptidão* e persistência de espécies através de diferentes escalas ecológicas. No primeiro capítulo, combinamos modelagem matemática, simulações numéricas e dados empíricos para compreendermos como a coevolução em redes mutualísticas locais molda a *aptidão* de espécies (Cosmo *et al.*, 2023a, no prelo). Para o segundo capítulo, expandimos o escopo do nosso trabalho para uma escala regional. Nesse capítulo, combinamos modelagem matemática e simulações numéricas para compreendermos como a coevolução local pode moldar a persistência de espécies em uma escala regional (Cosmo *et al.* 2023b).

Capítulo 1

Indirect effects shape species fitness in coevolved mutualistic networks

*This manuscript has been accepted for publication in *Nature.*

Indirect effects shape species fitness in coevolved mutualistic networks

Leandro G. Cosmo[1*], Ana Paula A. Assis[2], Marcus A. Aguiar[3], Mathias M. Pires[4], Alfredo Valido[5], Pedro Jordano[6], John N. Thompson[7], Jordi Bascompte[8], Paulo R. Guimarães Jr.[9]

[1]*Programa de Pós-Graduação em Ecologia, Departamento de Ecologia, Instituto de Biociências, Universidade de São Paulo, São Paulo, Brazil*.

[2]*Departamento de Genética e Biologia Evolutiva, Instituto de Biociências, Universidade de São Paulo, São Paulo, Brazil*.

[3]*Instituto de Física 'Gleb Wataghin', Universidade Estadual de Campinas, Campinas, Brazil*

[4]*Departamento de Biologia Animal, Instituto de Biologia, Universidade Estadual de Campinas, Campinas, Brazil*.

[5]*Island Ecology and Evolution Research Group, Institute of Natural Products and Agrobiology (IPNA-CSIC), C/Astrofísico Francisco Sánchez 3, 38206 La Laguna, Tenerife (Canary Islands, Spain).*

[6]*Estación Biológica de Doñana, CSIC, av. Americo Vespucio 26, 41092, Sevilla, Spain; Departamento de Biología Vegetal y Ecología, Universidad de Sevilla, Sevilla, Spain*.

[7]*Department of Ecology and Evolutionary Biology, University of California, Santa Cruz, 130 McAllister Way, Santa Cruz, California, 95060, USA.*

[8]*Department of Evolutionary Biology and Environmental Studies, University of Zurich, Winterthurerstrasse 190, Zurich, CH-8057, Switzerland.*

[9]*Departamento de Ecologia, Instituto de Biociências, Universidade de São Paulo, São Paulo, Brazil.*

[*]Corresponding author: lgcosmo@usp.br

One of the main forces that sustain Earth's biodiversity are ecological interactions. Yet, a major challenge in ecology and evolution is to determine how these interactions affect fitness when we progress from isolated pairwise interactions to entire networks of interacting species[1–4]. In networks, chains of effects result in indirect effects among non-interacting species, potentially affecting the fitness outcomes of ecological interactions (such as mutualisms)[5–7]. Applying analytical techniques and numerical simulations to 186 empirical mutualistic networks, we show how direct and indirect effects determine changes in the fitness of species coevolving in these networks. Although species fitness partially increases with the number of mutualistic partners, most of the fitness variation across species was driven by indirect effects. We found that indirect effects prevent coevolving species from adapting to mutualistic partners and other sources of selective pressures in the environment, thereby decreasing fitness. Such decreases are distributed in a predictable way within networks: peripheral species receive more indirect effects and experiment higher reductions in fitness than central species. This topological effect was also evident when we analyzed an empirical study of invasion by honeybees. As honeybees become integrated as a central species within networks, they boost indirect effects and reduce the fitness of several other species. Overall, our study shows how and why indirect effects can govern the adaptive landscape of species-rich mutualistic assemblages.

Fitness – the ability of organisms to survive and reproduce – is the fundamental biological currency that underlies the ecology and evolution of biodiversity[8,9]. Variation in fitness among organisms mediates processes and patterns at multiple scales, from the persistence and evolution of populations to the reorganization and functionality of ecological communities[10,11]. In nature, much of fitness variation is the outcome of ecological interactions, ranging from antagonisms to mutualisms[12–14]. Mutualisms are particularly intriguing because some of the most diverse ecosystems, such as coral reefs and tropical forests, are strongly supported by

interactions of mutual benefit[13]. Mutualistic interactions, by definition, increase the fitness of interacting individuals and thus can also raise the average fitness across the individuals of a given species[15] (hereafter "species fitness"). Fitness increases may be fueled by reciprocal evolutionary changes in traits (i.e., coevolution), which in turn may cascade back and further change species fitness[16]. Such fitness-coevolution-trait feedbacks may be altered by interactions with other species within ecological communities[3,17,18]. Consequently, species fitness may evolve through a combination of direct reciprocal selection on each pair of interacting species and indirect effects mediated by selection acting on species that are not linked directly as interacting partners[5,18]. Indirect effects, in turn, may create or intensify conflicting selective pressures, thereby reshaping the adaptive landscape and the distribution of species fitness within an interaction network[5,19]. This combination of direct and indirect effects may pervade most interaction networks among free-living species, where interactions typically show very low specificity.

Here, we use a combination of mathematical modeling and empirical mutualistic networks to understand how indirect effects shape species fitness. Our starting point is a classic discrete time quantitative genetics equation that describes how a continuous phenotypic trait evolves in response to a selection gradient (Methods)[20]. In evolutionary biology, the selection gradient describes the relationship between species fitness and a continuous phenotypic trait by dictating the strength and direction of natural selection on this trait[20]. For mutualistic species, natural selection can come from at least two distinct sources. First, selection from mutualistic partners favor complementarity of traits, for instance when the proboscis of a butterfly matches the length of the floral tube of plants, or in multi-species assemblages, when the plant trait fits within the range of potential animal partners[21–23]. The second selective force comes from all other sources in the environment unrelated to mutualisms, such as abiotic factors, that favor an optimal trait value for each species (hereafter "environmental optima")[24–27]. Thus, in our

coevolutionary model we assumed that these two sources of selective pressures comprise the selection gradient and drive the evolution of a species trait (Methods):

$$\bar{z}_i^{(t+1)} = \bar{z}_i^{(t)} + \sigma^2_{Gz_i}\varrho_i\left[m_i\sum_{j,j\neq i}^{N} q_{ij}^{(t)}\left(\bar{z}_j^{(t)} - \bar{z}_i^{(t)}\right) + (1-m_i)\left(\theta_i - \bar{z}_i^{(t)}\right)\right] \quad (1)$$

Equation (1) relates how the trait of a species ($\bar{z}_i$) evolves according to the available additive genetic variance on the trait ($\sigma^2_{Gz_i}$), as well as the selection gradient outlined earlier, represented by the other terms in the equation. The first term in the selection gradient, $\sum_{j,j\neq i}^{N} q_{ij}^{(t)}\left(\bar{z}_j^{(t)} - \bar{z}_i^{(t)}\right)$, measures the selective pressures coming from each mutualistic partner *j*, with each partner *j* favoring trait complementarity with a relative strength $q_{ij}^{(t)}$ (see Methods for details). In turn, the second term, $\left(\theta_i - \bar{z}_i^{(t)}\right)$, describes the component of the selection gradient that drives the evolution of species traits towards the environmental optima. Other parameters in equation (1) include m_i, which measures the proportional contribution of mutualisms as selective pressures; and ϱ_i, which measures the sensitivity of the selection gradient to the different values of trait $\bar{z}_i$.

The selection gradient corresponds to the slope of the relationship between the natural logarithm of species fitness and mean trait values, $\frac{dln\overline{W_i}}{d\bar{z}_i}$. Therefore, it is possible to integrate the selection gradient to derive the fitness of each species as a function of trait values. Using this approach, we derived the fitness function that underlies our coevolutionary model:

$$\overline{W_i} = e^{\frac{1}{2}\varrho_i\left[\frac{m_i}{\alpha}\ln\left(\frac{s_i}{k_i}\right) - (1-m_i)(\theta_i-\bar{z}_i)^2\right]} \quad (2)$$

Equation (2) represents the fitness of a given species *i* relative to its theoretical maximum fitness and describes the relationship between a species' phenotypic trait (represented by $\bar{z}_i$) and its fitness. Thus, $0 < \overline{W_i} \leq 1$, the upper bound corresponding to the case of species *i*

achieving the maximum possible fitness for a species with the same number of mutualistic partners (Methods).

The function described in equation (2) shows that species fitness depends on two main components, each representing a different aspect of the fitness landscape. First, it depends on a mutualistic component in which fitness increases with the average trait matching of species across its mutualistic partners, $\frac{s_i}{k_i}$. The term $s_i = \sum_{j=1, j\neq i}^{N} a_{ij} e^{-\alpha(\bar{z}_j - \bar{z}_i)^2}$ represents the total trait matching with all j mutualistic partners, while $k_i = \sum_{j=1, j\neq i}^{N} a_{ij}$ is the total number of mutualistic partners of species i ($a_{ij} = 1$ if species i interacts with species j and 0 otherwise). The parameter α controls the sensitivity of trait matching to differences in the trait values of mutualistic partners. The second component, represented by $(\theta_i - \bar{z}_i)^2$, describes the squared distance between a species' trait value and the environmental optimum, θ_i. The less distant species traits are from their environmental optima, the larger fitness is. Therefore, species achieve the maximum possible fitness ($\overline{w_i} = 1$) when their traits perfectly match the traits of all mutualistic partners and the environmental optimum (Methods).

Using the fitness function and our coevolutionary model, we first explored how coevolving in a mutualistic network affects species fitness. We performed numerical simulations of our model parameterized with the structure of 186 empirical networks encompassing a wide range of network topologies and types of mutualisms worldwide (Methods). The coevolutionary dynamics quickly reached a global stable equilibrium at which traits and, consequently, species fitness cease to change (Extended Data Fig. 1., Methods). Trait values and species fitness at equilibrium are analytically predictable even if not all species are guaranteed to survive throughout the coevolutionary dynamics (Extended Data Fig. 1, Supplementary methods). At the equilibrium, fitness of species that coevolved in networks varied 5 times more than the fitness of isolated pairs of coevolved species (SD = 0.025 in networks vs 0.005 in pairs, Fig.

1a). This increased variation in the fitness of species that coevolved within networks was due in part to the number of direct partners. Species fitness was higher for species with two or more direct partners than for species in the network interacting with only one direct partner, leading to a bimodal distribution of fitness values (Fig. 1a-1b). The larger variability in fitness for species that coevolve in mutualistic networks still holds under a wide range of scenarios in which other ecological processes may drive species with low fitness extinct and the extant species coevolve to a new equilibrium (Extended Data Fig. 2, Supplementary methods). Furthermore, the bimodality in the distribution of species fitness becomes less noticeable as extinctions increases, but only disappear under conditions of catastrophic extinctions exceeding 40% of the species within the network (Extended Data Fig. 2, Supplementary methods). The increase in fitness for species with two or more partners was expected and occurs because a higher number of partners evens out differences in the contribution of individual mutualistic partner species to fitness, increasing fitness due to geometric mean effects[28–31] (Supplementary methods). Even so, the effects of the number of partners quickly saturated and poorly explained the variability in species fitness (Fig. 1b), indicating a potential role of indirect effects in shaping fitness variation across species.

After having quantified the overall effects of coevolution in networks for species fitness and identifying the potential importance of indirect effects, we next derived an analytical approximation that explicitly assesses how indirect evolutionary effects shape the fitness of species coevolving within networks (Supplementary methods). By combining the fitness function (equation 2) and the equation for species traits at coevolutionary equilibrium (Methods), we obtained the following approximation:

$$\overline{w_i}^{*} \cong e^{-\frac{1}{2}\varrho_i\{m_i[(\langle\theta\rangle-\theta_i)(m_i+F_i)-\theta_i+\langle z\rangle]^2 + (1-m_i)(\theta_i-\langle\theta\rangle)^2(m_i+F_i)^2\}} \quad (3)$$

where $\overline{w_i}^*$ is the fitness of species *i* at the coevolutionary equilibrium; $\langle\theta\rangle$ represents the mean environmental optimum across all species other than *i* in the network; $\langle z\rangle$ is the average trait value across mutualistic partners of *i*; and F_i represents the proportional contribution of indirect evolutionary effects to the evolution of species *i*.

Our analytical approximation showed that indirect evolutionary effects prevent coevolving species from simultaneously achieving high trait matching with mutualistic partners and trait values favored by environmental selection. Thus, the larger the contribution of indirect effects generated by other species to the evolution of a given species *i*, the smaller the fitness of *i* was (Fig. 2a). Our analytical results also showed that indirect effects are strongly affected by network structure: indirect effects are minimized if a species is the central species of a network, whereas peripheral species receive more indirect effects. Consequently, the fitness of peripheral species is lower than the fitness of central species due to this increased contribution of indirect effects (Supplementary methods).

The relationship between species fitness and indirect effects was strong and held for numerical simulations that relaxed the simplifying assumptions of our analytical approximation (Fig. 2a-c) and incorporated the network structure of empirical mutualisms. Sensitivity analysis further indicated that the role of indirect effects in species fitness only substantially weakens when mutualistic selection is either very weak, very strong, or the environmental optima of species are very narrowly distributed in the network ($m_i \leq 0.1$ or $m_i \geq 0.9$, Extended Data Fig. 3-5, Supplementary methods). Furthermore, how indirect evolutionary effects shape fitness still hold even when the species with the lowest fitness become extinct, for instance, because of the ecological dynamics in the system (Extended Data Fig. 6, Supplementary Methods). Except at these extremes of m_i values then, indirect evolutionary effects may strongly shape species fitness within coevolving mutualistic networks. These extremes should not be commonly found

in nature, as we have evidence that (1) the selection imposed on species traits by mutualistic interactions and other sources in the environment are similar in strength to each other, even for highly intimate mutualisms (e.g., symbiosis)[32-35]; and (2) mutualistic networks are composed of different organisms, each one with its own life history and developmental constraints. In turn, species life history and developmental constraint can be radically distinct among species and shape how traits respond to selection[12]. Therefore, our results suggest that indirect evolutionary effects should have a pervasive role in shaping the fitness of mutualistic species in ecological communities.

Human activities that homogenize ecological communities can lead to a reorganization of direct and indirect interactions, ultimately changing the outcome of coevolution and altering species fitness[27,36–38]. One important example would be the introduction of a new species into a network. As a case study, we explored the potential consequences of the reorganization of direct and indirect effects by the introduction of the European honeybee (*Apis mellifera*), which often becomes a central species within pollination networks worldwide[39–42]. We first performed numerical simulations on 73 empirical networks that include *A. mellifera* (Methods, Fig. 3a) by first removing it from the network and running the coevolutionary model until it reached equilibrium. Then, we connected *A. mellifera* back to the network to simulate an invasion and evaluated how the fitness of all other native species was affected after reaching a new equilibrium. This approach allowed us to use our controlled scenario as a theoretical benchmark. Nevertheless, this certainly represents a simplistic assumption as it neglects the reduction of number of species, mutualistic interactions, and the potential rewiring of native pollinators after the invasion. We will relax these assumptions later by considering a field experiment involving a pollination network before and after the introduction of *A. mellifera* by beekeeping practices[39].

Our simulations show that invasive species such as *A. mellifera* can substantially affect the fitness of native species (Fig. 3b) and reshape their adaptive landscapes (Fig. 3c). Specifically, we found that the effects of the invasion differed between species that directly interact with honeybees and those that do only indirectly. The fitness of the honeybee's direct partners on average increased after the invasion ($n=10^3$ simulations, Fig. 4a, green histogram bars), whereas for species indirectly interacting with the honeybee, the overall effect of the invasion on fitness was negative ($n=10^3$ simulations, Fig. 4a, red histogram bars). In our simulations, the average change in fitness was positive only if the increase in fitness of gaining a new mutualistic partner (the honeybee) compensated the decrease in fitness caused by changes in indirect evolutionary effects (Fig. 4b). In contrast, for species that interact only indirectly with the honeybee, fitness decreased because the invasion increased the contribution of indirect evolutionary effects to the fitness of these species (Fig. 4c). As our previous results showed, increasing the contribution of indirect evolutionary effects hinders species fitness because indirect effects difficult species to adapt at the same time to mutualistic partners and the environment. These results held for different values of mutualistic selection (Extended Data Figs. 7-9, Supplementary methods).

However, when *A. mellifera* invades a network in nature, some native pollinators become disconnected from the network (i.e., functionally extinct), and those left in the system rewire interactions and lose mutualistic partners by resource competition[39]. We explored these additional consequences using the data from an experimental field study in which the mutualistic networks before and after the arrival of *A. mellifera* are available[39]. These simulations showed that the fitness of 68% of the native species decreased after the introduction of *A. mellifera* because the honeybee not only increased the contribution of indirect evolutionary effects, but also reduced drastically the number of mutualistic partners of nearly all native plant species in the network (Extended Data Fig. 10). Together with our theoretical

benchmark, these results indicate that mutualistic interactions with an invasive species can decrease the fitness of most native species in networks through a reorganization of indirect evolutionary effects. Yet, these negative effects in fitness can be buffered if species are able to obtain new mutualistic partners with similar effectiveness after the invasion, but the experimental evidence suggests this would be rarely the case, especially at very high densities of the invader species[39].

Our results highlight that mutualists coevolve in a dynamic "seascape" within which adaptive peaks can be transient and cause natural selection to push mutualists to lower or higher fitness points depending on the structure and reorganization of indirect evolutionary effects[43]. Specifically, indirect effects resulting from coevolution constrain species fitness. Consequently, we predict that selection may favor the evolution of lifestyles that reduce the negative impact of indirect evolutionary effects, especially in species-rich assemblages with low interaction specificity. Two examples would be specialists and supergeneralists. Regarding the former, their dependence on mutualistic interactions is so high that it minimizes the negative impact of indirect evolutionary effects on fitness. Regarding supergeneralists, fitness is less affected by indirect effects because they rely upon the resources directly provided by multiple partners, thus maximizing direct effects over indirect ones[1,18]. Furthermore, when such supergeneralist invade native communities, this may reduce fitness of mutualists through indirect evolutionary effects, an overlooked outcome of biological invasions. On the other hand, a generalized effect of environmental drivers (e.g., climate change effects on pollinators) may deeply influence the sign and magnitude of indirect effects, translating in larger fitness losses among species. More generally, our results highlight how and why the structure of ecological networks can govern the fitness, the adaptive landscape, and, consequently, the persistence of species across Earth's ecosystems.

References

1. Thompson, J. N. The coevolving web of life. *Am. Nat.* **173**, 125–140 (2009).
2. Thompson, J. N. Mutualistic webs of species. *Science* **312**, 372–373 (2006).
3. Bascompte, J. & Jordano, P. Plant-animal mutualistic networks: The architecture of biodiversity. *Annu. Rev. Ecol. Evol. Syst.* **38**, 567–593 (2007).
4. Bascompte, J. Disentangling the web of life. *Science* **325**, 416–419 (2009).
5. Guimarães, P. R., Pires, M. M., Jordano, P., Bascompte, J. & Thompson, J. N. Indirect effects drive coevolution in mutualistic networks. *Nature* **550**, 511–514 (2017).
6. Wootton, J. T. The nature and consequences of indirect effects in ecological communities. *Annu. Rev. Ecol. Syst.* **25**, 443–466 (1994).
7. Strauss, S. Y. Indirect effects in community ecology: Their definition, study and importance. *Trends Ecol. Evol.* **6**, 206–210 (1991).
8. Darwin, C. *On the Origin of Species by Means of Natural Selection, or the Preservation of Favoured Races in the Struggle for Life*. (Murray, London U.K., 1861).
9. Fisher, R. A. *The Genetical Theory of Natural Selection*. (Oxford University Press, Oxford, 1930).
10. Reed, D. H. Relationship between population size and fitness. *Conserv. Biol.* **19**, 563–568 (2005).
11. Orr, H. A. Fitness and its role in evolutionary genetics. *Nat. Rev. Genet.* **10**, 531–539 (2009).
12. Thompson, J. N. *Relentless Evolution*. (University of Chicago Press, 2013).
13. Bronstein, J. L. *Mutualism*. (Oxford University Press, Oxford, 2015).
14. Bronstein, J. L. Our current understanding of mutualism. *Q. Rev. Biol.* **69**, 31–51 (1994).

15. Bronstein, J. L., Dieckmann, U. & Ferrière, R. Coevolutionary dynamics and the conservation of mutualisms. in *Evolutionary Conservation Biology* (eds. Ferrière, R., Dieckmann, U. & Couvet, D.) 305-326 (Cambridge University Press, 2009).
16. Thompson, J. N. *The Geographic Mosaic of Coevolution*. (University of Chicago Press, 2005).
17. Nuismer, S. L., Jordano, P. & Bascompte, J. Coevolution and the architecture of mutualistic networks. *Evolution* **67**, 338–354 (2013).
18. Guimarães, P. R., Jr, Jordano, P. & Thompson, J. N. Evolution and coevolution in mutualistic networks. *Ecol. Lett.* **14**, 877–885 (2011).
19. Kauffman, S. A. & Johnsen, S. Coevolution to the edge of chaos: coupled fitness landscapes, poised states, and coevolutionary avalanches. *J. Theor. Biol.* **149**, 467–505 (1991).
20. Lande, R. Natural selection and random genetic drift in phenotypic evolution. *Evolution* **30**, 314 (1976).
21. Santamaría, L. & Rodríguez-Gironés, M. A. Linkage rules for plant–pollinator networks: Trait complementarity or exploitation barriers? *PLoS Biol.* **5**, e31 (2007).
22. Rohr, R. P., Naisbit, R. E., Mazza, C. & Bersier, L.-F. Matching-centrality decomposition and the forecasting of new links in networks. *Proc. Biol. Sci.* **283**, (2016).
23. Peralta, G. *et al.* Trait matching and phenological overlap increase the spatio-temporal stability and functionality of plant-pollinator interactions. *Ecol. Lett.* **23**, 1107–1116 (2020).
24. Galen, C. High and dry: Drought stress, sex-allocation trade-offs, and selection on flower size in the alpine wildflower *Polemonium viscosum* (Polemoniaceae). *Am. Nat.* **156**, 72–83 (2000).

25. Irwin, R. E., Adler, L. S. & Brody, A. K. The dual role of floral traits: Pollinator attraction and plant defense. *Ecology* **85**, 1503–1511 (2004).
26. Strauss, S. Y. & Whittall, J. B. Non-pollinator agents of selection on floral traits. in *Ecology and Evolution of Flowers* (eds Harder, L.D. and Barrett, S.C.H.) 120-138 (Oxford University Press, 2006).
27. Galetti, M. *et al.* Functional extinction of birds drives rapid evolutionary changes in seed size. *Science* **340**, 1086–1090 (2013).
28. Yoshimura, J. & Jansen, V. A. A. Evolution and population dynamics in stochastic environments. *Res. Popul. Ecol.* **38**, 165–182 (1996).
29. Bascompte, J., Possingham, H. & Roughgarden, J. Patchy populations in stochastic environments: Critical number of patches for persistence. *Am. Nat.* **159**, 128–137 (2002).
30. Waser, N. M., Chittka, L., Price, M. V., Williams, N. M. & Ollerton, J. Generalization in pollination systems, and why it matters. *Ecology* **77**, 1043–1060 (1996).
31. Levins, R. The effect of random variations of different types on population growth. *Proc. Natl. Acad. Sci. U. S. A.* **62**, 1061–1065 (1969).
32. Piculell, B. J., Hoeksema, J. D. & Thompson, J. N. Interactions of biotic and abiotic environmental factors in an ectomycorrhizal symbiosis, and the potential for selection mosaics. *BMC Biol.* **6**, 23 (2008).
33. Batstone, R. T., Peters, M. A. E., Simonsen, A. K., Stinchcombe, J. R. & Frederickson, M. E. Environmental variation impacts trait expression and selection in the legume-rhizobium symbiosis. *Am. J. Bot.* **107**, 195–208 (2020).
34. Caruso, C. M., Eisen, K. E., Martin, R. A. & Sletvold, N. A meta-analysis of the agents of selection on floral traits. *Evolution* **73**, 4–14 (2019).

35. Munguía-Rosas, M. A., Ollerton, J., Parra-Tabla, V. & De-Nova, J. A. Meta-analysis of phenotypic selection on flowering phenology suggests that early flowering plants are favoured. *Ecol. Lett.* **14**, 511–521 (2011).
36. Fricke, E. C. & Svenning, J. C. Accelerating homogenization of the global plant–frugivore meta-network. *Nature* **585**, 74–78 (2020).
37. Mackin, C. R., Peña, J. F., Blanco, M. A., Balfour, N. J. & Castellanos, M. C. Rapid evolution of a floral trait following acquisition of novel pollinators. *J. Ecol.* **109**, 2234–2246 (2021).
38. Stuart, Y. E. *et al.* Rapid evolution of a native species following invasion by a congener. *Science* **346**, 463–466 (2014).
39. Valido, A., Rodríguez-Rodríguez, M. C. & Jordano, P. Honeybees disrupt the structure and functionality of plant-pollinator networks. *Sci. Rep.* **9**, 4711 (2019).
40. Aizen, M. A., Morales, C. L. & Morales, J. M. Invasive mutualists erode native pollination webs. *PLoS Biol.* **6**, e31 (2008).
41. Traveset, A. & Richardson, D. M. Mutualistic interactions and biological invasions. *Annu. Rev. Ecol. Evol. Syst.* **45**, 89–113 (2014).
42. Traveset, A. & Richardson, D. M. Biological invasions as disruptors of plant reproductive mutualisms. *Trends Ecol. Evol.* **21**, 208–216 (2006).
43. Merrel, D. J. *The Adaptive Seascape: The Mechanism of Evolution*. 259 (University of Minnesota Press, 1994).

Figure legends

Figure 1 | **Coevolution in mutualistic networks increases the variability in species fitness.** **a,** Histogram showing the distribution of species fitness (rescaled relative to the average) that

coevolved in a single mutualistic pair (green histogram bars), or within the 186 empirical networks used to parameterize the model (violet histogram bars). **b,** When coevolving within networks, species fitness increased up to a saturation point with the number of mutualistic partners, but largely varied among species with the same number of partners. Each fitness value corresponds to the mean value for 10^3 numerical simulations of our model. In both panels, fitness values are rescaled relative to the average of each scenario (coevolution in pairs or in networks) in such a way that zero indicates the average of the distribution in each scenario. Note that on panel **(b)** only species coevolving within networks are shown. Parameter values are as follows: $m_i = 0.5$, $\sigma^2_{G z_i} = 1.0$, ϱ_i=0.2, $\alpha = 0.2$. θ_i and initial trait values were sampled from a uniform distribution U [0, 10].

Figure 2 | Species position within networks and indirect evolutionary effects shape species fitness in coevolved mutualistic networks. a, Analytical approximation (solid line and shaded region) predicts that indirect evolutionary effects decrease the fitness of species coevolving in mutualistic networks. Points of lighter and darker colors represent species with one and more than one partner, respectively. This effect held for numerical simulations (n=10^3 numerical simulations for each of the 186 empirical networks), as shown for species within an example plant-pollinator network (points and inset), and **b,** for species across all empirical networks after controlling for the effects of the number of mutualistic partners. **c,** Example for a seed-dispersal network (inset) showing how species in peripheral positions receive more indirect effects and have a lower fitness than core species. The color of points represents species fitness such that the darker the color, the higher the fitness value. In panel **a,** the line represents the mean predicted fitness and shaded regions standard deviations when sampling species environmental optima (θ_i and $\langle\theta\rangle$) and $\langle z\rangle$ from a normal distribution, θ_i~N(0.0, 0.1), $\langle\theta\rangle$~N(2.5, 0.1) and $\langle z\rangle$~N(2.5, 0.1). Points in all panels correspond to the mean value of species fitness (panels **a** and **b**) or contribution of indirect effects (panel **c**) across 10^3 numerical

simulations. Other parameter values are as follows: $m_i = 0.5$, $\sigma^2_{Gz_i} = 1.0$, ϱ_i=0.2, $\alpha = 0.2$. For numerical simulations, θ_i and initial trait values were sampled from a uniform distribution U [0, 10]. In panels **a** and **b,** the *x*-axis represents the proportional contribution of indirect evolutionary effects (equation 3).

Figure 3 | **Example of how the reorganization of indirect effects through a biological invasion can reshape species fitness within networks**. **a,** Geographical location of the empirical networks used to parameterize the invasion simulations by honeybees. **b,** Examples of the rapid rate at which an invader can either increase or decrease the fitness of two native species within a network (insert). **c,** The reorganization of indirect effects following invasion reshapes the adaptive landscape of the native species, slightly favoring different trait values and changing fitness. Dashed and solid lines represent the adaptive landscape of species before and after coevolving with the invader, respectively. Parameter values are as follows: $m_i = 0.5$, $\sigma^2_{Gz_i} = 1.0$, ϱ_i=0.2, $\alpha = 0.2$. θ_i and initial trait values were sampled from a uniform distribution U [0, 10].

Figure 4 | **Indirect evolutionary effects shape the fitness consequences of simulated network invasions. a,** Histograms showing the average change in species fitness (across all 10^3 simulations) after coevolving with the invasive species. The frequency in the *y*-axis represents log(Counts). **b-c,** Relationship between the average change in species fitness after the invasion, and the change in the total contribution of indirect evolutionary effects coming from the network for **b,** direct partners and **c,** indirect partners of the invasive species. Points and histogram bars represent the average values across all simulations (n=10^3 numerical simulations, 73 networks). The *x*-axis on panel **a,** and *y*-axis on panels **b-c,** are rescaled relative to the maximum absolute value of average change in fitness across all species. Parameter values

are as follows: $m_i = 0.5$, $\sigma^2_{Gz_i} = 1.0$, ϱ_i=0.2, $\alpha = 0.2$. θ_i and initial trait values were sampled from a uniform distribution U [0, 10].

Methods

Modeling coevolution in mutualistic networks

The starting point of our model is the classic quantitative genetics equation by Russell Lande[20]. This equation relates how the mean value of a continuous trait ($\bar{z}_i$) of a species changes between successive generations in response to the selective pressures in the environment:

$$\Delta\bar{z}_i = \sigma^2_{Gz_i} \frac{dln\overline{W_i}^{(t)}}{d\bar{z}_i^{(t)}} \quad (4)$$

where $\sigma^2_{Gz_i}$ is the additive genetic variance of trait z_i. The term $\frac{dln\overline{W_i}^{(t)}}{d\bar{z}_i^{(t)}}$ is the selection gradient and connects how changes in $\bar{z}_i$ affect the mean fitness of species i. In natural communities, the traits of species that mediates mutualistic interactions are subject to the selective pressures of its interacting partners and other sources in the environment. Thus, we assumed that the selection gradient, $\frac{dln\overline{W_i}}{d\bar{z}_i}$, is composed of two sources of selective pressures. First, we assumed that for a given species *i*, mutualisms contribute to a proportion m_i of the evolution of trait $\bar{z}_i$. Following empirical evidence and previous work[5,26,27,44], we further assumed that (1) mutualistic interactions of species *i* with each partner *j* favor trait complementarity, e.g., the complementarity between insect mouthparts and the floral tubes of plants; and (2) each mutualistic partner *j* of species *i* contributes to a given amount (q_{ij}) to the selective pressures that act upon trait $\bar{z}_i$. Second, we assumed that the selective pressures from other features of the environment, such as abiotic factors, contribute to the remaining proportion $(1 - m_i)$ of

the evolution of trait $\bar{z}_i$ and favor an optimal trait value (hereafter called environmental optima, θ_i). Under these assumptions, the selection gradient, $\frac{dln\overline{W_i}}{d\bar{z}_i}$, can be described as:

$$\frac{dln\overline{W_i}^{(t)}}{d\bar{z}_i^{(t)}} = \varrho_i \left[m_i \sum_{j,j\neq i}^{N} q_{ij}^{(t)} \left(\bar{z}_j^{(t)} - \bar{z}_i^{(t)} \right) + (1 - m_i)\left(\theta_i - \bar{z}_i^{(t)} \right) \right] \quad (5)$$

where ϱ_i is a constant that measures the sensitivity of species fitness to changes in the values of $\bar{z}_i^{(t)}$. The term $q_{ij}^{(t)}$quantifies the evolutionary contribution of a given mutualistic partner *j* to the selection imposed on $\bar{z}_i^{(t)}$. We assumed that $q_{ij}^{(t)}$ depends on a trait matching rule such that $q_{ij}^{(t)}$ increases with the trait matching between species *i* and a partner *j*, relative to all other *k* partners of *i*, $q_{ij}^{(t)} = \frac{a_{ij} e^{-\alpha\left(\bar{z}_j^{(t)} - \bar{z}_i^{(t)}\right)^2}}{\sum_{k=1,k\neq i}^{N} a_{ik} e^{-\alpha\left(\bar{z}_k^{(t)} - \bar{z}_i^{(t)}\right)^2}}$, in which $a_{ij}(a_{ik}) = 1$ if species *i* interacts with species *j(k)* in the network or equals 0 otherwise; and α is a parameter that controls the sensitivity of $q_{ij}^{(t)}$ to the distance between species traits. Combining equations (4) and (5) results in our coevolutionary model:

$$\bar{z}_i^{(t+1)} = \bar{z}_i^{(t)} + \sigma_{Gz_i}^2 \varrho_i \left[m_i \sum_{j,j\neq i}^{N} q_{ij}^{(t)} \left(\bar{z}_j^{(t)} - \bar{z}_i^{(t)} \right) + (1 - m_i)\left(\theta_i - \bar{z}_i^{(t)} \right) \right] \quad (1)$$

Linking coevolution and species fitness

In our model, the selection gradient, $\frac{dln\overline{W_i}}{d\bar{z}_i}$ connects the evolution of species traits to how mutualisms and the environment affect their mean fitness[5]. To derive the expression that explicitly links coevolution to species mean fitness, $\overline{w_i}(\bar{z}_i)$, we solved equation (5) to obtain species absolute fitness (Supplementary methods). Assuming a selection gradient first and then integrating it to find fitness, results in an equation that describes an entire family of fitness

functions that could lead to the same selection gradient (see Supplementary methods for additional examples):

$$\overline{W_i} = \mathrm{e}^{\varrho_i\left[\frac{m_i}{2\alpha}\ln\left(\sum_{j=1,j\neq i}^{N} a_{ij}e^{-\alpha\left(\bar{z}_j-\bar{z}_i\right)^2}\right)+(1-m_i)\left(\theta_i\bar{z}_i-\frac{\bar{z}_i^{\,2}}{2}\right)\right]+c_i} \quad (6)$$

where c_i is a constant that emerges from the integration of the selection gradient. Thus, instead of a specific function, equation (6) is a general representation of an entire family of fitness functions depending on the choice of the constant c_i. In fact, it can be shown that equation (6) can lead to other fitness functions adopted in previous work by choosing different values for c_i (Supplementary methods). Since in equation (6) species fitness scales up with the number of mutualistic partners, with the value of the environmental optima (θ_i) and depends on this arbitrary constant (c_i), we performed two additional steps. First, we found the conditions under which species achieve their maximum theoretical absolute fitness. The absolute fitness of species will be maximized whenever species are at their adaptive peaks, i.e., when $\frac{dln\overline{W_i}}{d\bar{z}_i} = 0$. From equation (4), since $0 < m_i < 1$, this condition is fulfilled when $\bar{z}_i = \bar{z}_j$ for all mutualistic partners *j*, and, at the same time, $\bar{z}_i = \theta_i$ (except for the trivial case in which $\varrho_i = 0$). That is, fitness is maximized when species are perfectly adapted to all mutualistic partners and the environmental optima (e.g., when all species share the same environmental optima). Plugging in this condition into equation (6) yields:

$$\overline{W_{max,i}} = \mathrm{e}^{\varrho_i\left[\frac{m_i}{2\alpha}\ln\left(\sum_{j=1,j\neq i}^{N} a_{ij}\right)+(1-m_i)\left(\frac{\theta_i^2}{2}\right)\right]+c_i} \quad (7)$$

Next, we computed species relative fitness ($\overline{w_i}$) as the ratio $\frac{\overline{W_i}}{\overline{W_{max,i}}}$, resulting in equation (2), indicating how close the species is to the maximum fitness value for a species with the same number of partners:

$$\overline{w_i} = e^{\frac{1}{2}\varrho_i\left[\frac{m_i}{\alpha}\ln\left(\frac{s_i}{k_i}\right)-(1-m_i)(\theta_i-z_i)^2\right]} \quad (2)$$

Linking indirect evolutionary effects to species fitness

Our coevolutionary model always leads to a stable equilibrium of species traits (and therefore species fitness). Using the simplifying assumption that $q_{ij}^{(t)} \approx q_{ij}$, from equation (1), species traits reach a coevolutionary equilibria when:

$$m_i \sum_{j=1, j\neq i}^{N} q_{ij}\left(\bar{z}_j^{\,*} - \bar{z}_i^{\,*}\right) + (1 - m_i)(\theta_i - \bar{z}_i^{\,*}) = 0 \quad (8)$$

Equation (8) leads to:

$$\bar{z}_i^{\,*} - m_i \sum_{j=1, j\neq i}^{N} q_{ij}\bar{z}_j^{\,*} = (1 - m_i)\theta_i \quad (9)$$

which, in matrix form can be rewritten as:

$$\vec{\boldsymbol{Z}}^* - \boldsymbol{Q}\vec{\boldsymbol{Z}}^* = \boldsymbol{\psi}\vec{\boldsymbol{\Theta}} \quad (10)$$

$$\vec{\boldsymbol{Z}}^* = (\boldsymbol{I} - \boldsymbol{Q})^{-1}\boldsymbol{\psi}\vec{\boldsymbol{\Theta}} \quad (11)$$

In equations (10)-(11) $\vec{\boldsymbol{Z}}^*$is a Nx1 vector of species traits at the coevolutionary equilibrium, $\boldsymbol{\psi}$ is a NxN diagonal matrix with $(1 - m_i)$ as its diagonal elements; $\vec{\boldsymbol{\Theta}}$ is a Nx1 vector of species environmental optima (θ_i); and $\boldsymbol{I}$ is the identity matrix. The **Q**-matrix is a matrix whose entries, $m_i q_{ij}$, contain the direct evolutionary effects between species *i* and *j*.

The matrix $\mathbf{T} = (\boldsymbol{I} - \boldsymbol{Q})^{-1}$ is a matrix that contains not only the direct, but also the indirect evolutionary effects that come from the multiple pathways connecting species in the network. This interpretation can be recovered by noticing that the **T**-matrix is the result of a matrix power series:

$$(\boldsymbol{I} - \boldsymbol{Q})^{-1} = \boldsymbol{Q^0} + \boldsymbol{Q^1} + \boldsymbol{Q^2} + \boldsymbol{Q^3} \ldots = \sum_{\boldsymbol{\ell=0}}^{\infty} \boldsymbol{Q^{\ell}} \quad (12)$$

The powers of the **Q**-matrix correspond to matrices that represent the effects of species on each other through multiple pathways in the network. Thus, while the **Q**-matrix represents the direct

evolutionary effects that species exert on each other, each power ℓ of the Q-matrix contains the effects that species *j* exert on species *i* through a chain of effects of length ℓ. For instance, the elements $q_{ij}^{(2)}$ of the matrix $\boldsymbol{Q^2}$contains the effects of species *j* on species *i* through pathways of length 2, such as the indirect evolutionary effect of one plant species on another plant mediated by a shared animal mutualist. Consequently, the **T**-matrix contains the sum of the evolutionary effects among species flowing through all possible pathways in the network. Using the **T**-matrix, we first partitioned the contribution of indirect evolutionary effects from the direct ones. Then, combining equation (11) with the fitness function allowed us to express species fitness as a function of the total amount of incoming evolutionary effects for each species (Supplementary methods), and to partition the contribution of direct and indirect evolutionary effects to fitness.

Numerical simulations

We evaluated how mutualistic coevolution in ecological networks is connected to species average fitness by combining numerical simulations and an analytical approximation of our coevolutionary model. These simulations were parameterized with the structure of 186 empirical networks (Supplementary Table 1). Our dataset comprised 186 empirical networks distributed among three types of mutualisms: plants with extrafloral nectaries that are protected by ants (n=4), animals that consume the fleshy fruits of plants and disperse their seeds (n=34), and plants whose flowers are pollinated by animals (n=148). These mutualistic interactions span a wide range of network structures of multiple-partner mutualisms. All these networks were obtained from the Web-of-Life dataset (www.web-of-life.es). Here we focus on mutualisms in which there are two distinct set of species, forming bipartite networks. But other types of mutualisms that do not form bipartite networks can also be used to parameterize our coevolutionary model[45]. Examples of such mutualisms include mimetic rings in which unpalatable species can display a similar warning signal (i.e., Müllerian mimetic rings) and

indirectly benefit each other by a decreased per capita attack rate from predators[45]. In simulations with the same network, we parameterized a_{ij} as 1 if species *i* and *j* interacted and 0 otherwise. Furthermore, initial trait values ($\overline{z_i}$), and environmental optimum values (θ_i) were sampled from a uniform distribution U [0, 10]. We sampled environmental optimum values from a uniform distribution because in mutualistic communities, species can widely differ in their life histories, physiological constrains, and therefore, on their environmental optima[12]. With this approach we did not assume any particular shape on the distribution of environmental optima of species, as in a uniform distribution all values occur with the same frequency (i.e., are equiprobable). However, our analytical approximation show that our results do not rely on a particular distribution of environmental optima of species, and we also present the results of numerical simulations for when the sampling range of the environmental optimum is narrower than the interval used in the main text (Extended Data Fig. 4b).

All other parameters were held constant and were the same for all species ($\sigma^2_{G z_i} = 1.0$, ϱ_i=0.2, $\alpha = 0.2$). We ran 1000 simulations for each combination of network and m_i values (m_i=0.1, 0.2, 0.3, 0.4, 0.5, 0.6, 0.7, 0.8, 0.9), in which we first allowed species traits to achieve asymptotic values (defined as $\left|z_i^{(t+1)} - z_i^{(t)}\right| < 10^{-4}$). Then, we used these asymptotic trait values in equation (2) to compute the fitness of each species. In the main text we present the results for the scenario in which $m_i = 0.5$, since in empirical ecological communities the selective pressures from mutualistic interactions and other sources in the environment have been shown to be similar in strength to each other[24,26,34,35]. However, we also present the results of the numerical simulations for all other m_i values in the Supplementary methods and as extended data figures (Extended Data Figs. 3-4).

We used these numerical simulations to test the predictions of our analytical approximations (Supplementary methods). From the results of our numerical simulations, we built the matrix

of total evolutionary effects, **T**-matrix, $\boldsymbol{T} = (\boldsymbol{I} - \boldsymbol{Q})^{-\mathbf{1}}$. In our model, the **T**-matrix is an NxN matrix containing the total evolutionary effects among all N species in a network that determines the trait values of species at the coevolutionary equilibrium (equation 11). The matrix of direct evolutionary effects, i.e., the **Q**-matrix, was built using species trait values at the coevolutionary equilibrium. Following previous work[18], we used the entries of the **T**-matrix, t_{ij}, to compute the contribution of indirect evolutionary effects to trait evolution as:

$$F_i = \frac{\sum_{j=1, j\neq i}^{N} \left(1 - a_{ij}\right) t_{ij}}{\sum_{j=1, j\neq i}^{N} t_{ij}} \quad (13)$$

where F_i is the contribution of indirect evolutionary effects to species *i* and $a_{ij} = 1$ if species *i* interacts with species *j* and $a_{ij} = 0$ otherwise. All numerical simulations were performed using the Julia programming language[46], while figures were produced in R (see ref. 47). The code to perform numerical simulations and reproduce our results is publicly available[48].

Numerical simulations exploring the invasion of a supergeneralist species

We evaluated how an introduced supergeneralist species shapes the fitness of the native species with numerical simulations parameterized with a subset of the networks we used (n=73 empirical networks, Supplementary Table 2). These empirical networks were used because they were collected from ecological communities within which the European honeybee, *Apis mellifera* is not a native species. This honeybee species is a known supergeneralist species that interacts with many species within networks. To simulate how the fitness of species changes after coevolving with the invader, we proceeded as follows. First, we created a "pre-invasion" network by completely disconnecting *A. mellifera* from the network. We used this pre-invasion network to simulate the coevolutionary dynamics of species before the invasion, allowed species traits to reach asymptotic values (defined as $\left|z_i^{(t+1)} - z_i^{(t)}\right| < 10^{-4}$ for all species), and used equation (2) to compute species fitness at these asymptotic values. Second, we "reintroduced" *A. mellifera* into the network, simulated the coevolutionary dynamics with the

resulting "post-invasion" network, allowed species traits to reach asymptotic values, and computed species fitness again. Then, using the values for species fitness resulting from coevolution in the pre- and post-invasion networks, we evaluated how species fitness changed as a result of the *A. mellifera* invasion. Indirect evolutionary effects for the pre- and post-invasion networks were computed following equation (13). For all numerical simulations, initial trait values and environmental optimum values were sampled from a uniform distribution U [0, 10]. All other parameters were held constant and were the same for all species ($\varphi_i = 0.2$, ϱ_i=0.2, $\alpha = 0.2$). For each combination of network and values of m_i (m_i=0.1, 0.2, 0.3, 0.4, 0.5, 0.6, 0.7, 0.8, 0.9), we ran 1000 numerical simulations (see Extended Data Figs. 7-9 and Supplementary methods for sensitivity analyses).

44. Nuismer, S. *Introduction to Coevolutionary Theory*. (W. H. Freeman, 2017).

45. Birskis-Barros, I., Freitas, A. V. L. & Guimarães, P. R. Habitat generalist species constrain the diversity of mimicry rings in heterogeneous habitats. Sci. Rep. **11**, 5072 (2021).

46. Bezanson, J., Edelman, A., Karpinski, S. & Shah, V. B. Julia: A fresh approach to numerical computing. *SIAM Rev.* **59**, 65–98 (2017).

47. R Core Team. R: A language and environment for statistical computing. Preprint at https://www.R-project.org/ (2022).

48. Cosmo, L.G. Indirect effects shape species fitness in coevolved mutualistic networks (version 1.0.0). Computer software. Zenodo. doi:10.5281/zenodo.7945239 (2023).

Acknowledgements

This study was financed in part by the Coordenação de Aperfeiçoamento de Pessoal de Nível Superior – Brasil (CAPES) – Finance Code 001. LGC is funded by a São Paulo Research Foundation PhD scholarship (FAPESP; grants #2019/22146-3 and #2022/07939-0), and thank R. Cogni, Marco A. R. Mello, Carolina R. Montoya and Mayra C. Vidal for the comments in

previous versions of this manuscript. PRG is funded by Brazil's Council for Scientific and Technological Development (CNPq grant #307134/2017-2), FAPESP (São Paulo Research Foundation; grant: #2018/14809-0), and the Royal Society, London (CHL/R1/180156). APA was supported by Coordenação de Aperfeiçoamento de Pessoal de Nível Superior – Brasil (CAPES) – Finance Code 001 and São Paulo Research Foundation (FAPESP grant #2016/14277-2). MMP is funded by Sao Paulo Research Foundation (FAPESP grant #2019/25478-7) and Brazil's Council for Scientific and Technological Development (CNPq, grant #313059/2022-5). MAA is funded by São Paulo Research Foundation (FAPESP, grant #2021/14335-0 - ICTP-SAIFR), and by Brazil's Council for Scientific and Technological Development (CNPq, grant #301082/2019-7). AV is supported by the Spanish Ministry of Science, Innovation, and Universities (PGC2018-099772-B-100). PJ is funded by the Spanish Ministry of Science, Innovation, and Universities (CGL2017-82847-P), LifeWatch ERIC-SUMHAL (LIFEWATCH-2019-09-CSIC-13)/FEDER-EU funding), and the VI and VII Research Funding Program from Universidad de Sevilla (2021/00000826). JB's research is supported by the Swiss National Science Foundation (grant 310030_197201).

Author contributions

All authors designed the study. L.G.C., P.R.G. and M.A.A. derived the fitness function. L.G.C. and P.R.G. developed the analytical approximations. L.G.C. performed simulations and conducted analyses. A.V. and P.J. contributed with the data and analysis of the field experiment. L.G.C., P.R.G. and J.B. wrote a first draft of the manuscript and all authors contributed substantially to the final draft.

Competing interest

The authors declare that they have no competing financial interests.

Additional information

Supplementary Information is available for this paper.

588 Correspondence and requests for materials should be addressed to Leandro G. Cosmo or Paulo
589 R. Guimarães Jr.
590 Reprints and permissions information is available at www.nature.com/reprints.
591 **Code availability**
592 All the code to perform the numerical simulations used in this study is available a GitHub
593 repository (https://github.com/lgcosmo/Cosmo_et_el_indirect_effects_fitness), and in Zenodo
594 (DOI: 10.5281/zenodo.7945239).
595 **Data availability**
596 The dataset of empirical networks used in this study is available in a GitHub repository
597 (https://github.com/lgcosmo/Cosmo_et_el_indirect_effects_fitness), in Zenodo
598 (doi:10.5281/zenodo.7945239), and in the Web-of-Life Database (www.web-of-life.es).
599 **Extended Data figure legends**
600 **Extended Data Figure 1 | Species traits and fitness quickly reach equilibrium values after**
601 **coevolving in mutualistic networks. a-c,** Example for an ant-plant mutualistic network (panel
602 **a**) of how species traits (panel **b**) and fitness (panel **c**) quickly reach a coevolutionary
603 equilibrium. **d**, The coevolutionary equilibrium is reached even if not all species survive
604 throughout the dynamics, as illustrated by three species that were randomly extinct from the
605 network (for illustrative purposes, species whose trait values reach zero). Each point and line
606 correspond to the values for each species in the network (represented by different colors). The
607 diamond-shaped points on the right of panel **b** represent the environmental optima of each
608 species (θ_i). The dashed lines in panel **d** represent the trait values at equilibrium predicted by
609 equation (11) using the matrix of the interactions among surviving species. Parameter values
610 are as follows: $\sigma^2_{Gz_i} = 1.0$, $\varrho_i = 0.2$, $\alpha = 0.2$, $m_i = 0.5$. Initial trait values and environmental
611 optima were sampled from a uniform distribution U [0, 10].

Extended Data Figure 2 | Coevolution in mutualistic networks increases the variability in species fitness when a certain percentage of the species with the lowest fitness become extinct, and the surviving species coevolve to a new equilibrium. Each set of panels represents a specific scenario where a certain percentage of the species in the network experience extinction after reaching the initial coevolutionary equilibrium. In all scenarios extinctions occurred in a specific order, starting with the species possessing the lowest fitness until a desired percentage of extinctions was reached. The corresponding extinction percentages for each scenario are as follows: **a-b**, 10%; **c-d**, 20%; **e-f**, 30%; **g-h**, 40%; and **i-j**, 50%. In all panels the red histogram bars depict the distribution of fitness of the surviving species in the new coevolutionary equilibrium for 10^3 numerical simulations parameterized with the initial structure of empirical networks (n=186 empirical networks). Green histogram bars correspond to the scenario in which species coevolve as isolated pairs and there are no extinctions. In the boxplots each point corresponds to the mean value for 10^3 numerical simulations for a given species coevolving in the empirical mutualistic networks (n=186 empirical networks). Fitness values are rescaled relative to the average of the scenario in which species coevolve in networks or as isolated pairs. Other parameter values are as follows: $\sigma^2_{Gz_i} = 1.0$, ϱ_i=0.2, $\alpha = 0.2$, and $m_i = 0.5$. θ_i and initial trait values were sampled from a uniform distribution U [0, 10].

Extended Data Figure 3 | Coevolution in mutualistic networks increases the variability in species fitness for different levels of strength of mutualistic selection. a, Histogram showing the distribution of mean equilibrium fitness of species for 10^3 numerical simulations of a pair of coevolving species (green histogram bars), or of species within the 186 empirical networks used to parameterize the model (red histogram bars), for different values of m_i (values above each panel). **b**, Boxplot showing how species fitness vary with the number of mutualistic partners for different values of m_i (the intensity of mutualistic selection, values above each

panel). Each point corresponds to the mean value for 10^3 numerical simulations for a given species. In all panels fitness values are rescaled relative to the average of each scenario and m_i (coevolution in pairs or in networks). Other parameter values are as follows: $\sigma^2_{Gz_i} = 1.0$, ϱ_i=0.2, $\alpha = 0.2$, and m_i as indicated on top of each panel. θ_i and initial trait values were sampled from a uniform distribution U [0, 10].

Extended Data Figure 4 | Indirect effects drive species fitness for different parameterizations of the model. a, Examples of how indirect evolutionary effects drive the fitness of species in numerical simulations across all empirical networks (n=186 empirical networks) for different values of m_i (values above each panel), for species with five mutualistic partners. **b**, Examples of how indirect evolutionary effects drive the fitness of species in numerical simulations across all empirical networks (n=186 empirical networks) for different intervals of θ_i (values above each panel), and sensitivity of species adaptive landscapes (ϱ_i, diferente colors) for species with five mutualistic partners. Points in all panels represent average results for 10^3 numerical simulations of each combination of empirical network and parameter values. Other parameter values are as follows: $\sigma^2_{Gz_i} = 1.0$ and $\alpha = 0.2$. Values of m_i and ϱ_i as indicated on each panel. In **a**, θ_i and initial trait values were sampled from a uniform distribution U [0, 10], while in **b** the upper bound of the uniform distribution is indicated in the values above each panel.

Extended Data Figure 5 | Peripheral species are more affected by indirect effects drive for different networks and levels of mutualistic selection. Results from numerical simulations parameterized with the structure of empirical networks (n=186 empirical networks), showing how the contribution of indirect evolutionary effects is smaller for core than peripheral species within the same network. This result holds for all values of m_i, the intensity of mutualistic selection (values above each panel). Each point corresponds to the average for 10^3 numerical simulations for each combination of species position (core or

peripheral), empirical network and m_i. Points of different colors correspond to species that were classified either as core species (red points) or peripheral species (blue points). Parameter values are as follows: $m_i = variable$, $\sigma^2_{Gz_i} = 1.0$, ϱ_i=0.2, $\alpha = 0.2$. θ_i and initial trait values were sampled from a uniform statistical distribution U [0, 10].

Extended Data Figure 6 | Indirect effects drive the fitness of surviving species when the least fit species become extinct, and the surviving ones coevolve to a new equilibrium. Each panel corresponds to scenarios in which a certain percentage of the species in the network underwent extinction after reaching a first coevolutionary equilibrium. For all scenarios extinctions occurred in a specific order, starting with the species possessing the lowest fitness, until a given percentage of extinctions was reached. The corresponding percentage of species extinct are as follows: **a**, scenario without extinctions; **b**, 10%; **c**, 20%; **d**, 30%; **e**, 40%; and **f**, 50%. Points in each panel represent average results for species with three mutualistic partners across 10^3 numerical simulations parameterized with the initial structure of 186 empirical networks. In panels **b-f**, indirect evolutionary effects were computed from the matrix of evolutionary effects (**Q**-matrix) among the surviving species (equation 13). Parameter values are as follows: $m_i = 0.5$, $\sigma^2_{Gz_i} = 1.0$, ϱ_i=0.2, $\alpha = 0.2$. θ_i and initial trait values were sampled from a uniform statistical distribution U [0, 10].

Extended Data Figure 7 | Invasion of a network by a supergeneralist changes the fitness of native species via coevolution for different levels of mutualistic selection. Histograms showing the average change in native species fitness (n=10^3 numerical simulations for each of the 73 empirical networks) after coevolving with the invasive species for different values of m_i (the intensity of mutualistic selection, values above each panel). The frequency in the y-axis represents log(Counts). Other parameter values are as follows: $\sigma^2_{Gz_i} = 1.0$, ϱ_i=0.2, $\alpha = 0.2$, and m_i as indicated on top of each panel. θ_i and initial trait values were sampled from a uniform distribution U [0, 10].

Extended Data Figure 8 | Direct and indirect evolutionary effects drive the change in fitness of native species directly interacting with a supergeneralist invader. Relationship between the average change in species fitness (n=10^3 numerical simulations for each of the 73 empirical networks) after the invasion and the change in the contribution of indirect evolutionary effects for direct partners of *A. mellifera* and for different values of m_i (the intensity of mutualistic selection, values above each panel). Parameter values are as follows: $\sigma^2_{Gz_i} = 1.0$, ϱ_i=0.2, $\alpha = 0.2$, and m_i as indicated on top of each panel. θ_i and initial trait values were sampled from a uniform distribution U [0, 10].

Extended Data Figure 9 | Indirect evolutionary effects drive the change in fitness of native species only indirectly interacting with a supergeneralist invader. Relationship between the average change in species fitness (n=10^3 numerical simulations for each of the 73 empirical networks) after the invasion and the change in the contribution of indirect evolutionary effects for indirect partners of *A. mellifera* and for different values of m_i (the intensity of mutualistic selection, values above each panel). Other parameter values are as follows: $\sigma^2_{Gz_i} = 1.0$, ϱ_i=0.2, $\alpha = 0.2$, and m_i as indicated on top of each panel. θ_i and initial trait values were sampled from a uniform distribution U [0, 10].

Extended Data Figure 10 | Indirect evolutionary effects and rewiring of interactions shape the fitness consequences of the invasion of a network by the supergeneralist *A. mellifera*. **a-b**, Representations of the **(a)** *pre-* and **(b)** *post-Apis* network structures, showing how the invasion by *A. mellifera* reorganizes interactions. **c-d**, Histograms showing **(c)** the change in the number of partners and **(d)** the change in fitness that native species experienced after coevolving with *A. mellifera*. **e**, Relationship between the change in indirect evolutionary effects caused by *A. mellifera* and the change in the fitness of native species. The results in panels **d** and **e** correspond to the average results for the native species of 10^3 numerical simulations of the coevolutionary dynamics in the *pre-* and *post-Apis* networks. Parameter

values are as follows: $m_i = 0.5$, $\sigma^2_{Gz_i} = 1.0$, ϱ_i=0.2, $\alpha = 0.2$. θ_i and initial trait values were sampled from a uniform statistical distribution U [0, 10].

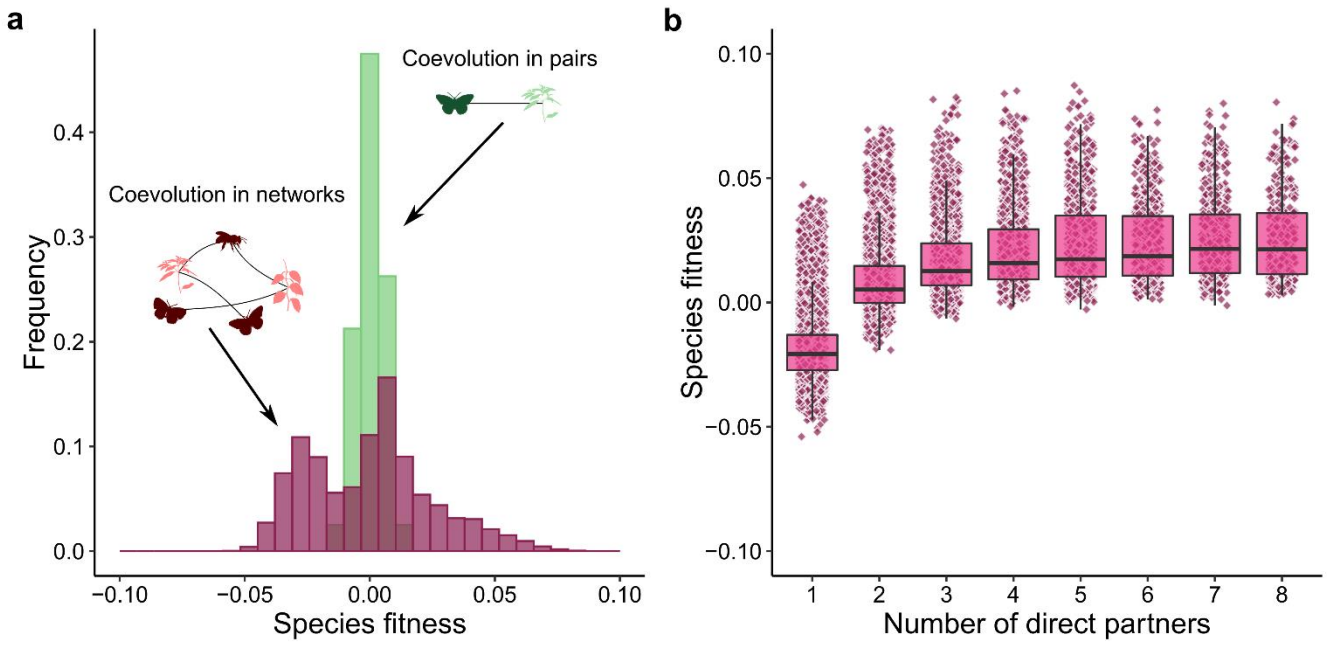

Figure 1 | **Coevolution in mutualistic networks increases the variability in species fitness. a,** Histogram showing the distribution of species fitness (rescaled relative to the average) that coevolved in a single mutualistic pair (green histogram bars), or within the 186 empirical networks used to parameterize the model (violet histogram bars). **b,** When coevolving within networks, species fitness increased up to a saturation point with the number of mutualistic partners, but largely varied among species with the same number of partners. Each fitness value corresponds to the mean value for 10^3 numerical simulations of our model. In both panels, fitness values are rescaled relative to the average of each scenario (coevolution in pairs or in networks) in such a way that zero indicates the average of the distribution in each scenario. Note that on panel **(b)** only species coevolving within networks are shown. Parameter values are as follows: $m_i = 0.5$, $\sigma^2_{Gz_i} = 1.0$, ϱ_i=0.2, $\alpha = 0.2$. θ_i and initial trait values were sampled from a uniform distribution U [0, 10].

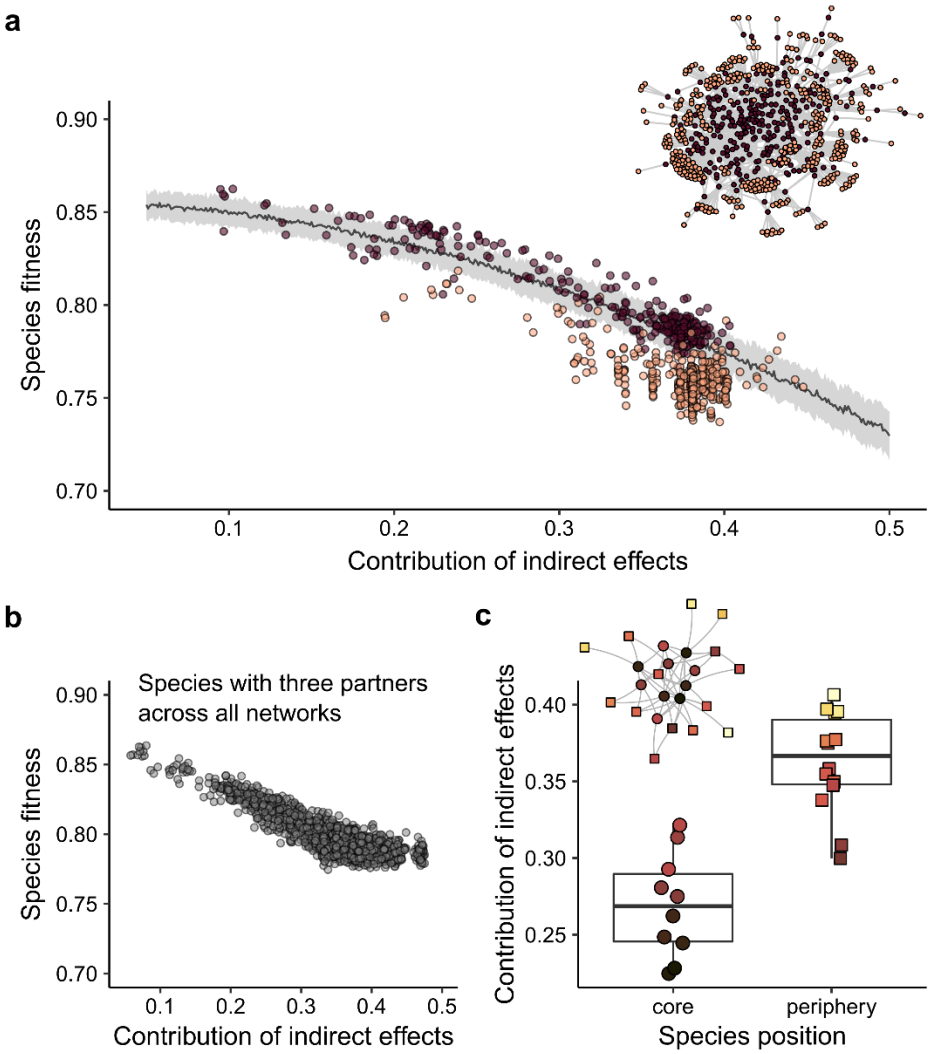

Figure 2 | Species position within networks and indirect evolutionary effects shape species fitness in coevolved mutualistic networks. a, Analytical approximation (solid line and shaded region) predicts that indirect evolutionary effects decrease the fitness of species coevolving in mutualistic networks. Points of lighter and darker colors represent species with one and more than one partner, respectively. This effect held for numerical simulations (n=10^3 numerical simulations for each of the 186 empirical networks), as shown for species within an example plant-pollinator network (points and inset), and **b,** for species across all empirical networks after controlling for the effects of the number of mutualistic partners. **c,** Example for a seed-dispersal network (inset) showing how species in peripheral positions receive more indirect effects and have a lower fitness than core species. The color of points represents species fitness such that the darker the color, the higher the fitness value. In panel **a,** the line represents the mean predicted fitness and shaded regions standard deviations when sampling species environmental optima (θ_i and $\langle\theta\rangle$) and $\langle z\rangle$ from a normal distribution, θ_i~N(0.0, 0.1), $\langle\theta\rangle$~N(2.5, 0.1) and $\langle z\rangle$~N(2.5, 0.1). Points in all panels correspond to the mean value of species fitness (panels **a** and **b**) or contribution of indirect effects (panel **c**) across 10^3 numerical simulations. Other parameter values are as follows: $m_i = 0.5$, $\sigma^2_{Gz_i} = 1.0$, ϱ_i=0.2, $\alpha = 0.2$. For numerical simulations, θ_i and initial trait values were sampled from a uniform distribution U [0, 10]. In panels **a** and **b,** the *x*-axis represents the proportional contribution of indirect evolutionary effects (equation 3).

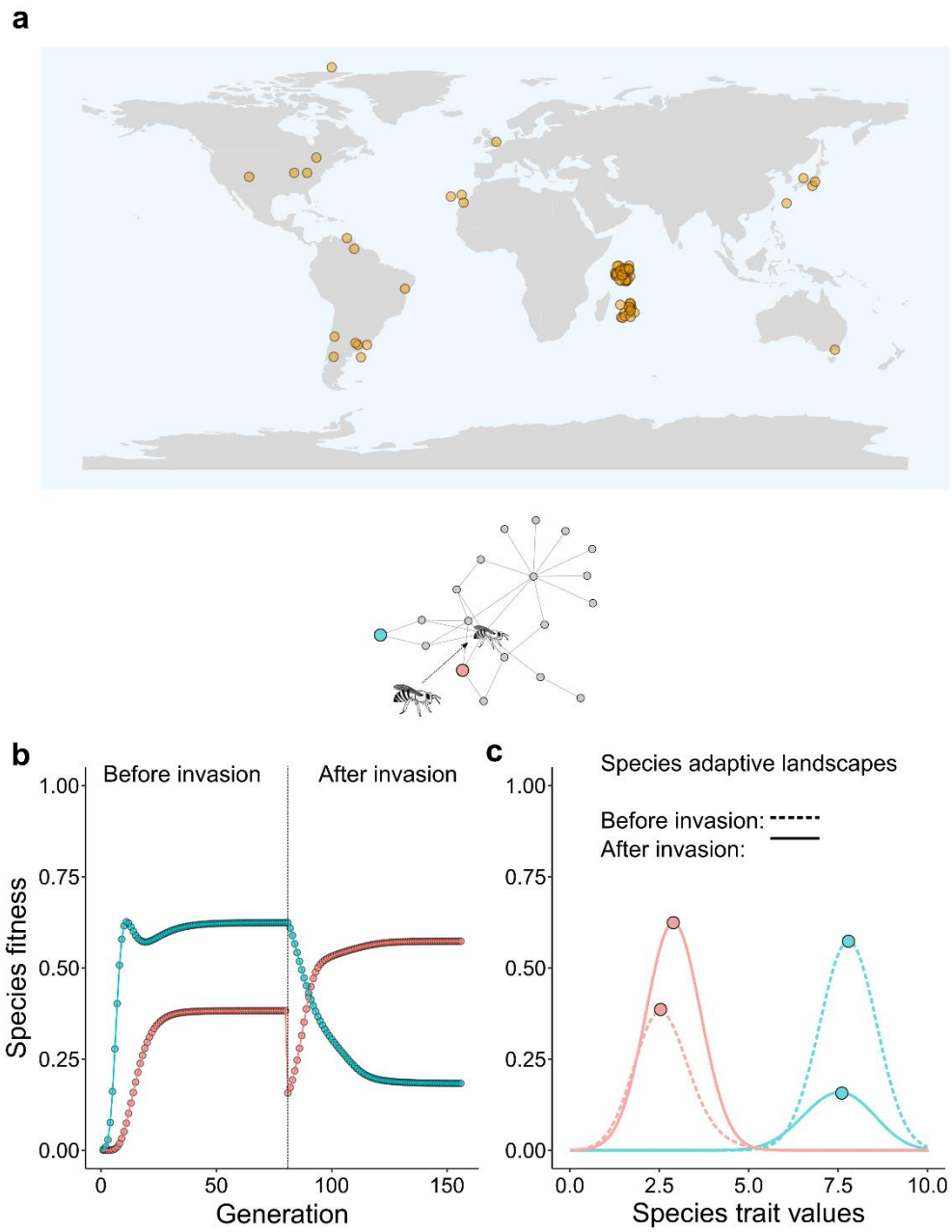

Figure 3 | Example of how the reorganization of indirect effects through a biological invasion can reshape species fitness within networks. **a,** Geographical location of the empirical networks used to parameterize the invasion simulations by honeybees. **b,** Examples of the rapid rate at which an invader can either increase or decrease the fitness of two native species within a network (insert). **c,** The reorganization of indirect effects following invasion reshapes the adaptive landscape of the native species, slightly favoring different trait values and changing fitness. Dashed and solid lines represent the adaptive landscape of species before and after coevolving with the invader, respectively. Parameter values are as follows: $m_i = 0.5$, $\sigma^2_{Gz_i} = 1.0$, ϱ_i=0.2, $\alpha = 0.2$. θ_i and initial trait values were sampled from a uniform distribution U [0, 10].

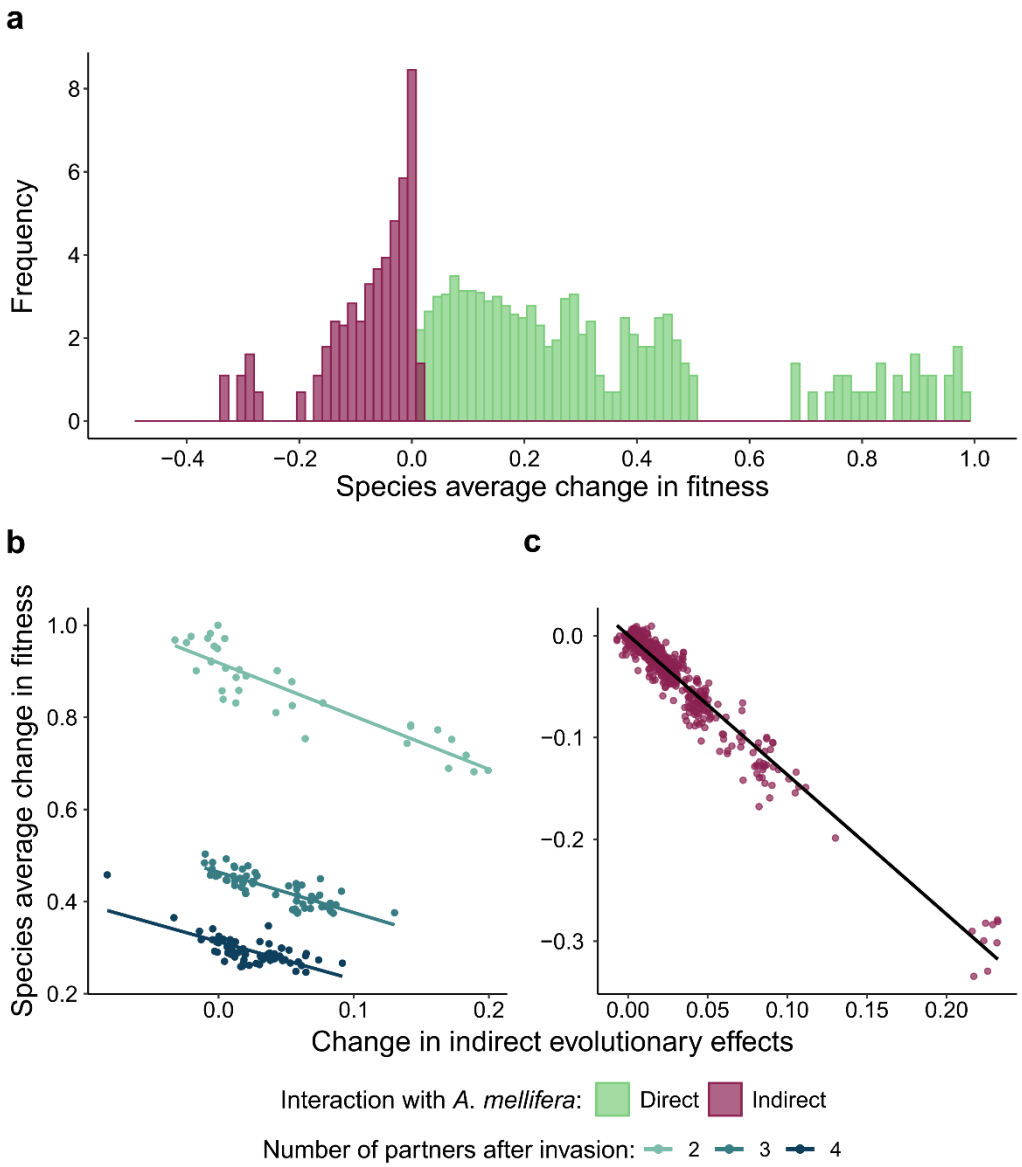

Figure 4 | Indirect evolutionary effects shape the fitness consequences of simulated network invasions. a, Histograms showing the average change in species fitness (across all 10^3 simulations) after coevolving with the invasive species. The frequency in the *y*-axis represents log(Counts). **b-c,** Relationship between the average change in species fitness after the invasion, and the change in the total contribution of indirect evolutionary effects coming from the network for **b,** direct partners and **c,** indirect partners of the invasive species. Points and histogram bars represent the average values across all simulations (n=10^3 numerical simulations, 73 networks). The *x*-axis on panel **a,** and *y*-axis on panels **b-c,** are rescaled relative to the maximum absolute value of average change in fitness across all species. Parameter values are as follows: $m_i = 0.5$, $\sigma^2_{G z_i} = 1.0$, ϱ_i=0.2, $\alpha = 0.2$. θ_i and initial trait values were sampled from a uniform distribution U [0, 10].

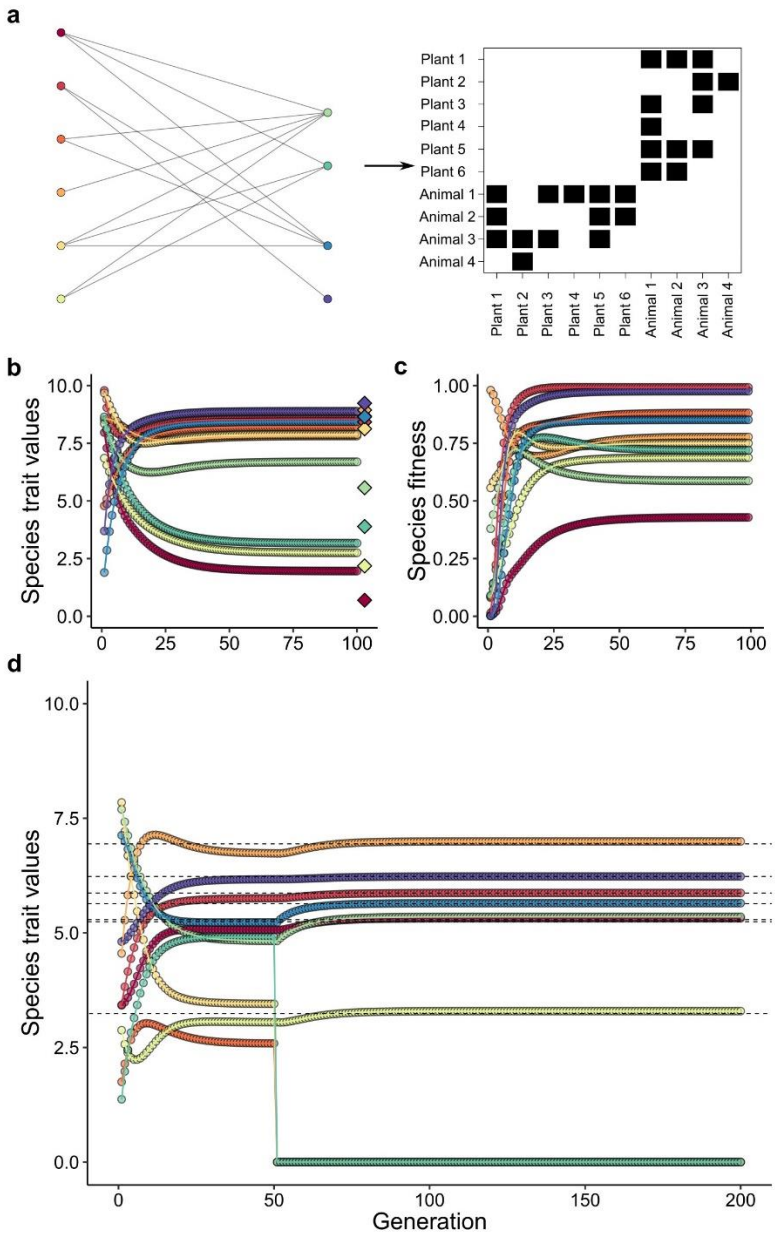

Extended Data Figure 1 | Species traits and fitness quickly reach equilibrium values after coevolving in mutualistic networks. a-c, Example for an ant-plant mutualistic network (panel **a**) of how species traits (panel **b**) and fitness (panel **c**) quickly reach a coevolutionary equilibrium. **d**, The coevolutionary equilibrium is reached even if not all species survive throughout the dynamics, as illustrated by three species that were randomly extinct from the network (for illustrative purposes, species whose trait values reach zero). Each point and line correspond to the values for each species in the network (represented by different colors). The diamond-shaped points on the right of panel **b** represent the environmental optima of each species (θ_i). The dashed lines in panel **d** represent the trait values at equilibrium predicted by equation (11) using the matrix of the interactions among surviving species. Parameter values are as follows: $\sigma^2_{Gz_i} = 1.0$, $\varrho_i = 0.2$, $\alpha = 0.2$, $m_i = 0.5$. Initial trait values and environmental optima were sampled from a uniform distribution U [0, 10].

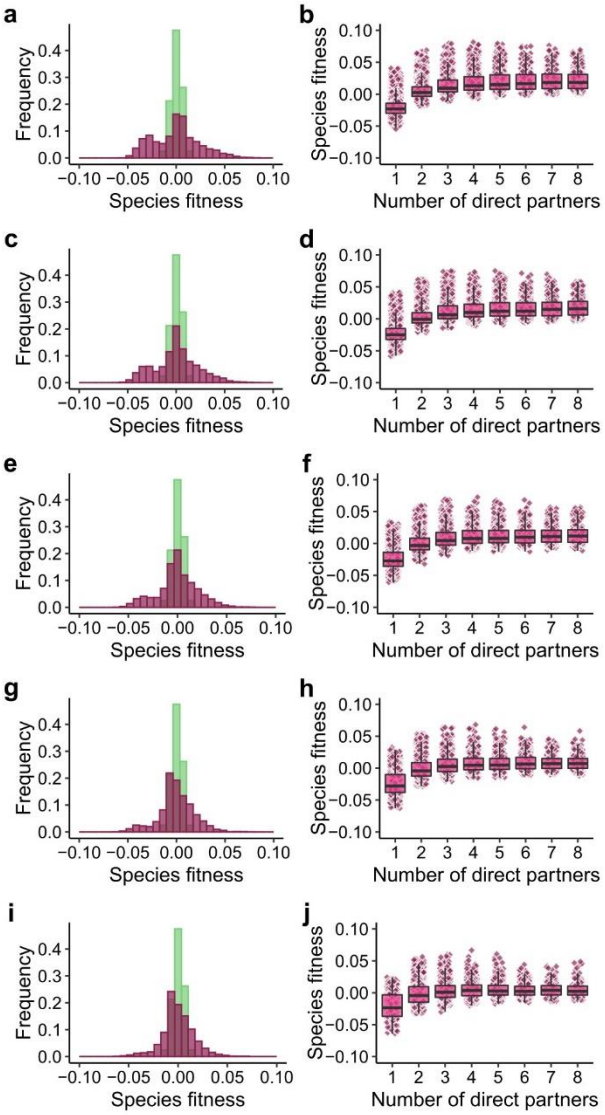

Extended Data Figure 2 | Coevolution in mutualistic networks increases the variability in species fitness when a certain percentage of the species with the lowest fitness become extinct, and the surviving species coevolve to a new equilibrium. Each set of panels represents a specific scenario where a certain percentage of the species in the network experience extinction after reaching the initial coevolutionary equilibrium. In all scenarios extinctions occurred in a specific order, starting with the species possessing the lowest fitness until a desired percentage of extinctions was reached. The corresponding extinction percentages for each scenario are as follows: **a-b**, 10%; **c-d**, 20%; **e-f**, 30%; **g-h**, 40%; and **i-j**, 50%. In all panels the red histogram bars depict the distribution of fitness of the surviving species in the new coevolutionary equilibrium for 10^3 numerical simulations parameterized with the initial structure of empirical networks (n=186 empirical networks). Green histogram bars correspond to the scenario in which species coevolve as isolated pairs and there are no extinctions. In the boxplots each point corresponds to the mean value for 10^3 numerical simulations for a given species coevolving in the empirical mutualistic networks (n=186 empirical networks). Fitness values are rescaled relative to the average of the scenario in which species coevolve in networks or as isolated pairs. Other parameter values are as follows: $\sigma^2_{Gz_i} = 1.0$, ϱ_i=0.2, $\alpha = 0.2$, and $m_i = 0.5$. θ_i and initial trait values were sampled from a uniform distribution U [0, 10].

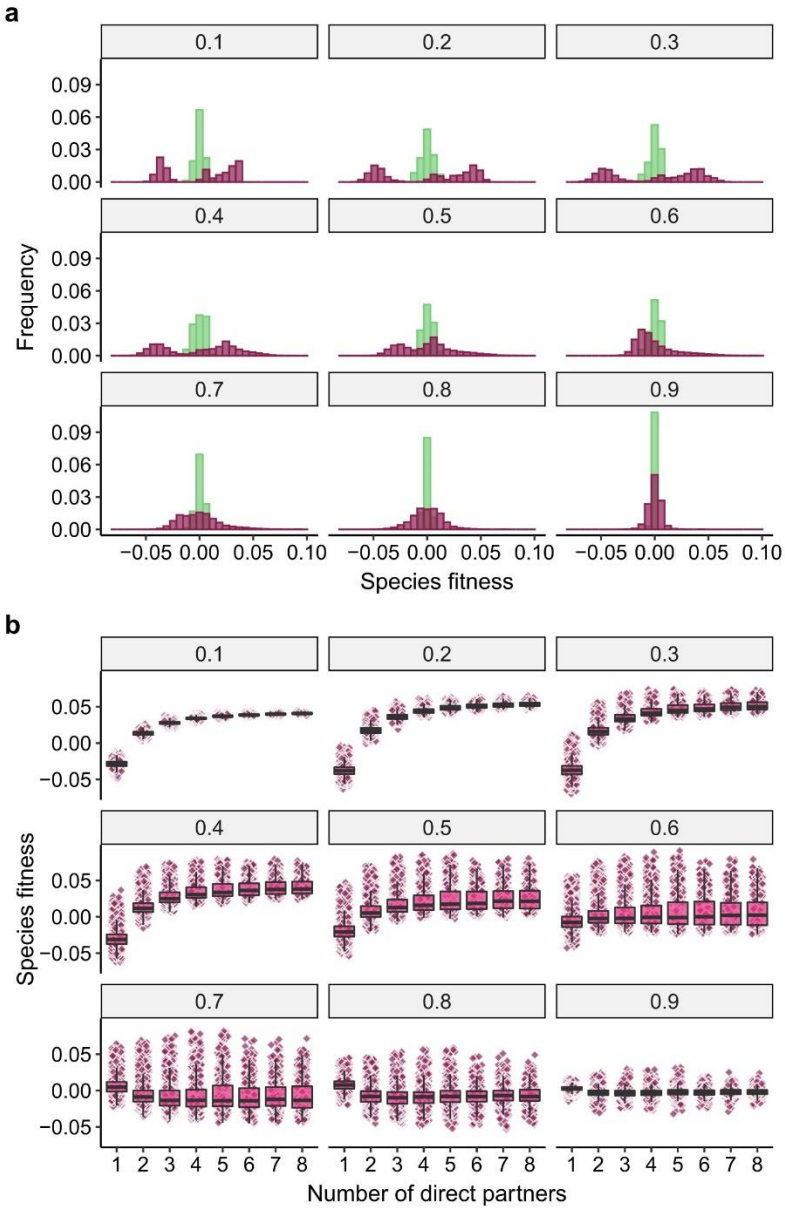

Extended Data Figure 3 | Coevolution in mutualistic networks increases the variability in species fitness for different levels of strength of mutualistic selection. a, Histogram showing the distribution of mean equilibrium fitness of species for 10^3 numerical simulations of a pair of coevolving species (green histogram bars), or of species within the 186 empirical networks used to parameterize the model (red histogram bars), for different values of m_i (values above each panel). **b**, Boxplot showing how species fitness vary with the number of mutualistic partners for different values of m_i (the intensity of mutualistic selection, values above each panel). Each point corresponds to the mean value for 10^3 numerical simulations for a given species. In all panels fitness values are rescaled relative to the average of each scenario and m_i (coevolution in pairs or in networks). Other parameter values are as follows: $\sigma^2_{Gz_i} = 1.0$, ϱ_i=0.2, $\alpha = 0.2$, and m_i as indicated on top of each panel. θ_i and initial trait values were sampled from a uniform distribution U [0, 10].

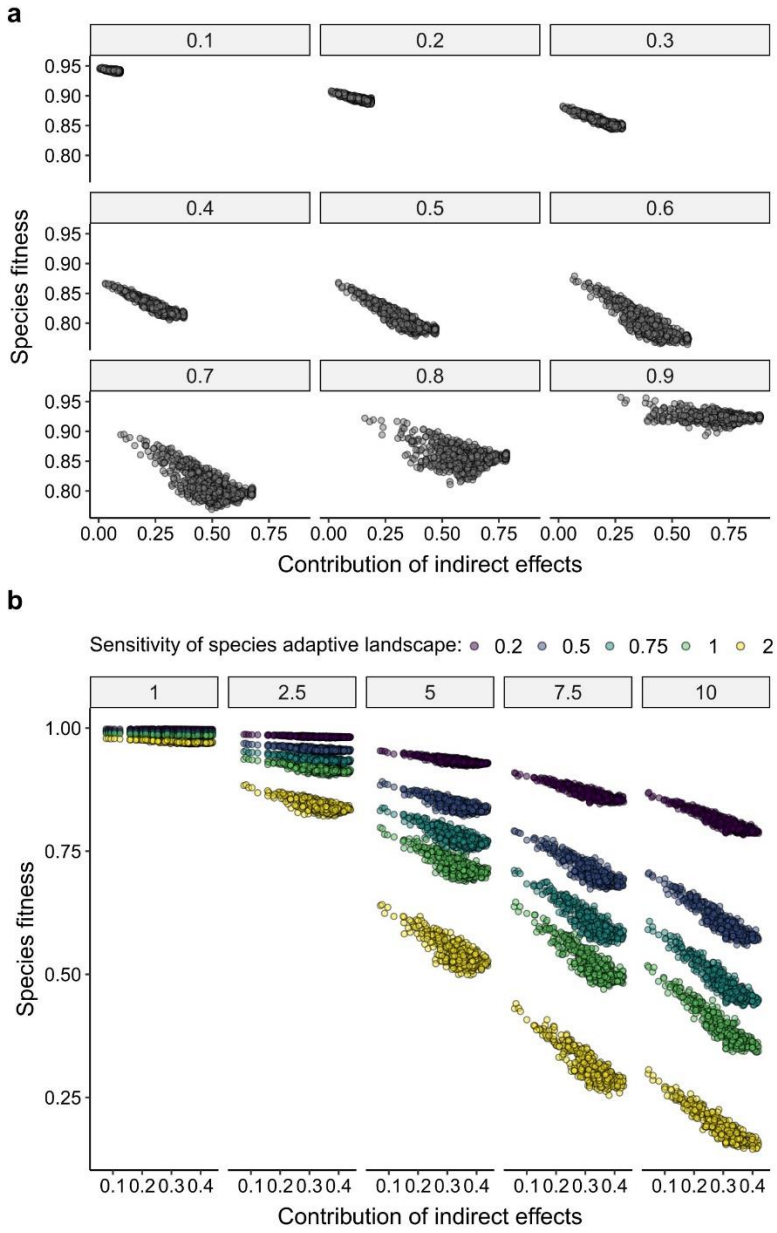

Extended Data Figure 4 | Indirect effects drive species fitness for different parameterizations of the model. a, Examples of how indirect evolutionary effects drive the fitness of species in numerical simulations across all empirical networks (n=186 empirical networks) for different values of m_i (values above each panel), for species with five mutualistic partners. **b**, Examples of how indirect evolutionary effects drive the fitness of species in numerical simulations across all empirical networks (n=186 empirical networks) for different intervals of θ_i (values above each panel), and sensitivity of species adaptive landscapes (ϱ_i, diferente colors) for species with five mutualistic partners. Points in all panels represent average results for 10^3 numerical simulations of each combination of empirical network and parameter values. Other parameter values are as follows: $\sigma^2_{Gz_i} = 1.0$ and $\alpha = 0.2$. Values of m_i and ϱ_i as indicated on each panel. In **a**, θ_i and initial trait values were sampled from a uniform distribution U [0, 10], while in **b** the upper bound of the uniform distribution is indicated in the values above each panel.

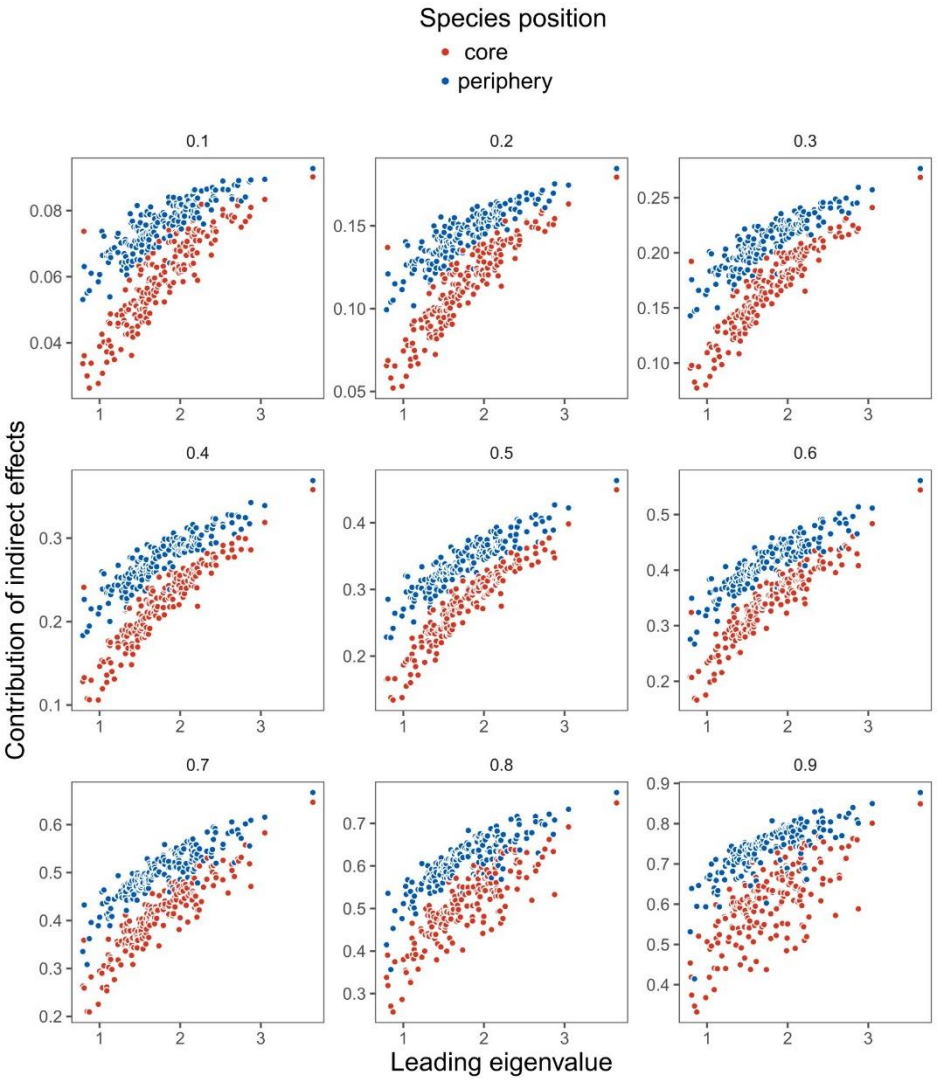

Extended Data Figure 5 | Peripheral species are more affected by indirect effects drive for different networks and levels of mutualistic selection. Results from numerical simulations parameterized with the structure of empirical networks (n=186 empirical networks), showing how the contribution of indirect evolutionary effects is smaller for core than peripheral species within the same network. This result holds for all values of m_i, the intensity of mutualistic selection (values above each panel). Each point corresponds to the average for 10^3 numerical simulations for each combination of species position (core or peripheral), empirical network and m_i. Points of different colors correspond to species that were classified either as core species (red points) or peripheral species (blue points). Parameter values are as follows: $m_i = variable$, $\sigma^2_{Gz_i} = 1.0$, ϱ_i=0.2, $\alpha = 0.2$. θ_i and initial trait values were sampled from a uniform statistical distribution U [0, 10].

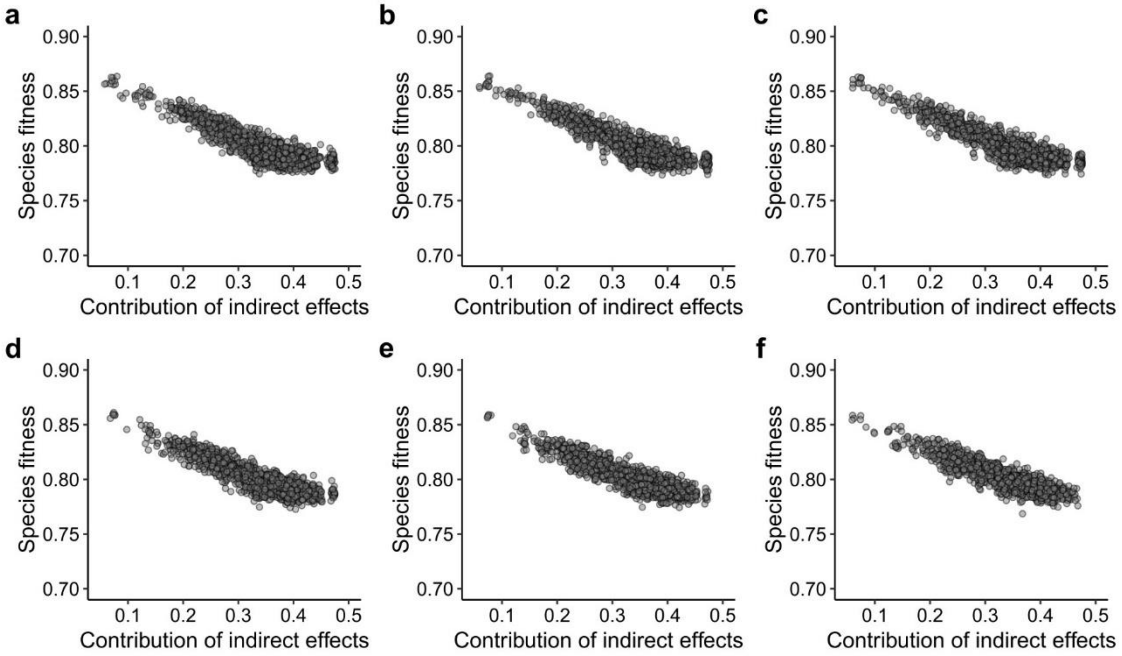

Extended Data Figure 6 | Indirect effects drive the fitness of surviving species when the least fit species become extinct, and the surviving ones coevolve to a new equilibrium. Each panel corresponds to scenarios in which a certain percentage of the species in the network underwent extinction after reaching a first coevolutionary equilibrium. For all scenarios extinctions occurred in a specific order, starting with the species possessing the lowest fitness, until a given percentage of extinctions was reached. The corresponding percentage of species extinct are as follows: **a**, scenario without extinctions; **b**, 10%; **c**, 20%; **d**, 30%; **e**, 40%; and **f**, 50%. Points in each panel represent average results for species with three mutualistic partners across 10^3 numerical simulations parameterized with the initial structure of 186 empirical networks. In panels **b-f**, indirect evolutionary effects were computed from the matrix of evolutionary effects (**Q**-matrix) among the surviving species (equation 13). Parameter values are as follows: $m_i = 0.5$, $\sigma^2_{Gz_i} = 1.0$, ϱ_i=0.2, $\alpha = 0.2$. θ_i and initial trait values were sampled from a uniform statistical distribution U [0, 10].

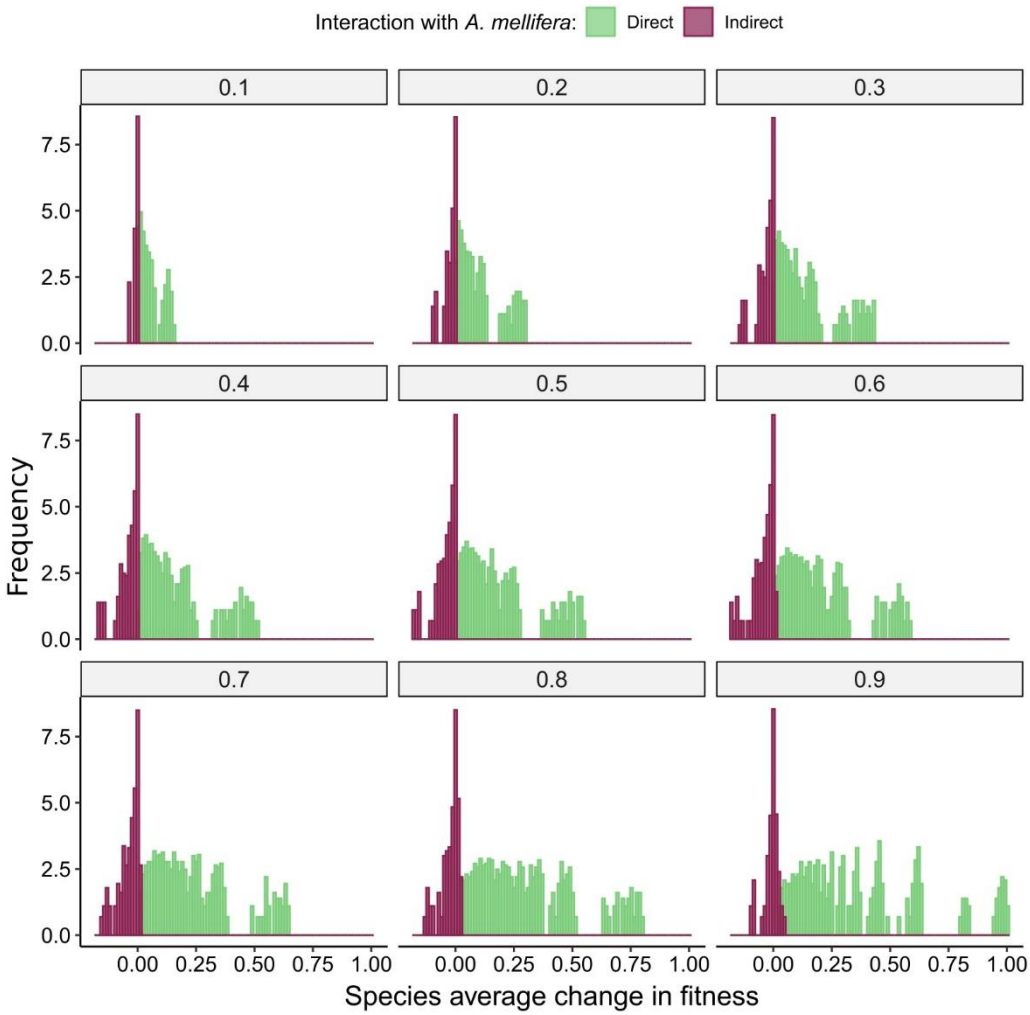

Extended Data Figure 7 | Invasion of a network by a supergeneralist changes the fitness of native species via coevolution for different levels of mutualistic selection. Histograms showing the average change in native species fitness (n=10^3 numerical simulations for each of the 73 empirical networks) after coevolving with the invasive species for different values of m_i (the intensity of mutualistic selection, values above each panel). The frequency in the y-axis represents log(Counts). Other parameter values are as follows: $\sigma^2_{Gz_i} = 1.0$, ϱ_i=0.2, $\alpha = 0.2$, and m_i as indicated on top of each panel. θ_i and initial trait values were sampled from a uniform distribution U [0, 10].

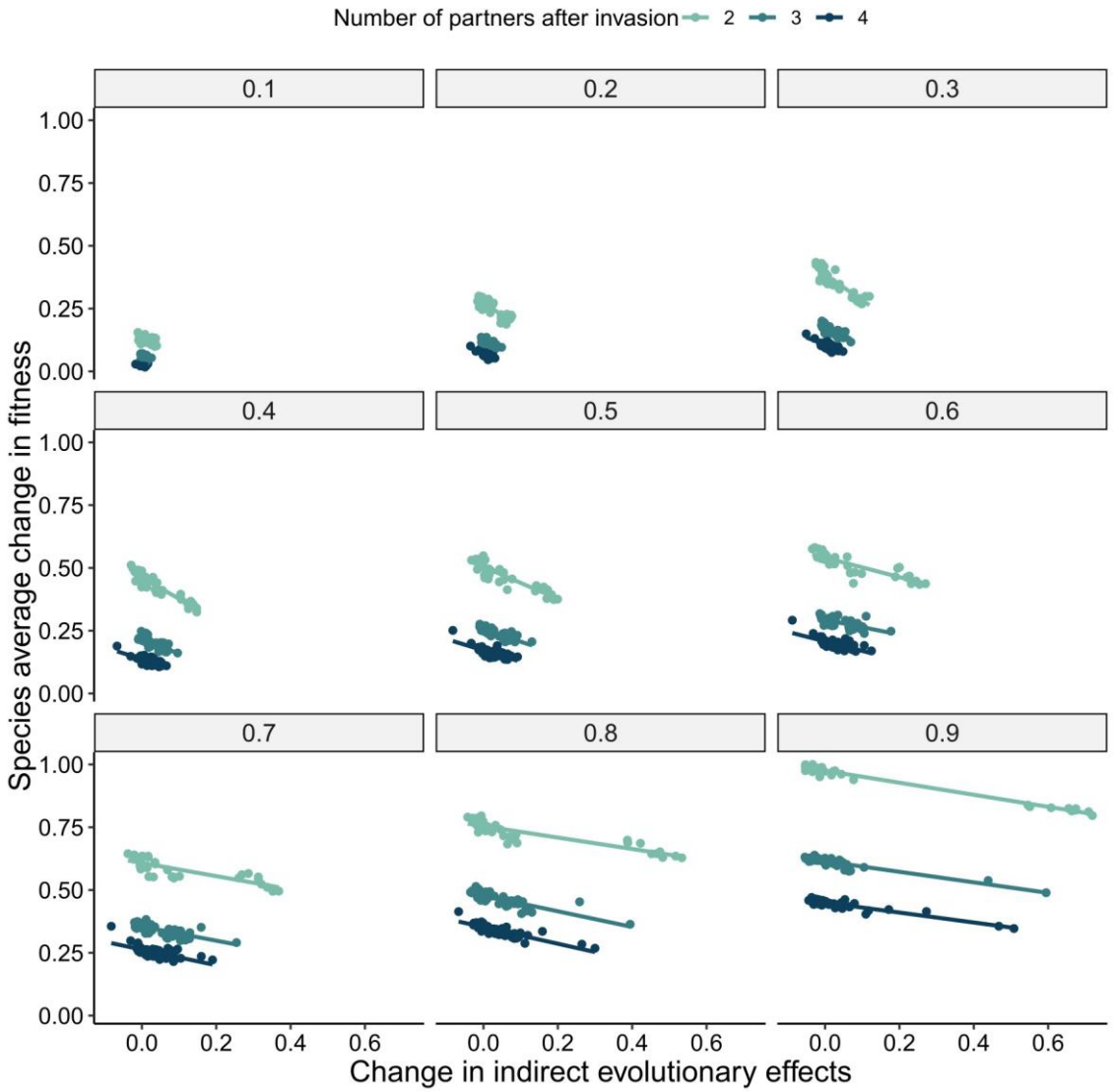

Extended Data Figure 8 | Direct and indirect evolutionary effects drive the change in fitness of native species directly interacting with a supergeneralist invader. Relationship between the average change in species fitness (n=10^3 numerical simulations for each of the 73 empirical networks) after the invasion and the change in the contribution of indirect evolutionary effects for direct partners of *A. mellifera* and for different values of m_i (the intensity of mutualistic selection, values above each panel). Parameter values are as follows: $\sigma^2_{Gz_i} = 1.0$, ϱ_i=0.2, $\alpha = 0.2$, and m_i as indicated on top of each panel. θ_i and initial trait values were sampled from a uniform distribution U [0, 10].

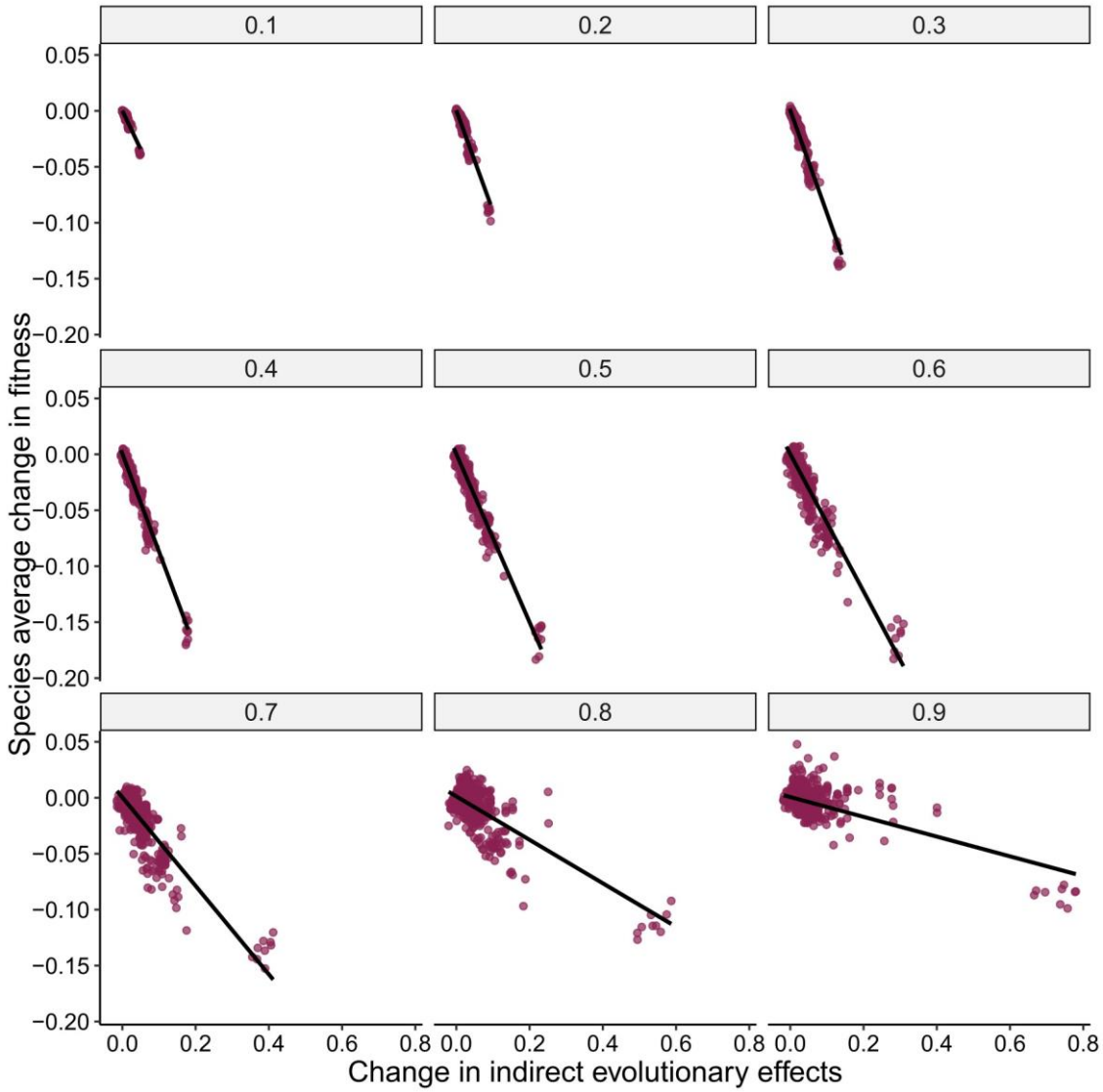

Extended Data Figure 9 | Indirect evolutionary effects drive the change in fitness of native species only indirectly interacting with a supergeneralist invader. Relationship between the average change in species fitness (n=10^3 numerical simulations for each of the 73 empirical networks) after the invasion and the change in the contribution of indirect evolutionary effects for indirect partners of *A. mellifera* and for different values of m_i (the intensity of mutualistic selection, values above each panel). Other parameter values are as follows: $\sigma^2_{Gz_i} = 1.0$, ϱ_i=0.2, $\alpha = 0.2$, and m_i as indicated on top of each panel. θ_i and initial trait values were sampled from a uniform distribution U [0, 10].

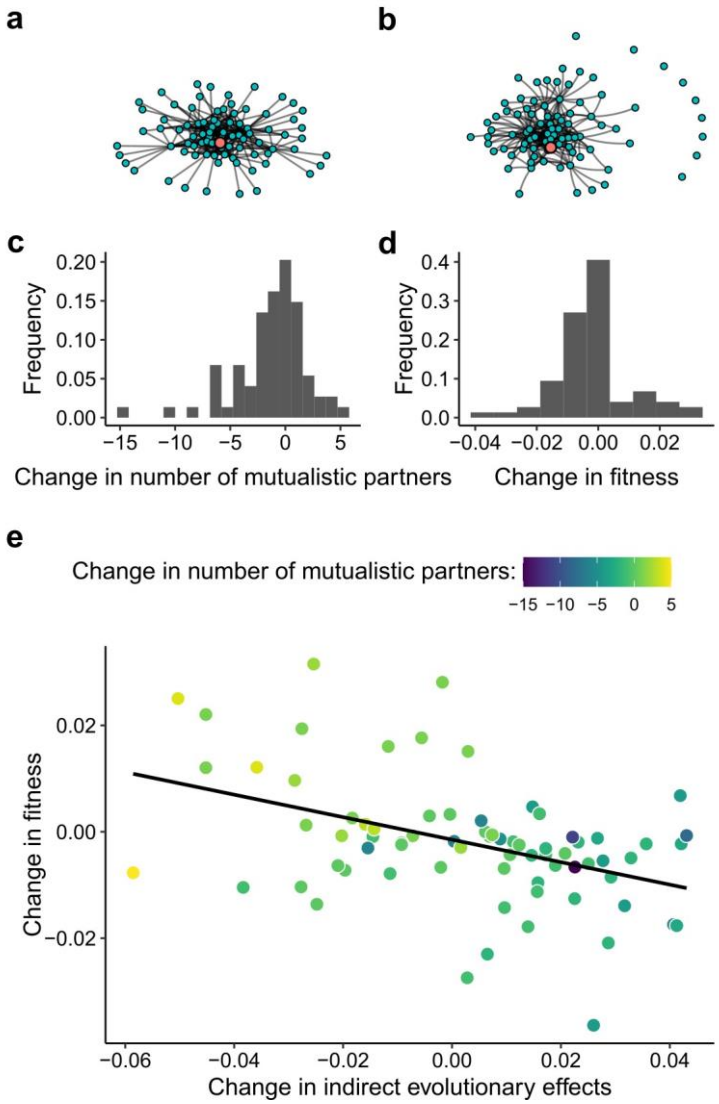

Extended Data Figure 10 | Indirect evolutionary effects and rewiring of interactions shape the fitness consequences of the invasion of a network by the supergeneralist *A. mellifera*. a-b, Representations of the **(a)** *pre-* and **(b)** *post-Apis* network structures, showing how the invasion by *A. mellifera* reorganizes interactions. **c-d**, Histograms showing **(c)** the change in the number of partners and **(d)** the change in fitness that native species experienced after coevolving with *A. mellifera*. **e**, Relationship between the change in indirect evolutionary effects caused by *A. mellifera* and the change in the fitness of native species. The results in panels **d** and **e** correspond to the average results for the native species of 10^3 numerical simulations of the coevolutionary dynamics in the *pre-* and *post-Apis* networks. Parameter values are as follows: $m_i = 0.5$, $\sigma^2_{Gz_i} = 1.0$, ϱ_i=0.2, $\alpha = 0.2$. θ_i and initial trait values were sampled from a uniform statistical distribution U [0, 10].

Supplementary Methods

Indirect effects shape species fitness in coevolved mutualistic networks

Leandro G. Cosmo, Ana Paula A. Assis, Marcus A. Aguiar, Mathias M. Pires, Alfredo Valido, Pedro Jordano, John N. Thompson, Jordi Bascompte, Paulo R. Guimarães Jr.

Contents

1 Coevolutionary dynamics in mutualistic networks

The dynamics underlying our coevolutionary model is similar to a diffusion equation underpinned by the species traits favored by the selection gradient[1]:

$$\bar{z}_i^{(t+1)} = \bar{z}_i^{(t)} + \sigma_{Gz_i}^2 \varrho_i \left[m_i \sum_{j,j\neq i}^{N} q_{ij}^{(t)} \left(\bar{z}_j^{(t)} - \bar{z}_i^{(t)} \right) + (1 - m_i)\left(\theta_i - \bar{z}_i^{(t)} \right) \right] \quad (1)$$

To understand the outcomes of the coevolutionary dynamics we studied the stability and the solutions of equation (1). Using the simplifying assumption that $q_{ij}^{(t)} \approx q_{ij}$, equation (1) can be rewritten in matrix notation as (see Ref 25 for more details):

$$\vec{\boldsymbol{Z}}^{(t+1)} = \vec{\boldsymbol{Z}}^{(t)} + \boldsymbol{\Phi}\mathbf{Q}\vec{\boldsymbol{Z}}^{(t)} - \boldsymbol{\Phi}\vec{\boldsymbol{Z}}^{(t)} + \boldsymbol{\Phi}\boldsymbol{\Psi}\vec{\boldsymbol{\Theta}} \quad (S1)$$

in which $\vec{\boldsymbol{Z}}^{(t)}$ is the Nx1 vector of species traits at time t; $\boldsymbol{\Phi}$ is a NxN diagonal matrix containing the product $\sigma_{Gz_i}^2 \varrho_i$ for each species i, $\mathbf{Q}$ is the NxN matrix of direct evolutionary effects among species, with entries $m_i q_{ij}$; $\boldsymbol{\Psi}$ is a NxN diagonal matrix with entries $(1 - m_i)$; and $\vec{\boldsymbol{\Theta}}$ is the Nx1 vector of species environmental optima. Rearranging the terms in equation (S1) leads to:

$$\vec{\boldsymbol{Z}}^{(t+1)} = (\boldsymbol{I} - \boldsymbol{\Phi} + \boldsymbol{\Phi}\mathbf{Q})\vec{\boldsymbol{Z}}^{(t)} + \boldsymbol{\Phi}\boldsymbol{\Psi}\vec{\boldsymbol{\Theta}} \quad (S2)$$

In turn, iterating equation (S2) results in:

$$\vec{\boldsymbol{Z}}^{(t)} = (\boldsymbol{I} - \boldsymbol{\Phi} + \boldsymbol{\Phi}\mathbf{Q})^t \vec{\boldsymbol{Z}}^{(0)} + \sum_{t=0}^{t-1} (\boldsymbol{I} - \boldsymbol{\Phi} + \boldsymbol{\Phi}\mathbf{Q})^t \, \boldsymbol{\Phi}\boldsymbol{\Psi}\vec{\boldsymbol{\Theta}} \quad (S3)$$

If species are under environmental selection ($0 < m_i < 1$) and $\sigma_{Gz_i}^2 \varrho_i < 1$, then the absolute value of the leading eigenvalue of the matrix $(\boldsymbol{I} - \boldsymbol{\Phi} + \boldsymbol{\Phi}\mathbf{Q})$ is less than

one. This implies that the first part of equation (S3) decays to 0 as $t \to \infty$ and that the summation $\sum_{t=0}^{t-1}(\boldsymbol{I}-\boldsymbol{\Phi}+\boldsymbol{\Phi Q})^{t}\,\boldsymbol{\Phi\Psi}\vec{\boldsymbol{\Theta}}$ converges to $(\boldsymbol{I}-\boldsymbol{I}+\boldsymbol{\Phi}-\boldsymbol{\Phi Q})^{-1}\boldsymbol{\Phi\Psi}\vec{\boldsymbol{\Theta}}$. Simplifying and substituting these results into equation (S3) yields:

$$\vec{\boldsymbol{Z}}^{*} = (\boldsymbol{I}-\boldsymbol{Q})^{-1}\boldsymbol{\Psi}\vec{\boldsymbol{\theta}} \tag{11}$$

which is the equilibrium solution derived into the main text. Thus, our coevolutionary model always converges to a global equilibrium given by equation (11). The stability of this global equilibrium is governed by the matrix $\boldsymbol{J} = (\boldsymbol{I}-\boldsymbol{\Phi}+\boldsymbol{\Phi Q})$ and the model is globally stable provided that $0 < m_i < 1$ and $\sigma_{Gz_i}^2 \varrho_i < 1$, i.e., the condition that assures that all of the eigenvalues of the matrix J are less than one in absolute value (by the Perron-Frobenius theorem).

The same equilibrium solution would be obtained in case we modeled coevolution using differential equations. Previous work showed that, in continuous time, the quantitative genetics equation underlying changes in species traits is[2,3]:

$$\frac{d\bar{z}_i}{dt} = \sigma_{Gz_i}^2 \frac{dln\overline{W_i}}{d\bar{z}_i} \tag{S4}$$

Substituting the equation for the selection gradient into equation (S4) yields:

$$\frac{d\bar{z}_i}{dt} = \sigma_{Gz_i}^2 \varrho_i \left[m_i \sum_{j,j\neq i}^{N} q_{ij}^{(t)} \left(\bar{z}_j{}^{(t)} - \bar{z}_i{}^{(t)}\right) + (1-m_i)\left(\theta_i - \bar{z}_i{}^{(t)}\right) \right] \tag{S5}$$

which has an identical equilibrium solution as equation (11), $\vec{\boldsymbol{Z}}^{*} = (\boldsymbol{I}-\boldsymbol{Q})^{-1}\boldsymbol{\Psi}\vec{\boldsymbol{\theta}}$. The matrix $\boldsymbol{T} = (\boldsymbol{I}-\boldsymbol{Q})^{-1}\boldsymbol{\Psi}$ resulting from our steady-state solutions is similar to the matrix used to compute Katz centrality in networks[4], $(\boldsymbol{I}-\boldsymbol{aC})^{-1}\vec{\boldsymbol{1}}$, in which C

is an adjacency matrix, $\vec{\mathbf{1}}$ is an all one vector and $\boldsymbol{a}$ is a scalar constant ($a < \frac{1}{\lambda_C^1}$, λ_C^1 being the leading eigenvalue of the adjacency matrix C), reinforcing the role of indirect effects propagating to multiple pathways in shaping dynamics. In fact, the T-matrix emerging directly from the long-term solution of our coevolutionary model is a generalization of Katz centrality and converges to it provided that (1) $\boldsymbol{Q} = \boldsymbol{aC}$, which implies that mutualistic selection is equal among all species and (2) the vector $\boldsymbol{\Psi}\vec{\boldsymbol{\theta}} = \vec{\mathbf{1}}$.

It is interesting to note that there are two trivial solutions of equation (1) in the limits in which $m_i = 1$ and $m_i = 0$. When $m_i = 1$, equation (S2) reduces to a diffusion process in a network. If the network is connected and $\sigma_{Gz_i}^2 \varrho_i < 1$, then the traits of all species are equal in the long-term solution. In turn, when $m_i = 0$, the traits of all species converge to their respective environmental optima, i.e., $\bar{z}_i = \theta_i$. These two trivial solutions represent scenarios in which species fitness are maximal for all species in the network.

Further analysis show that these results are robust to the extinction of species in the network. If species are extinct throughout the coevolutionary dynamics, the trait values of all species still converge to the equilibrium point predicted by equation (11) for the modified Q-matrix, $\vec{\boldsymbol{\Theta}}$ vector, and T-matrix of the surviving species. Since (1) it is these trait values at the equilibrium that determine fitness; and (2) equation (11) is the foundation upon which we build our analytical study

linking indirect effects to fitness, our results hold even when not all species are guaranteed to survive throughout the coevolutionary dynamics.

2 Modeling the fitness consequences of coevolution in mutualistic networks

2.1 Linking coevolution to species fitness

Here we derive the expression that explicitly links coevolution to species mean fitness, $\overline{w_i}(\bar{z}_i)$. From equation (5) of the main text:

$$\int d\ln\overline{W_i} = \int \varrho_i \left[m_i \sum_{j,j\neq i}^{N} q_{ij}\left(\bar{z}_j - \bar{z}_i\right) + (1-m_i)(\theta_i - \bar{z}_i) \right] d\bar{z}_i \qquad \text{(S6)}$$

Equation (S6) leads to:

$$\ln\overline{W_i} = \varrho_i \left[m_i \int \sum_{j=1,j\neq i}^{N} \frac{a_{ij} e^{-\alpha\left(\bar{z}_j - \bar{z}_i\right)^2}}{\sum_{k=1,k\neq i}^{N} a_{ij} e^{-\alpha\left(\bar{z}_k - \bar{z}_i\right)^2}} \left(\bar{z}_j - \bar{z}_i\right) d\bar{z}_i + (1-m_i) \int (\theta_i - \bar{z}_i) d\bar{z}_i \right] \qquad \text{(S7)}$$

The first integral in equation (S7) can be solved by substitution noting that the integrand is of the form $\frac{g\prime(x)}{g(x)}$. Thus, if we let $u = \sum_{j=1,j\neq i}^{N} a_{ij} e^{-\alpha\left(\bar{z}_j - \bar{z}_i\right)^2}$, we have that $du = 2\alpha \sum_{j=1,j\neq i}^{N} a_{ij} e^{-\alpha\left(\bar{z}_j - \bar{z}_i\right)^2} \left(\bar{z}_j - \bar{z}_i\right) d\bar{z}_i$ and $\frac{du}{2\alpha} = \sum_{j=1,j\neq i}^{N} a_{ij} e^{-\alpha\left(\bar{z}_j - \bar{z}_i\right)^2} d\bar{z}_i$.

Through this substitution the first integral becomes:

$$\int \frac{1}{2\alpha}\frac{1}{u} du = \frac{1}{2\alpha}\ln(u) = \frac{1}{2\alpha}\left[\ln\left(\sum_{j=1,j\neq i}^{N} a_{ij} e^{-\alpha\left(\bar{z}_j - \bar{z}_i\right)^2} \right) + c_{1i} \right] \qquad \text{(S8)}$$

The second integral in equation (S7) can be readily solved and results in:

$$\int (\theta_i - \bar{z}_i) d\bar{z}_i = \theta_i \bar{z}_i - \frac{{\bar{z}_i}^2}{2} + c_{2i} \qquad \text{(S9)}$$

Combining equations (S7-S9):

$$ln\overline{W_i} = \varrho_i \left[\frac{m_i}{2\alpha} \ln \left(\sum_{j=1, j \neq i}^{N} a_{ij} e^{-\alpha \left(\bar{z}_j - \bar{z}_i \right)^2} \right) + (1 - m_i) \left(\theta_i \bar{z}_i - \frac{\bar{z}_i^{\,2}}{2} \right) \right] + c_i \qquad (S10)$$

and exponentiating both sides:

$$\overline{W_i} = \mathrm{e}^{\varrho_i \left[\frac{m_i}{2\alpha} \ln \left(\sum_{j=1, j \neq i}^{N} a_{ij} e^{-\alpha \left(\bar{z}_j - \bar{z}_i \right)^2} \right) + (1 - m_i) \left(\theta_i \bar{z}_i - \frac{\bar{z}_i^{\,2}}{2} \right) \right] + c_i} \qquad (6)$$

where $c_i = \varrho_i \left[\frac{m_i}{2\alpha} c_{1i} + (1 - m_i) c_{2i} \right]$ is a constant of integration that characterizes the entire family of fitness functions that can lead to the same selection gradient. In this fitness function, however, the mean fitness of a given species increases with the number of mutualistic partners and depends on the arbitrary constant c_i. Thus, to compare the mean fitness of species with a different number of mutualistic partners and with different values for c_i, we obtained the conditions and an equation for when $\overline{W_i}$ is maximum. This allowed us to quantify species fitness as the ratio of their realized to their theoretical maximum fitness. When $0 < m_i < 1$, species achieve their maximum fitness if their trait values perfectly match the environmental optimum ($\bar{z}_i = \theta_i$) and the traits of mutualistic partners ($\bar{z}_i = \bar{z}_j$ for all j partners, Methods). Therefore, substituting these conditions in equation (6) leads to:

$$\overline{W_{max,i}} = \mathrm{e}^{\varrho_i \left[\frac{m_i}{2\alpha} \ln \left(\sum_{j=1, j \neq i}^{N} a_{ij} \right) + (1 - m_i) \left(\frac{\theta_i^2}{2} \right) \right] + c_i} \qquad (7)$$

and

$$\overline{w_i} = \frac{\overline{W_i}}{\overline{W_{max,i}}} = e^{\frac{1}{2}\varrho_i\left[\frac{m_i}{\alpha}\ln\left(\frac{s_i}{k_i}\right) - (1-m_i)(\theta_i-\bar{z}_i)^2\right]} \quad (2)$$

where $s_i = \sum_{j=1,j\neq i}^{N} a_{ij} e^{-\alpha\left(\bar{z}_j-\bar{z}_i\right)^2}$ and $k_i = \sum_{j=1,j\neq i}^{N} a_{ij}$.

It is also important to note that the use of equation (2) does not change the selection gradient as we can obtain the same equation directly from equation (6) by setting $c_{1i} = -ln\left(\sum_{j=1,j\neq i}^{N} a_{ij}\right)$ and $c_{2i} = -\frac{\theta_i^2}{2}$.

3 Robustness of the fitness function to different modelling assumptions

Using our approach of directly assuming the selection gradient and then integrating it, leads to an equation describing an entire family of fitness functions. This increases the generality of our results to different modeling assumptions. Two relevant examples would be the assumptions about the costs of mutualistic interactions or competitive/facilitative effects among species that share mutualistic partners[5–9]. Regarding the former, in many mutualisms' species produce resources that their partners use (e.g. nectar in plant-pollinator interactions or the nutritional contents of fruit pulp in plant-frugivore interactions) and therefore mutualisms may show significant costs. Mathematically, these costs could be described as a partner-specific deduction in the absolute fitness of species:

$$d_i = -m_i \sum_{j=1}^{N} a_{ij}\mu_{ij} \quad (S11)$$

where d_i is the total cost of mutualistic interactions for species *i* and μ_{ij} is the cost of interacting with each mutualistic partner *j*. Combining equations (S11) and (6) to apply this cost results in:

$$\overline{W_i} = \mathrm{e}^{\varrho_i\left[\frac{m_i}{2\alpha}\ln\left(\sum_{j=1,j\neq i}^{N} a_{ij}e^{-\alpha\left(\bar{z}_j-\bar{z}_i\right)^2}\right)-m_i\sum_{j=1}^{N} a_{ij}\mu_{ij}+(1-m_i)\left(\theta_i\bar{z}_i-\frac{\bar{z}_i^{\,2}}{2}\right)\right]} \quad (S12)$$

In turn, equation (S12) is equivalent to setting $c_{1i} = -2\alpha\sum_{j=1}^{N} a_{ij}\mu_{ij}$ and $c_{2i} = 0$. In respect to the later, species that share mutualistic partners can facilitate or compete for the interactions and commodities provide by species. This could be modeled as an increase or decrease in the total benefits provided by mutualisms to each species *i* depending on the fraction of partners shared with another species *j*:

$$p_i = m_i\sum_{j=1}^{N}\gamma_{ij}\frac{\sum_{k=1}^{N} a_{ik}a_{jk}}{\sum_{k=1}^{N} a_{ik}} \quad (S13)$$

in which p_i is the total effect of sharing partners on the fitness of species *i* and γ_{ij} is the effect on the fitness of species *i* for sharing partners with species *j*. The effects of sharing mutualistic partners described in equation (S13) could be obtained by setting $c_{1i} = 2\alpha\sum_{j=1}^{N}\gamma_{ij}\frac{\sum_{k=1}^{N} a_{ik}a_{jk}}{\sum_{j=1}^{N} a_{ij}}$ and $c_{2i} = 0$, resulting in the following fitness function:

$$\overline{W_i} = \mathrm{e}^{\varrho_i\left[\frac{m_i}{2\alpha}\ln\left(\sum_{j=1,j\neq i}^{N} a_{ij}e^{-\alpha\left(\bar{z}_j-\bar{z}_i\right)^2}\right)+m_i\sum_{j=1}^{N}\gamma_{ij}\frac{\sum_{k=1}^{N} a_{ik}a_{jk}}{\sum_{k=1}^{N} a_{ik}}+(1-m_i)\left(\theta_i\bar{z}_i-\frac{\bar{z}_i^{\,2}}{2}\right)\right]} \quad (S14)$$

Thus, our fitness function can accommodate a wide range of different modeling assumptions, as long as the mathematical functions underlying the assumptions do not explicitly depend on the same trait that mediates the mutualistic interaction

(z_i). In these particular cases, these effects will add or reduce the species fitness and, therefore, these terms do not change the outcomes of indirect effects in shaping fitness that we describe in the main text.

Additionally, it can be shown that setting different values to the integration constants yield fitness functions that have been used previously to model coevolution in mutualisms. For instance, for isolated pairs of interacting species our fitness function reduces to:

$$e^{-\frac{\varrho_i}{2}\left[m_i(\bar{z}_j-\bar{z}_i)^2-\frac{m_i}{2\alpha}c_{1i}+(1-m_i)\left(\theta_i\bar{z}_i-\frac{\bar{z}_i^{\,2}}{2}+c_{2i}\right)\right]} \quad (S15)$$

In other studies, is often assumed that the fitness of individuals are driven by two components[10]. First, the probability of successful interactions with individuals of mutualistic partners, $P_X(x,y)=e^{-\beta(y-x)^2}$ and $P_Y(y,x)=e^{-\beta(x-y)^2}$ in which x and y correspond to random variables encoding the distribution of the traits of individuals of mutualistic species X and Y. Second with the probability of the traits of individuals matching other abiotic factors in the environment, $P_X(x,\theta_X)=e^{-\gamma(\theta_X-x)^2}$ or , $P_Y(y,\theta_Y)=e^{-\gamma(\theta_Y-y)^2}$. Assuming that fitness is multiplicative results in the following pair of functions:

$$W_X=e^{-\beta(y-x)^2}e^{-\gamma(\theta_X-x)^2}=e^{-[\beta(y-x)^2+\gamma(\theta_X-x)^2]} \quad (S16.1)$$

$$W_Y=e^{-\beta(x-y)^2}e^{-\gamma(\theta_Y-y)^2}=e^{-[\beta(x-y)^2+\gamma(\theta_Y-y)^2]} \quad (S16.2)$$

If traits and environmental optima among individuals are normally distributed, the expected fitness of the population of species X and Y can be approximated as[11]:

$$\overline{W_X}\cong e^{-[\beta(\bar{y}-\bar{x})^2+\gamma(\theta_X-x)^2+2\sigma_x^2+\sigma_y^2]} \quad (S17.1)$$

$$\overline{W_Y} \cong e^{-[\beta(\bar{x}-\bar{y})^2+\gamma(\theta_Y-y)^2+2\sigma_y^2+\sigma_x^2]} \quad (S17.2)$$

In which σ_x^2 and σ_y^2 represent the phenotypic variances of, respectively, traits x and y in the populations of species X and Y. These two resulting fitness functions for species X and Y can be obtained by setting: (1) $c_{1i} = \frac{2}{\varrho_i}\frac{2\alpha}{m_i}\left(2\sigma_x^2 + \sigma_y^2\right)$ or $c_{1i} = \frac{2}{\varrho_i}\frac{2\alpha}{m_i}\left(2\sigma_y^2 + \sigma_x^2\right)$; (2) $c_{2i} = -\frac{\theta_x^2}{2}$ or $c_{2i} = -\frac{\theta_y^2}{2}$; and (3) using the equivalence $\beta = \frac{\varrho_i}{2}m_i$ and $\gamma = \frac{\varrho_i}{2}(1-m_i)$ in equation (6). Similarly, for mutualists coevolving in networks, the fitness of individuals of species i can be modeled as[12]:

$$W_i = \sum_{j=1}^{N} a_{ij}\, e^{-\beta\left(z_j-z_i\right)^2} e^{-\gamma(\theta_i-z_i)^2} = \mathrm{e}^{\left[\ln\left(\sum_{j=1}^{N} a_{ij} e^{-\beta\left(z_j-z_i\right)^2}\right)-\gamma(\theta_i-z_i)^2\right]} \quad (S18)$$

in which z correspond to random variables encoding the distribution of the traits of individuals of mutualistic species. From equation (S18), if the traits of all species are independent and normally distributed and have low variances in respect to the mean, the mean fitness of the population can be approximated as:

$$\overline{W_i} \cong \mathrm{e}^{\left[\ln\left(\sum_{j=1}^{N} a_{ij} e^{-\beta\left(\bar{z}_j-\bar{z}_i\right)^2}\right)-\gamma(\theta_i-\bar{z}_i)^2-\sum_{j=1}^{N} a_{ij}\left(2\sigma_{z_i}^2+\sigma_{z_j}^2\right)\right]} \quad (S19)$$

in which σ_z^2 correspond to the phenotypic variances of species traits. Equation (S19) can be obtained from our fitness equation by assuming the parameter equalities (1) $\varrho_i = \frac{2\alpha}{m_i}$, $\beta = \alpha$, $\gamma = \frac{(1-m_i)}{\varrho_i}$; (2) by setting $c_{1i} = -\sum_{j=1}^{N} a_{ij}\left(2\sigma_{z_i}^2 + \sigma_{z_j}^2\right)$; and (3) setting $c_{2i} = -\frac{\theta_i^2}{2}$. Thus, our results are robust to assuming different fitness functions as the ones that have been previously assumed when modeling coevolution in mutualisms.

4 Sensitivity analyses of numerical simulations and analytical approximations

On the main text we first explored how participating in a network affects the average fitness of species after generations of coevolution. The results shown in Figure 1 correspond to the results of simulations in which the level of mutualistic selection is $m_i = 0.5$. Here, we show how different levels of mutualistic selection, m_i, affects the results shown in Figure 1 of the main text. (Extended Data Fig. 3). Our results show that unless mutualistic selection is very strong ($m_i = 0.9$), species fitness is much more variable when species coevolve in networks than in pairs. Thus, the results reported in the main text are robust to different levels of mutualistic selection.

Regarding other parameters of the model - namely $\sigma^2_{Gz_i}$, ϱ_i, and α - our analytical approach shows that they not qualitatively affect our results. In the coevolutionary dynamics our analytical approximations for the solutions of the model show that all these three parameters do not affect the outcome of coevolution, only the speed at which species reach equilibrium trait values. For the fitness function, upon inspection equation (2) shows that $\sigma^2_{Gz_i}$ does not play a role, while ϱ_i only rescales the values of fitness for each species *i*. This result is consistent with our definition of ϱ_i as the overall slope of the selection gradient. Throughout the text we used a relatively small value for ϱ_i ($\varrho_i = 0.2$), but increasing it amplify the magnitude of the effects that we reported. The parameter α divides the term $ln\left(\frac{s_i}{k_i}\right)$ in equation

(2). From the properties of logarithms, the relationship between α and $ln\left(\frac{s_i}{k_i}\right)$ can be rewritten as $ln\left(\frac{s_i}{k_i}\right)^{\frac{1}{\alpha}}$. Using a mean field assumption in which $\bar{z}_j \approx \langle z \rangle$, we can re-express $ln\left(\frac{s_i}{k_i}\right)^{\frac{1}{\alpha}}$ as $ln\left(\frac{s_i}{k_i}\right)^{\frac{1}{\alpha}} \approx ln\left(e^{-\alpha(\langle z \rangle - \bar{z}_i)^2}\right)^{\frac{1}{\alpha}} \approx -(\langle z \rangle - \bar{z}_i)^2$. Thus, as long as $\bar{z}_j$ are not too different among the j mutualistic partners of species i (which is reasonable given that mutualisms favor trait similarity), then the effect of α on our results should be negligible.

4.1 Robustness of the model to the extinction of species

In natural systems it is possible that the species with the lowest fitness become extinct as a result of the ecological dynamics in the community. Thus, we tested the robustness of our results to eventual extinctions with an additional set of simulations. In these simulations, we first allowed species trait and fitness values to reach a coevolutionary equilibrium. Next, we performed simultaneous extinctions of a percentage of the species in the network. These extinctions occurred in a particular order, starting with the ones possessing the lowest fitness at the coevolutionary equilibrium until a given desired percentage of species in the network became extinct. Then, after the extinction event we allowed the surviving species to coevolve to a new equilibrium and computed species fitness and indirect evolutionary effects among the surviving species. Indirect evolutionary effects were computed using equation (13) and the matrix of direct evolutionary effects among

236 the surviving species (Q-matrix). The simulations were parameterized with the
237 initial structure of the same 186 empirical networks used in the main text.
238 We simulated five different scenarios progressively increasing the percentage of
239 species that went extinct, from 10% to 50% of the species in each network. We did
240 not go above 50% of extinctions because even under 40% of extinctions a large
241 portion of the surviving species were completely disconnected from the networks.
242 Furthermore, in mutualistic networks the ecological dynamics should not result in
243 large extinction events, since the structure of mutualistic networks have been shown
244 to increase resilience, biodiversity and minimize the effect of ecological processes
245 that could lead to extinctions (e.g. competition)13-15. After the extinction event,
246 some species eventually become disconnected from the network. These species were
247 also considered extinct which, in natural systems, may be a result of
248 coextinctions16. Thus, for scenarios above 40% of extinctions, this percentage may
249 underestimate the actual extinctions that occurred in each network.
250 Our results show that the variability in species fitness remains large. The
251 bimodality in the distribution of species fitness becomes less noticeable when
252 extinctions increase, but only disappears above 40% of extinctions (Extended Data
253 Fig. 2). This variability in fitness is driven by indirect effects that emerge from the
254 coevolutionary dynamics among the surviving species, even when 50% of the species
255 in the network went extinct (Extended Data Fig. 6). Therefore, our conclusions
256 about how indirect evolutionary effects shape fitness still hold even when species

with low fitness can eventually become extinct as a result of the ecological dynamics in communities.

4.2 Analytical approximation linking indirect evolutionary effects to species fitness

To link species fitness to the contribution of indirect evolutionary effects, we combined our fitness function (equation 2) with the analytical solution for the trait values of species at the coevolutionary equilibrium. In our model coevolution leads to a stable equilibrium of species traits, $\vec{\boldsymbol{Z}}^* = (\boldsymbol{I} - \boldsymbol{Q})^{-1}\boldsymbol{\Psi}\vec{\boldsymbol{\theta}}$, where $\vec{\boldsymbol{Z}}^*$ is an N×1 vector representing species traits at equilibrium, I is the identity matrix, Q is an N×N matrix whose entries represent the direct evolutionary effects of mutualistic interactions, $\boldsymbol{\Psi}$ is an N×N diagonal matrix with diagonal entries equals $1 - m_i$ for all species *i*, and $\vec{\boldsymbol{\theta}}$ is an N×1 vector representing species environmental optima[1]. The entries of matrix $\boldsymbol{T} = (\boldsymbol{I} - \boldsymbol{Q})^{-1}\boldsymbol{\Psi}$, t_{ij}, describe the total direct and indirect contribution of species j to the evolution of species *i*. Therefore, at the coevolutionary equilibrium the T-matrix connects direct and indirect evolutionary effects to the environmental optimum of species:

$$\boldsymbol{Z}^* = \boldsymbol{T}\boldsymbol{\theta} \qquad (S20)$$

or equivalently:

$$\bar{z}_i^{\,*} = \sum_{j=1}^{N} t_{ij}\theta_j \qquad (S21)$$

Using equation (2) and (S21), we can derive and expression for the fitness of species at the coevolutionary equilibrium:

$$\overline{w_i} = e^{\frac{1}{2}\varrho_i\left[\frac{m_i}{\alpha}\ln\left(\frac{\sum_{j=1,j\neq i}^{N} a_{ij}e^{-\alpha\left(\bar{z}_j^{\,*}-\bar{z}_i^{\,*}\right)^2}}{k_i}\right)-(1-m_i)(\theta_i-\bar{z}_i^{\,*})^2\right]} \qquad (S22)$$

To make further progress in equation (S22) we make a few simplifying assumptions. First, we use a mean-field approximation and assume that $\bar{z}_j^{\,*} \cong \langle z \rangle$, so that equation (S22) simplifies to:

$$\overline{w_i}^{*} \cong e^{-\frac{1}{2}\varrho_i\left[m_i(\langle z\rangle-\bar{z}_i^{\,*})^2+(1-m_i)(\theta_i-\bar{z}_i^{\,*})^2\right]} \qquad (S23)$$

Equation (S23) shows that the fitness of species is a negative exponential function that decreases with the squared distance of the trait of species i to all mutualistic partners and to the environmental optima. Therefore, the larger the distances $m_i(\langle z \rangle - \bar{z}_i^{\,*})^2$ and $(1-m_i)(\theta_i - \bar{z}_i^{\,*})^2$, the smaller the fitness of species i after generations of coevolution. To link indirect evolutionary effects to these two distances, we substitute $\bar{z}_i^{\,*}$ with equation (S21):

$$\overline{w_i}^{*} \cong e^{-\frac{1}{2}\varrho_i\left[m_i\left(\langle z\rangle-\sum_{j=1}^{N} t_{ij}\theta_j\right)^2+(1-m_i)\left(\theta_i-\sum_{j=1}^{N} t_{ij}\theta_j\right)^2\right]} \qquad (S24)$$

The term $\sum_{j=1}^{N} t_{ij}\theta_j$ can be further disentangled as:

$$\sum_{j=1}^{N} t_{ij}\theta_j = t_{ii}\theta_i + \sum_{j=1,j\neq i}^{N} t_{ij}\theta_j \qquad (S25)$$

In the T-matrix, $\sum_{j=1}^{N} t_{ij} = 1$ so that $t_{ii} = 1 - \sum_{j=1, j\neq i}^{N} t_{ij}$. Using the mean-field assumption that $\theta_j \cong \langle\theta\rangle$, equation (S24) can be further rewritten as:

$$\overline{w_i}^{*} \cong e^{-\frac{1}{2}\varrho_i\left\{m_i\left[(\langle\theta\rangle-\theta_i)\sum_{j=1,j\neq i}^{N} t_{ij}-\theta_i+\langle z\rangle\right]^2+(1-m_i)(\theta_i-\langle\theta\rangle)^2\left(\sum_{j=1,j\neq i}^{N} t_{ij}\right)^2\right\}} \quad (S26)$$

The term $\sum_{j=1,j\neq i}^{N} t_{ij}$ corresponds to the total amount, both direct and indirect, of evolutionary effects that species i receives. Thus, we can partition $\sum_{j=1,j\neq i}^{N} t_{ij}$ into its direct and indirect components:

$$\sum_{j=1,j\neq i}^{N} t_{ij} = \sum_{j=1,j\neq i}^{N} q_{ij} + \sum_{j=1,j\neq i}^{N} f_{ij} = m_i + F_i \quad (S27)$$

where f_{ij} corresponds to the contribution of species j to the indirect evolutionary effects received by species i, and F_i is the total contribution of indirect evolutionary effects to the evolution of i. Using equation (S27) into equation (S26):

$$\overline{w_i}^{*} \cong e^{-\frac{1}{2}\varrho_i\{m_i[(\langle\theta\rangle-\theta_i)(m_i+F_i)-\theta_i+\langle z\rangle]^2+(1-m_i)(\theta_i-\theta)^2(m_i+F_i)^2\}} \quad (3)$$

Upon inspection, equation (3) shows that when $\varrho_i \neq 0$, the fitness of species is maximized when:

$$m_i[(\langle\theta\rangle-\theta_i)(m_i+F_i)-\theta_i+z]+(1-m_i)(\theta_i-\langle\theta\rangle)^2(m_i+F_i)^2=0 \quad (S28)$$

Therefore, from equation (S28) the larger the contribution of indirect evolutionary effects, i.e. F_i, the greater the distance between species i trait, the traits of mutualistic partners of i, and the environmental optimum of i. Thus, to understand the relationship between species fitness and the contribution of indirect evolutionary effects, we analytically computed species fitness through equation (3) for different values of F_i. Values for $\langle\theta\rangle$, θ_i and $\langle z\rangle$ were sampled from a normal

distribution, while the remaining parameters were kept at a fixed value, while we set $m_i = 0.5$.

4.3 Relationship between species fitness and indirect effects in numerical simulations

In the main text we reported the results of the relationship between indirect evolutionary effects and species fitness for $m_i = 0.5$. Here we show how this relationship changes from a scenario in which mutualistic selection is very weak ($m_i = 0.1$) to very strong ($m_i = 0.9$). Our results show that the relationship between indirect effects and species fitness holds except for the extremes, when $m_i = 0.1$ or $m_i = 0.9$ (Extended Data Fig. 4). The relationship breaks at these extremes because when $m_i = 0.1$, the contribution of indirect effects is almost negligible but, on the other hand, when $m_i = 0.9$ the contribution of indirect effects is very high for all species and there is little variation among species.

4.4 Evolutionary effects and core-periphery structure in mutualistic networks

We now turn our attention to which species within networks are the most affected by indirect evolutionary effects. Mutualistic, species-rich networks are often characterized by variation in patterns of interaction across species, with a few highly connected, central species and multiple poorly connected species in the periphery of the network. Mutualistic networks are species-rich, centralized

networks. Centralized networks are characterized by a core-periphery structure in which core species are highly connected species that interact with both other highly connected species and with peripheral, poorly connected species[18]. In contrast, poorly connected species do not usually interact with each other. Therefore, it is likely that the contribution of indirect evolutionary effects changes for species that occupy either the core or the periphery of the network. Here, we tested this prediction combining an analytical approximation for the most centralized type of network – a star network – with numerical simulations parameterized with empirical networks.

4.5 Analytical approximation linking indirect evolutionary effects to the core-periphery structure of networks

We first study the relationship between network structure and the contribution of indirect evolutionary effects. As we previously discussed, we can calculate the total amount of evolutionary effects that a given species receives from the network using the diagonal entries of the T-matrix, t_{ii}, such that:

$$1 - t_{ii} = \sum_{j=1, j\neq i}^{N} t_{ij} \qquad (S29)$$

where $\sum_{j=1,j\neq i}^{N} t_{ij}$ corresponds to the total amount of evolutionary effects that species receive from all others in the network.

In the T-matrix, t_{ii} corresponds to feedback cycles of evolutionary effects that return to species *i*. Because most mutualistic networks are two-mode networks described by bipartite graphs, only even pathways contribute to feedback cycles and therefore for a network with N species:

$$t_{ii} = (1-m)\left[q_{ii}^0 + \sum_j^N q_{ij}^t q_{ji}^t + \sum_j^N \sum_l^N \sum_k^N q_{ij}^t q_{jl}^t q_{lk}^t q_{ki}^t + \cdots\right] \qquad (S30)$$

To explore if central and peripheral species vary in their evolutionary effects, we first use a mean-field approximation in which we assume that $m_i = m$ for any given species *i* and that we can approximate the interaction strength q_{ij}^t by:

$$q_{ij}^t \cong a_{ij}\,\frac{m}{k_i} \qquad (S31)$$

in which m is the strength of mutualistic selection and k_i is the number of partners of species *i*. We study the simplest and the centralized core-periphery network, a star network. In a star network, there is a single core species (the hub) that interacts with *N-1* species and there are N peripheral species that interact directly only with the hub. By combining equations (S30) and (S31) we have the feedback cycles for central species *i* and peripheral species *j*, respectively:

$$t_{ii}^{(C)} = (1-m)\left[1 + \sum_j^N a_{ij}a_{ji}\frac{m^2}{(N-1)} + \sum_j^N \sum_k^N a_{ij}a_{ji}a_{ik}a_{ki}\frac{m^4}{(N-1)^2} + \cdots\right] \qquad (S32.1)$$

$$t_{jj}^{(P)} = (1-m)\left[1 + a_{ji}a_{ij}\frac{m^2}{(N-1)} + \sum_k^N a_{ji}a_{ij}a_{jk}a_{kj}\frac{m^4}{(N-1)^2} + \cdots\right] \qquad (S32.2)$$

$$t_{ii}^{(C)} = (1-m)\left[1 + \frac{m^2}{(N-1)}(N-1) + \frac{m^4}{(N-1)^2}(N-1)^2 + \cdots\right] \qquad (S32.3)$$

$$t_{jj}^{(P)} = (1-m)\left[1 + \frac{m^2}{(N-1)} + \frac{m^4}{(N-1)^2}(N-1) + \cdots\right] \qquad (S32.4)$$

$$t_{ii}^{(C)} = (1-m)(m^0 + m^2 + m^4 + \cdots) = (1-m)\sum_{\ell=0}^{\infty} m^{2\ell} = \frac{1-m}{1-m^2} \qquad (S32.5)$$

$$t_{jj}^{(P)} = (1-m)\left(1 + \frac{m^2}{N-1} + \frac{m^4}{N-1} + \cdots\right) \qquad (S32.6)$$

$$t_{jj}^{(P)} = (1-m)\left(1 + \frac{1}{N-1}\sum_{\ell=1}^{\infty} m^{2\ell}\right) = (1-m) + \frac{(1-m)m^2}{(N-1)(1-m^2)} \qquad (S32.7)$$

Thus, the core species generates higher feedback cycles than peripheral species. Using equation (S29), (S32.5) and (S32.7):

$$u_i^{(C)} = 1 - t_{ii}^{(C)} = 1 - \frac{1-m}{1-m^2} = 1 - \left(\frac{1}{1+m}\right) \qquad (S33)$$

$$u_j^{(P)} = 1 - t_{jj}^{(P)} = 1 - \left[(1-m) + \frac{(1-m)m^2}{(N-1)(1-m^2)}\right] = m - \left[\frac{m^2}{(N-1)(1+m)}\right] \qquad (S34)$$

where $u_i^{(C)}$ and $u_j^{(P)}$ are the total amount of evolutionary effects received by the core and peripheral species, respectively. Since in our coevolutionary model species with the same number of partners receive the same total amount of direct evolutionary effects, $\sum_{j=1}^{N} q_{ij} = m$, any increase in the total amount of evolutionary effects that species receive comes from indirect evolutionary effects. Thus, upon inspection, equations (S33) and (S34) show that as the number of species in the star network increases, peripheral species receive more indirect evolutionary effects. In fact, as long as $N \geq 3$, peripheral species receive more indirect evolutionary effects than core species do. Furthermore, the larger the size of the star network, the larger the amount of indirect evolutionary effects that peripheral species receive, while indirect evolutionary effects are independent of network size for core species.

4.6 Indirect evolutionary effects and the core-periphery structure of empirical networks

We tested the predictions of our analytical approximation by performing numerical simulations with the set of empirical networks used in the main text. First, we classified the species of each empirical network that we used for our numerical simulations (n=186 networks) into "core" species or "peripheral" species. We classified a species *i* as a "core" species if $\sum_{j=1}^{N} a_{ij} > \frac{1}{N}\sum_{i=1}^{N}\sum_{j=1}^{N} a_{ij}$, where $a_{ij} = 1$ if species *i* interact with another species j and $a_{ij} = 0$ otherwise; and N is equal to the number of plant or animal species if *i* is a plant species or an animal species, respectively. Next, we used the results of our numerical simulations to understand how the contribution of indirect evolutionary effects changes between species that occupy the core or the periphery of networks. Since the overall contribution of indirect evolutionary effects can also change across networks, we controlled for potential differences driven by network structure using the leading eigenvalue of the network's adjacency matrix. We used the leading eigenvalue because previous work showed that it increases with the size of the network and is closely related to indirect evolutionary effects via the proliferation of pathways in the network[1,19].

The result from the numerical simulations agrees with our analytical predictions: independently of the value of mutualistic selection, within the same network, core species received a smaller amount of indirect evolutionary effects than peripheral

406 species (Extended Data Fig. 5). However, the contribution of indirect evolutionary
407 effects also changes across networks, such that a core species coevolving in one
408 network can receive a larger amount of indirect evolutionary effects than a
409 peripheral species coevolving in a different network. Therefore, the contribution of
410 indirect evolutionary effects depends on the interaction between the species position
411 within network and whether the overall network structure favors or hinders indirect
412 evolutionary effects.

413 *4.7 Numerical simulations for the invasion of a supergeneralist in networks*

414 On the main text we reported the results for the numerical simulations when $m_i =$
415 0.5. Here we report the results for different values of m_i. Our supplementary
416 analysis shows that the results reported in the main text hold for different values
417 of m_i (Extended Data Fig. 7-9). Independent of the value of m_i, the fitness of most
418 of the species that did not interact with *A. mellifera* decreased after the invasion,
419 while for species that directly interacted with *A. mellifera,* fitness increased
420 (Extended Data Fig. 7). This effect is just related to the increase (+1) in the
421 number of partners (i.e., direct effects). Furthermore, the change in indirect
422 evolutionary effects caused by the invasion also predicted changes in species fitness,
423 both for species that directly interacted with *A. mellifera* (Extended Data Fig. 8)
424 and for species that did not directly interact with *A. mellifera* (Extended Data Fig.
425 9).

4.8 Numerical simulations for the invasion of A. mellifera in an empirical network with rewiring of interactions

In the main text, we evaluated how coevolution with an introduced supergeneralist shapes species fitness by parameterizing our numerical simulations with the structure of 73 empirical networks within which *A. mellifera* is a known invader (Supplementary Table 2). However, in these simulations we assumed that the only change between the *pre-* and *post- A. mellifera* invasion networks was the inclusion of *A. mellifera* itself. Thus, in these simulations we neglect the possibility that species rewire their interactions after the invasion of *A. mellifera* in the network, but also the loss of native partners by resource competition.

Here, we performed a complementary set of simulations using an empirical dataset where the mutualistic networks before and after the arrival *A. mellifera* are available[20]. We performed 1000 numerical simulations in which we first allowed species to coevolve until traits reached asymptotic values for the empirical *pre-Apis* network (Extended Data Fig. 10a). Then, we changed the structure of the network to the *Apis* network (Extended Data Fig. 10b), allowed traits to reach asymptotic values, and evaluated how species fitness and the contribution of indirect evolutionary effects changed between the *pre-Apis* and *Apis-* scenarios. However, since in this empirical dataset there are species that are disconnected (e.g., functionally extinct) from the network after the invasion by *A. mellifera*, we only

446 quantified the coevolutionary effects of the invasion for species that are present
447 both in the *pre-* and *Apis-* networks.
448 Our results show that most of the species lose mutualistic partners after the
449 invasion (Extended Data Fig. 10c). As a consequence, the fitness of most species
450 decreases after the invasion (Extended Data Fig. 10d) because *A. mellifera* not only
451 reorganizes indirect evolutionary effects, but also reduces the number of mutualistic
452 partners via the rewiring of interactions and the functional extinction of other
453 species in the network (Extended Data Fig. 10e). Therefore, our results suggests
454 that if species are not able to retain mutualistic partners after the invasion by a
455 supergeneralist, fitness decreases after generations of coevolution. This result
456 translates well to the empirical data, in which native species show consistent
457 reductions in fitness estimators (e.g., seed set and seed mass) for individual plants
458 of different species when facing the consequences of *A. mellifera* invasion. However,
459 the availability of empirical data to test that in other systems is currently limited,
460 and we are aware of only two other studies that simultaneously measured network
461 structure and estimate the fitness of species[21,22]. In fact, the results of these studies
462 also match our model predictions that core species should have a higher fitness than
463 peripheral ones, but it remains empirically untested whether these differences in
464 fitness are a result of coevolution. Thus, we believe that our study will motivate
465 and facilitate future work to explicitly test our model predictions on how
466 coevolution in networks and indirect effects shape species fitness.

5 References

1. Guimarães, P. R., Pires, M. M., Jordano, P., Bascompte, J. & Thompson, J. N. Indirect effects drive coevolution in mutualistic networks. *Nature* **550**, 511–514 (2017).

2. Rice, S. *Evolutionary Theory: Mathematical and Conceptual Foundations*. (Sinauer Associates, 2004).

3. Lande, R. A quantitative genetic theory of life history evolution. *Ecology* **63**, 607–615 (1982).

4. Katz, L. A new status index derived from sociometric analysis. *Psychometrika* **18**, 39–43 (1953).

5. Johnson, C. A. & Bronstein, J. L. Coexistence and competitive exclusion in mutualism. *Ecology* **100**, e02708 (2019).

6. Ferriere, R., Bronstein, J. L., Rinaldi, S., Law, R. & Gauduchon, M. Cheating and the evolutionary stability of mutualisms. *Proc. Biol. Sci.* **269**, 773–780 (2002).

7. Ghazoul, J. Floral diversity and the facilitation of pollination. *J. Ecol.* **94**, 295–304 (2006).

8. Jones, E. I., Bronstein, J. L. & Ferrière, R. The fundamental role of competition in the ecology and evolution of mutualisms. *Ann. N. Y. Acad. Sci.* **1256**, 66–88 (2012).

9. Schmitt, R. J. & Holbrook, S. J. Mutualism can mediate competition and promote coexistence. *Ecol. Lett.* **6**, 898–902 (2003).

10. Nuismer, S. *Introduction to Coevolutionary Theory*. (W. H. Freeman, 2017).

11. Walsh, B. & Lynch, M. *Evolution and Selection of Quantitative Traits*. (Oxford University Press, 2018).

12. Nuismer, S. L., Week, B. & Aizen, M. A. Coevolution slows the disassembly of mutualistic networks. *Am. Nat.* **192**, 490–502 (2018).

13. Bastolla, U. *et al.* The architecture of mutualistic networks minimizes competition and increases biodiversity. *Nature* **458**, 1018–1020 (2009).

14. Bascompte, J. & Scheffer, M. The resilience of plant-pollinator networks. *Annu. Rev. Entomol.* (2022).

15. Rohr, R. P., Saavedra, S. & Bascompte, J. Ecological networks. On the structural stability of mutualistic systems. *Science* **345**, 1253497 (2014).

16. Bascompte, J., Jordano, P. & Olesen, J. M. Asymmetric coevolutionary networks facilitate biodiversity maintenance. *Science* **312**, 431–433 (2006).

17. Pires, M. M. *et al.* The indirect paths to cascading effects of extinctions in mutualistic networks. *Ecology* **101**, e03080 (2020).

18. Bascompte, J., Jordano, P., Melián, C. J. & Olesen, J. M. The nested assembly of plant-animal mutualistic networks. *Proc. Natl. Acad. Sci. U. S. A.* **100**, 9383–9387 (2003).

19. Borrett, S. R., Fath, B. D. & Patten, B. C. Functional integration of ecological networks through pathway proliferation. *J. Theor. Biol.* **245**, 98–111 (2007).

20. Valido, A., Rodríguez-Rodríguez, M. C. & Jordano, P. Honeybees disrupt the structure and functionality of plant-pollinator networks. *Sci. Rep.* **9**, 4711 (2019).

21. Lázaro, A., Gómez-Martínez, C., Alomar, D., González-Estévez, M. A. & Traveset, A. Linking species-level network metrics to flower traits and plant fitness. *J. Ecol.* 1–12 (2019).

22. Bergamo, P. J., Traveset, A. & Lázaro, A. Pollinator-mediated indirect effects on plant fecundity revealed by network indices. *Am. Nat.* **198**, 734–749 (2021).

Capítulo 2

Mutualistic coevolution and community diversity favour persistence in metacommunities under environmental changes

PROCEEDINGS B

royalsocietypublishing.org/journal/rspb

Research

Cite this article: Cosmo LG, Sales LP, Guimarães Jr PR, Pires MM. 2023 Mutualistic coevolution and community diversity favour persistence in metacommunities under environmental changes. *Proc. R. Soc. B* **290**: 20221909.
https://doi.org/10.1098/rspb.2022.1909

Received: 22 September 2022
Accepted: 2 December 2022

Subject Category:
Ecology

Subject Areas:
ecology, evolution, theoretical biology

Keywords:
metacommunity, mutualistic interactions, mutualistic networks, coevolution, environmental changes

Author for correspondence:
Leandro G. Cosmo
e-mail: lgcosmo@usp.br

Electronic supplementary material is available online at https://doi.org/10.6084/m9.figshare.c.6350191.

THE ROYAL SOCIETY PUBLISHING

Mutualistic coevolution and community diversity favour persistence in metacommunities under environmental changes

Leandro G. Cosmo[1], Lilian P. Sales[3,4], Paulo R. Guimarães Jr[2] and Mathias M. Pires[3]

[1]Programa de Pós-Graduação em Ecologia, Departamento de Ecologia, Instituto de Biociências, Universidade de São Paulo - USP, São Paulo, SP, Brazil
[2]Departamento de Ecologia, Instituto de Biociências, Universidade de São Paulo - USP, São Paulo, SP, Brazil
[3]Departamento de Biologia Animal, Instituto de Biologia, Universidade Estadual de Campinas - UNICAMP, Campinas, SP, Brazil
[4]Biology Department, Faculty of Arts and Science, Concordia University, Montreal, Canada

LGC, 0000-0003-2541-2645

Linking local to regional ecological and evolutionary processes is key to understand the response of Earth's biodiversity to environmental changes. Here we integrate evolution and mutualistic coevolution in a model of metacommunity dynamics and use numerical simulations to understand how coevolution can shape species distribution and persistence in landscapes varying in space and time. Our simulations show that coevolution and species richness can synergistically shape distribution patterns by increasing colonization and reducing extinction of populations in metacommunities. Although conflicting selective pressures emerging from mutualisms may increase mismatches with the local environment and the rate of local extinctions, coevolution increases trait matching among mutualists at the landscape scale, counteracting local maladaptation and favouring colonization and range expansions. Our results show that by facilitating colonization, coevolution can also buffer the effects of environmental changes, preventing species extinctions and the collapse of metacommunities. Our findings reveal the mechanisms whereby coevolution can favour persistence under environmental changes and highlight that these positive effects are greater in more diverse systems that retain landscape connectivity.

1. Introduction

Species are subjected to natural spatio-temporal variation in environmental conditions, but to persist in a changing environment a species may need to track suitable environment by colonizing novel sites or quickly adapt to novel local conditions [1–4]. Colonization success and adaptation are not fully determined by the abiotic environment but modulated by the multiple ecological interactions species establish in local ecological communities. Mutualisms, for instance, can increase dispersal potential [5] as well as allow species to expand their realized niches by increasing environmental suitability under unfavourable conditions [6]. Ecological interactions may also give rise to coevolutionary dynamics when species exert reciprocal selective pressures on each other [7–10]. Evolution in response to the physical environment and coevolutionary outcomes emerging from interactions may either converge, accelerating local adaptation, or diverge, generating conflicting dynamics [11–13]. The interplay between evolution and coevolution might, therefore, shape the response of biodiversity to changing environments [14]. How evolution in response to environmental and biotic pressures shape biodiversity patterns is a pressing question in the context of the global anthropogenic changes and the rise of novel biotas [15–20].

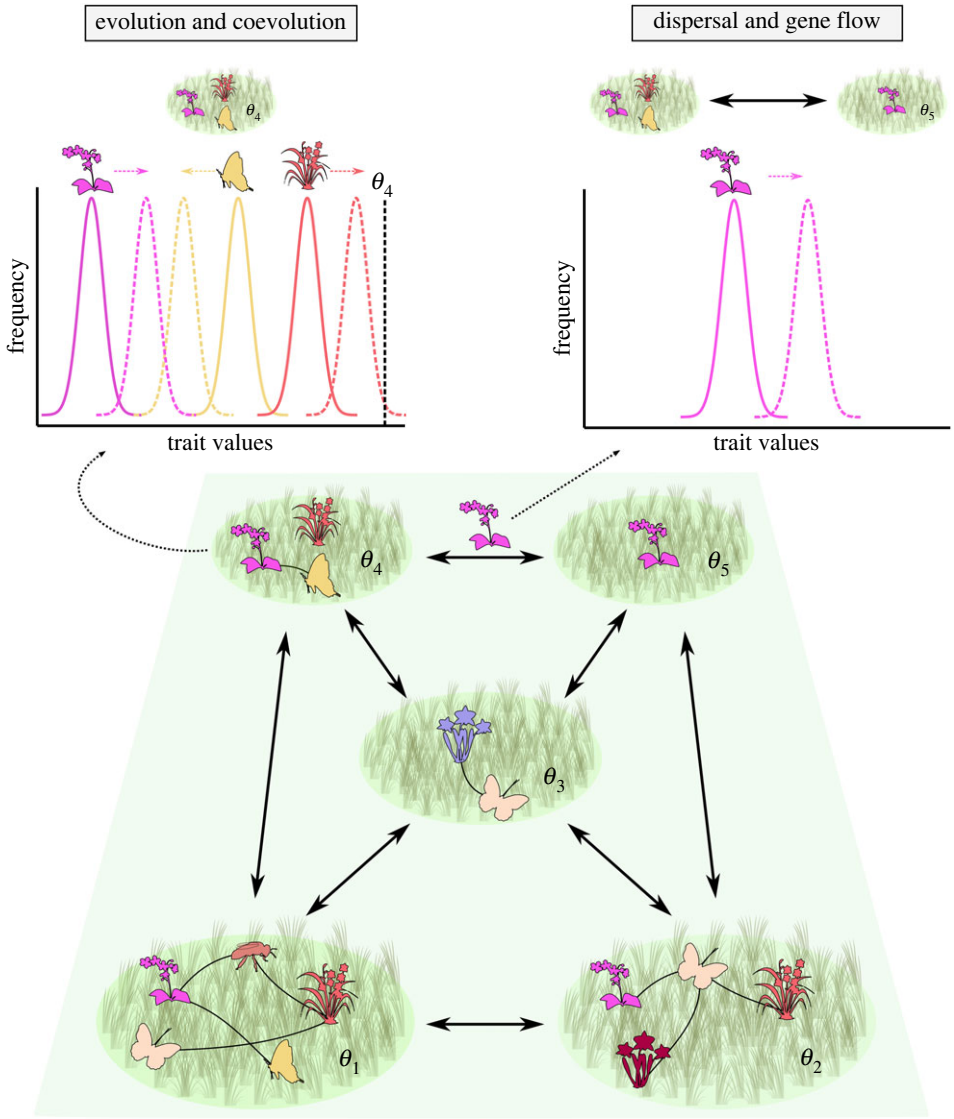

Figure 1. Representation of coevolving mutualists in a metacommunity. Within local patches, populations of different species (here indicated as coloured silhouettes) are subjected to different selective pressures imposed by local the environment (θ). In addition, species within local communities interact forming networks with varying configurations (interactions are depicted as solid lines connecting silhouettes within patches). While species-species interactions promote coevolution, traits also evolve in response to the selective pressures of the local environment (as represented in the upper panels). Trait evolution is depicted in the upper left panels as the change in the mean value of traits from the current generation (solid lines) to the next generation (dashed lines). At the regional scale, local populations can colonize other patches or become locally extinct, reshaping the distribution of genotypes and phenotypes in the metacommunity (from the solid to the dashed lines in the upper right panel). Under this framework, the colonization dynamics connects the local effects of evolution and coevolution to other patches in the metacommunity.

Empirical and theoretical studies have shed light on the consequences of mutualistic coevolution for interacting species [10,21,22]. Coevolution between mutualistic pairs favours the complementarity of traits, for instance, when the mouth parts of a pollinating insect matches the floral tube of a plant [23]. In this context, trait complementarity may increase the overall survival and reproduction of mutualistic partners, but it may also lead to highly specialized and intimate interactions in which the loss of a mutualistic partner highly increases the risk of co-extinctions [24–26]. Progressing to species-rich communities, theory predicts that coevolution can increase the similarity of traits among all mutualists resulting in evolutionary convergence [27–30]. In a changing environment, trait similarity may prevent co-extinctions because convergence increases functional redundancy, allowing mutualists to compensate for the extinction of partners through rewiring [31,32]. Thus, pairwise and multispecies coevolution may lead to different outcomes: from an increased risk of coextinction to the coevolutionary rescue of ecological functions from environmental changes.

When considering larger spatial scales, however, the outcome of coevolution may further depend on how populations of the same species are distributed and connected through gene flow across space [10]. Spatial heterogeneity may impose different local evolutionary regimes, but colonization dynamics may alter the distribution of genotypes and phenotypes of populations across space, which feeds back and affects local evolutionary and coevolutionary dynamics [33–38] (figure 1). For instance, variation in mutualistic selection across space can create geographical mosaics of adaptation [39–44]. By contrast, when two species-rich, local communities are linked by gene flow, mutualistic coevolution increases the convergence and matching of traits among all species of the two local communities [45]. While the effects of spatial processes on coevolution are starting to be unravelled [39,41,42,45,46], we still know little about how coevolution can affect distribution patterns in a

heterogeneous environment or whether coevolution favours or hinders persistence across space under environmental changes.

Here, we use numerical simulations to investigate how patterns of adaptation and coadaptation in two-species and multispecific scenarios affect patterns of population persistence in heterogeneous and changing environments. To do so, we developed a spatially explicit framework of a coevolving metacommunity by combining a mathematical model of evolution (in response to environmental selection) and coevolution (in response to mutualistic interactions) with colonization and extinction dynamics. Specifically, we explored the following questions: (1) how does coevolution in species-rich communities affects patterns of colonization, extinctions and the persistence of populations at the metacommunity scale? (2) How does coevolution in species-rich communities affect the persistence of local populations and species under environmental changes? The results of our numerical simulations show that mutualistic coevolution and species richness synergistically drive patterns of occupancy, colonization, extinction and trait matching in metacommunities. Furthermore, we show that coevolution can buffer negative effects of environmental changes, preventing the extinction of species and the collapse of metacommunities, especially in species-rich systems.

2. Methods

(a) Model description

We developed a spatially explicit metacommunity modelling framework that combines a coevolutionary model with colonization and extinction dynamics in a cellular automaton representing an ecological metacommunity where populations of S species can occur within any of K patches. Our model builds upon previous models of mutualisms in metacommunities [47–49]. However, instead of assuming fixed colonization and rates, we explicitly link these rates to the mean trait values of populations via a patch suitability function. We motivate our model using plant–insect mutualisms such as those between plants and insect pollinators. However, our overall framework can also be applied to other mutualistic interactions mediated by a trait matching mechanism, for instance, birds that disperse seeds [50]. For simplicity, we assumed that of the total pool of S species there are S/2 plants and S/2 animals in the metacommunity. The populations of plants and animals are assumed to be sufficiently large so that each one can be described by the mean trait value, z, of its individuals. Furthermore, we assumed that at each patch K there is a different environmental optimum for each species i, which can be summarized by a single value, θ_{ik}. Biologically this value can be interpreted as an average value of all the environmental factors in a patch that significantly affect the fitness of species i, for instance, linear combinations of variables related to temperature and precipitation. We initially assumed that the local environmental optimum of each species i at each patch k, θ_{ik}, did not vary over time (figure 1). By doing so, we simulated a heterogeneous but constant adaptive landscape where each local population is subjected to selective forces from the environment and from the local mutualistic partners. Later, we evaluated the effect of environmental change on emerging patterns of coevolution, colonization and extinction at the metacommunity level by varying the local environmental optima of species over time.

Each of these K patches can be occupied by one population of each species. When populations of plants and animals co-occur, they may interact and exert selective pressures on each other. Because functional mutualistic interactions often depend on the matching of the traits of the interacting individuals [26] (e.g. when the mouth part of an insect pollinator matches the floral tube of a plant), we modelled the probability of successful interactions as a trait matching rule:

$$p(a_{ijk}^{(t)} = 1) = \mathrm{e}^{-\alpha(z_{jk}^{(t)} - z_{ik}^{(t)})^2}, \tag{2.1}$$

in which $p(a_{ijk}^{(t)} = 1)$ is the probability of a successful interaction between individuals of co-occurring populations of species i and j in patch k, and α is a parameter that controls how sensitive $p_{ijk}^{(t)}$ is to differences between the trait values of species i, $z_{ik}^{(t)}$, and species j, $z_{jk}^{(t)}$.

At each time step of our model four events occur. First, at each patch k a local interaction network is formed by the local pairwise interactions according to equation (2.1). Second, the populations of each species evolve (see below) in response to the selective pressures of the environment and, when they interact, coevolve in response to their mutualistic partner's traits. Third, following evolution and coevolution, these populations can colonize adjacent patches. Finally, after all populations had the opportunity to colonize adjacent patches, local populations may become extinct depending on the local species-specific patch suitability.

(b) Evolution and coevolution

In our model, mutualistic interactions are a function of the trait matching between populations of different species and may change as populations evolve. As a consequence, at each time step of the model these interactions can give rise to distinct local interaction networks. To model evolution and coevolution, we adapted a model of coevolution in mutualistic networks [51] to our framework. This coevolutionary model is grounded on quantitative genetics [52] and connects the evolution of species' traits to the mean fitness consequences of mutualistic interactions and other selective pressures in the environment. For a given population of species i, in patch k, the change in the mean trait value z_{ik} from one generation to the next is given by:

$$z_{ik}^{(t+1)} = z_{ik}^{(t)} + \sigma^2_{Gz_{ik}} \frac{\partial \ln(\overline{w_{ik}})}{\partial z_{ik}^{(t)}}, \tag{2.2}$$

where $\sigma^2_{Gz_{ik}}$ is the additive genetic variance of traitz_i at patch k and the selection gradient, $\partial \ln(\overline{w_{ik}})/\partial z_{ik}^{(t)}$ describes how a change in the mean value of z_{ik} affects the mean fitness, $\overline{w_{ik}}$ of population i. We assumed that mutualistic interactions contribute with a proportion m_{ik} to the selection gradient, while other selective pressures in the environment contributes with $1 - m_{ik}$. Hence, the higher the value of m_{ik}, the stronger the effects of mutualistic interactions on the mean fitness of populations and therefore, on trait evolution when compared to other selective pressures in the environment. Because of the dependence of some mutualisms on trait complementarity [28,53], we assumed that the selection gradient favours complementarity with the traits of co-occurring mutualistic partners (z_{jk}) and with other selective pressures of the environment in patch k (θ_k):

$$z_{ik}^{(t+1)} = z_{ik}^{(t)} + \sigma^2_{Gz_{ik}} \varrho_{ik} \left[m_{ik} \sum_{j=1, j\neq i}^{S} q_{ijk}^{(t)} (z_{jk}^{(t)} - z_{ik}^{(t)}) + (1 - m_{ik})(\theta_{ik} - z_{ik}^{(t)}) \right]. \tag{2.3}$$

The parameter ϱ_{ik} controls the sensitivity of species fitness to the function that defines the selection gradient, i.e. the terms within the brackets. These terms within brackets correspond to the fitness effects of trait matching with mutualistic partners and the fitness effects of trait matching with the environment, respectively. We defined $q_{ijk}^{(t)}$ as the importance of a given mutualistic partner j for species i at time t and at patch k and assumed that $q_{ijk}^{(t)}$, depends on a trait matching rule relative to all mutualistic partners:

$$q_{ijk}^{(t)} = m_{ik} \frac{a_{ijk}^{(t)} \mathrm{e}^{-\alpha(z_{jk}^{(t)} - z_{ik}^{(t)})^2}}{\sum_{j=1, j\neq i}^{S} a_{ijk}^{(t)} \mathrm{e}^{-\alpha(z_{jk}^{(t)} - z_{ik}^{(t)})^2}}. \tag{2.4}$$

Furthermore, we assume that if $\sum_{j=1,j\neq i}^{S} a_{ijk}^{(t)} = 0$, i.e. at a given time step, species i does not interact with any mutualist at patch k, then $m_{ik} = 0$ and all the evolution of trait $z_{ik}^{(t)}$ occurs only in response to the environment θ_{ik}:

$$z_{ik}^{(t+1)} = z_{ik}^{(t)} + \sigma^2_{Gz_{ik}} \varrho_{ik}(\theta_{ik} - z_{ik}^{(t)}). \tag{2.5}$$

Because some of the parameters used in the model such as m_{ik} and ϱ_{ik}, are hard to estimate, especially in a multispecific context, we could not parameterize the model based on empirical systems. Thus, we explore a wide range of variation in those parameters in our analyses to understand whether our results are robust to parameter choice (see below).

(c) Patch suitability, colonization and extinction

Following evolution and coevolution, at each time step, species can colonize empty adjacent patches depending on how suitable the patch is to the colonizing species. Thus, similar to what is observed in empirical systems, the abiotic and biotic features filter whether or not colonization of adjacent patches will be successful [54–56]. To simplify species-environment relationships, we assumed that the suitability of patch k for species i, γ_{ik}, depends exclusively on the mean trait complementarity with mutualistic partners and the trait complementarity with the environment, according to:

$$\gamma_{ik}^{(t)} = e^{-\varrho_{ik}\left[m_{ik}\left(\sum_{j=1,j\neq i}^{S} a_{ijk}^{(t)}\left(z_{jk}^{(t)} - z_{ik}^{(t)}\right)^2 / \sum_{j=1,j\neq i}^{S} a_{ijk}^{(t)}\right) + (1-m_{ik})\left(\theta_{ik} - z_{ik}^{(t)}\right)^2\right]}. \tag{2.6}$$

Thus, $0 < \gamma_{ik}^{(t)} \leq 1$ and assumes its maximum value ($\gamma_{ik}^{(t)} = 1$) only when traits perfectly match the traits of all mutualistic partners and the environmental optimum. Furthermore, in equation (2.6) suitability increases only if species traits match both mutualistic partners traits and the local environmental optimum. Because we only model facultative mutualisms, if a patch k does not hold any mutualistic partner (i.e. $\sum_{j=1,j\neq i}^{S} a_{ijk}^{(t)} = 0$), we set $m_{ik} = 0$ and assumed that the suitability of the patch k is solely determined by the trait complementarity with the environment:

$$\gamma_{ik}^{(t)} = e^{-\varrho_{ik}\left(\theta_{ik} - z_{ik}^{(t)}\right)^2}. \tag{2.7}$$

In the colonization events, each species in each patch can colonize empty patches among any of the other eight adjacent patches with periodic boundary conditions (i.e. the Moore neighbourhood in a cellular automata). We assume that the probability of success of each colonization event is equal to the suitability of each k adjacent patch, $s_{ik}^{(t)}$. When a colonization event is successful, if the patch that receives dispersers is already occupied by another population of the same species, then there is gene flow among the dispersing and resident populations. For simplicity, we assume that following dispersal the new mean trait value of a population of a given species is comprised of a fraction of 0.95 of the resident population trait value and another 0.05 fraction averaged over the trait values of all other successfully dispersing populations of that species. If the patch is not already occupied by a population of the same species, it is then occupied with a trait value composed of the average trait values of all successfully dispersing populations. We also explored situations in which the contribution of gene flow is larger than 0.05 (from 0.1 to 0.5 in 0.1 steps), which yielded similar qualitative results (electronic supplementary material, Information).

Besides affecting colonization, we assume suitability also determines population persistence. We assumed that the extinction of a given population of species i that occurs in patch k depends on the suitability of the occupied patch for that species and occurs with probability $1 - \gamma_{ik}^{(t)}$. Thus, we modelled both the colonization of adjacent patches and extinction of populations as probabilistic events that depend on the suitability of patches. A given population will be more likely to colonize patches with greater suitability and undergo extinction in those patches where suitability is low or has become lower over time. Although we are specifically interested in colonization/extinction dynamics, we implicitly model demographic effects because fitness vary across time and space and environmental suitability affects local population density [57].

(d) Numerical simulations

We performed numerical simulations of our model using the Julia programming language v. 1.5.3 [58]. In these simulations we explored how different levels of strength of mutualistic interactions ($m_{ik} = 0.0 - 0.9$), species richness (2, 4, 8, 16 and 32 species) and spatial and temporal variation in the environment affected patterns of distribution of traits and populations in the metacommunity. For simplicity, we initially fixed the relative importance of mutualisms, m_{ik}, to be the same for all species in all patches in each simulation.

We ran 100 simulations per combination of value of m_{ik}, species pool and environmental conditions (fixed versus changing environment). At the beginning of each simulation, we sampled the values of the environmental optimum (θ_{ik}) and initial trait values from a uniform distribution U [0, 10]. To avoid situations in which all populations of a given species become extinct at the beginning of the simulation, the initial number of populations for all species were fixed as $\sqrt{K}$. For convenience we fixed the number of patches K to 100 (hence the initial number of populations of each species to 10). All simulations ran for 1200 time steps, which was enough for species traits in all patches to achieve quasi-equilibrium values.

To test how coevolution can modulate the response to environmental changes, we performed simulations while assuming directional changes on the environmental optima of each patch. We simulate environmental change by incrementing the values of the environmental optimum (θ_{ik}) by 0.25 at the end of each time step. In these simulations, all the remaining parameters of the model were held fixed and were the same for all populations/species ($\sigma^2_{Gz_{ik}} = 1.0$, $\varrho_{ik} = 0.1$, $\alpha = 0.1$). Since the strength of mutualistic interactions can also vary across space [10], we also performed an additional set of simulations in which we allowed m_{ik} to vary among patches (electronic supplementary material, Information). Varying m_{ik} across the space from neutral ($m_{ik} = 0$) to strong ($m_{ik} = 1.0$) allowed us to test how a geographical mosaic of coevolution can affect species response to environmental changes. Furthermore, we also explored the sensitivity of our model to different parameter values (increasing ϱ_{ik} in 10% steps up to a 50% increase, from 0.1 to 0.15) which yielded equivalent results (electronic supplementary material, Information).

At the end of each simulation, we measured six state variables. All variables were averaged across all time steps and species. We measured: (1) the trait matching (calculated via equation (2.1)) of species with mutualistic partners at local patches averaged over all partners; (2) the average trait matching between all possible pairs of species in the entire metacommunity (hereinafter called regional trait matching); (3) patch occupancy, defined as the proportion of patches occupied by populations of a given species; (4) the fraction of successful colonization events, defined as the proportion of successful colonization attempts in subsequent time steps; (5) the fraction of populations' extinctions, defined as the proportion of all populations that went extinct in subsequent time steps; and (6) the fraction of the total regional pool of surviving species at the end of simulations.

3. Results

(a) Coevolution and species richness shapes colonization and extinction dynamics

We first performed simulations of our model in a scenario in which the environment is heterogeneous but static over time.

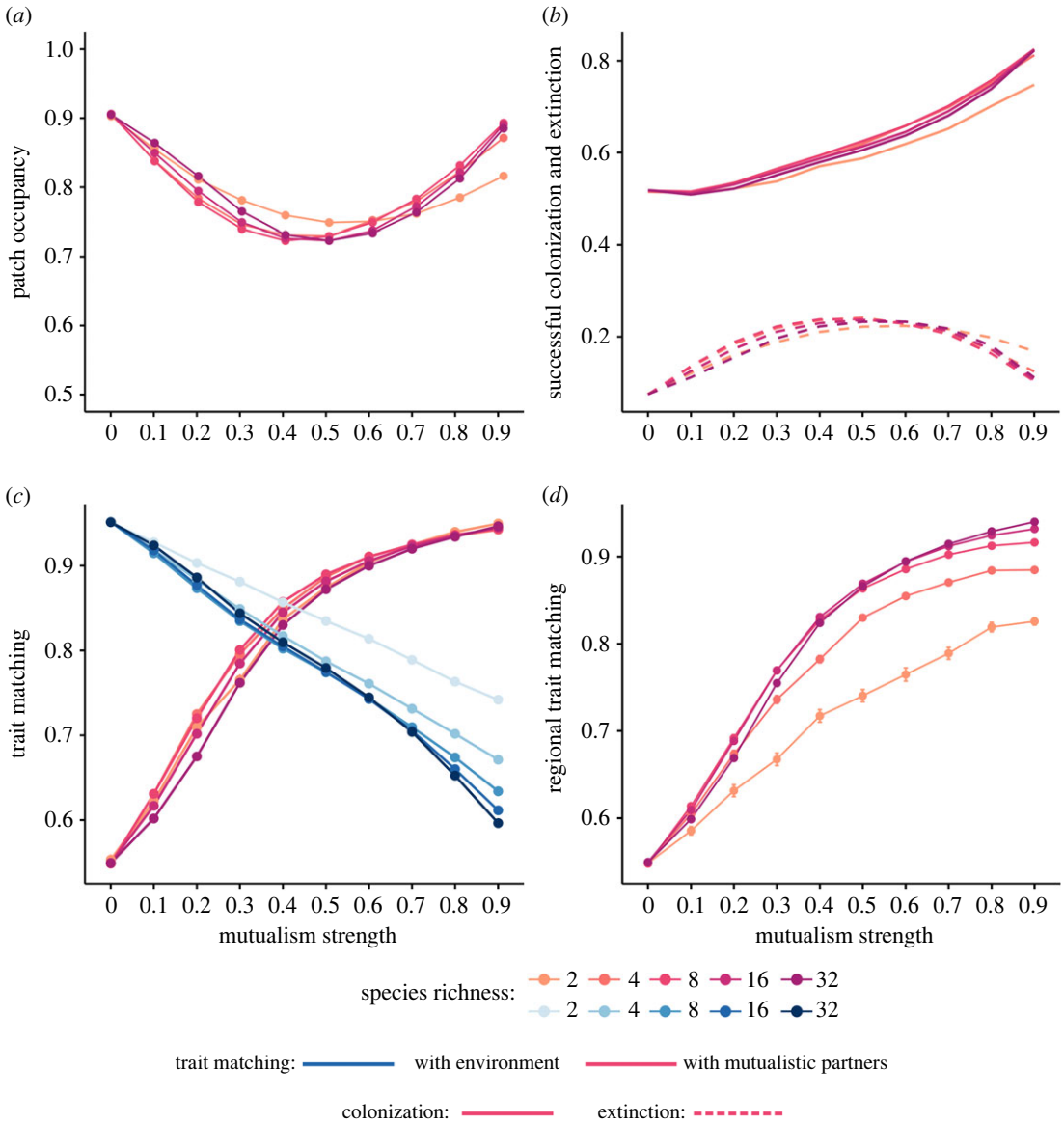

Figure 2. Mutualistic coevolution shapes patterns of (*a*) occupancy, (*b*) colonization and extinction and (*c*,*d*) trait matching in metacommunities. In (*b*), solid lines represent the rate of colonization and dashed lines the rate of extinction of populations. On panel (*c*), green lines and points represent the local trait matching of populations with the environment, while red lines the local trait matching with mutualistic partners. Points represents the mean value for 100 simulations and bars 95% confidence intervals. Parameter values are as follows: $m_{ik} = 0.0 - 0.9$, $\sigma^2_{Gz_{ik}} = 1.0$, $\varrho_{ik} = 0.1$, $\alpha = 0.1$.

Our simulations show that under this scenario, multispecific coevolution has nonlinear effects on metacommunity dynamics. Up to moderate levels of mutualism strength ($m_{ik} = 0.1$–0.5), coevolution decreases patch occupancy (figure 2*a*). However, as m_{ik} increases further, patch occupancy goes back to the same levels as the scenario without coevolution ($m_{ik} =$ 0, figure 2*a*). Such changes in patch occupancy occur because at low levels of m, mutualistic coevolution simultaneously increases the rate of successful colonization and the rate of local extinctions (figure 2*b*). The rates of colonization and extinction are further modulated by species richness such that for the same levels of m_{ik} higher species richness in the metacommunity increased the rate of colonization relative to the rate of local extinction (figure 2*b*). The effects of coevolution on colonization and extinction rates result from how coevolution shapes patterns of local and regional trait matching in the metacommunity (figure 2*c*,*d*). As m_{ik} increases, the conflicting selective pressure from mutualisms decreases the local trait matching of populations with the environment, increasing local extinctions (figure 2*c*). However, at high m, trait matching with mutualistic partners throughout the entire metacommunity, compensates mismatches with the environment, by increasing the likelihood that populations have suitable mutualistic partners at any patch, which increases the rate of successful colonization (figure 2*d*). Local and regional trait matching also increase with species richness, which explains why increasing richness has a positive effect on occupancy (figure 2*c*,*d*).

(b) Coevolution and species richness buffer the effects of environmental changes

We next performed simulations in which the environment changes over time. Our simulations show that when coevolution strength is low, patch occupancy is much lower than expected for static environmental settings (figure 3*a*). Increasing coevolution strength and species richness raises occupancy sharply by synergistically creating a more positive balance between the rates of population colonization and extinction (figure 3*b*). Indeed, as coevolution strength increases, mean

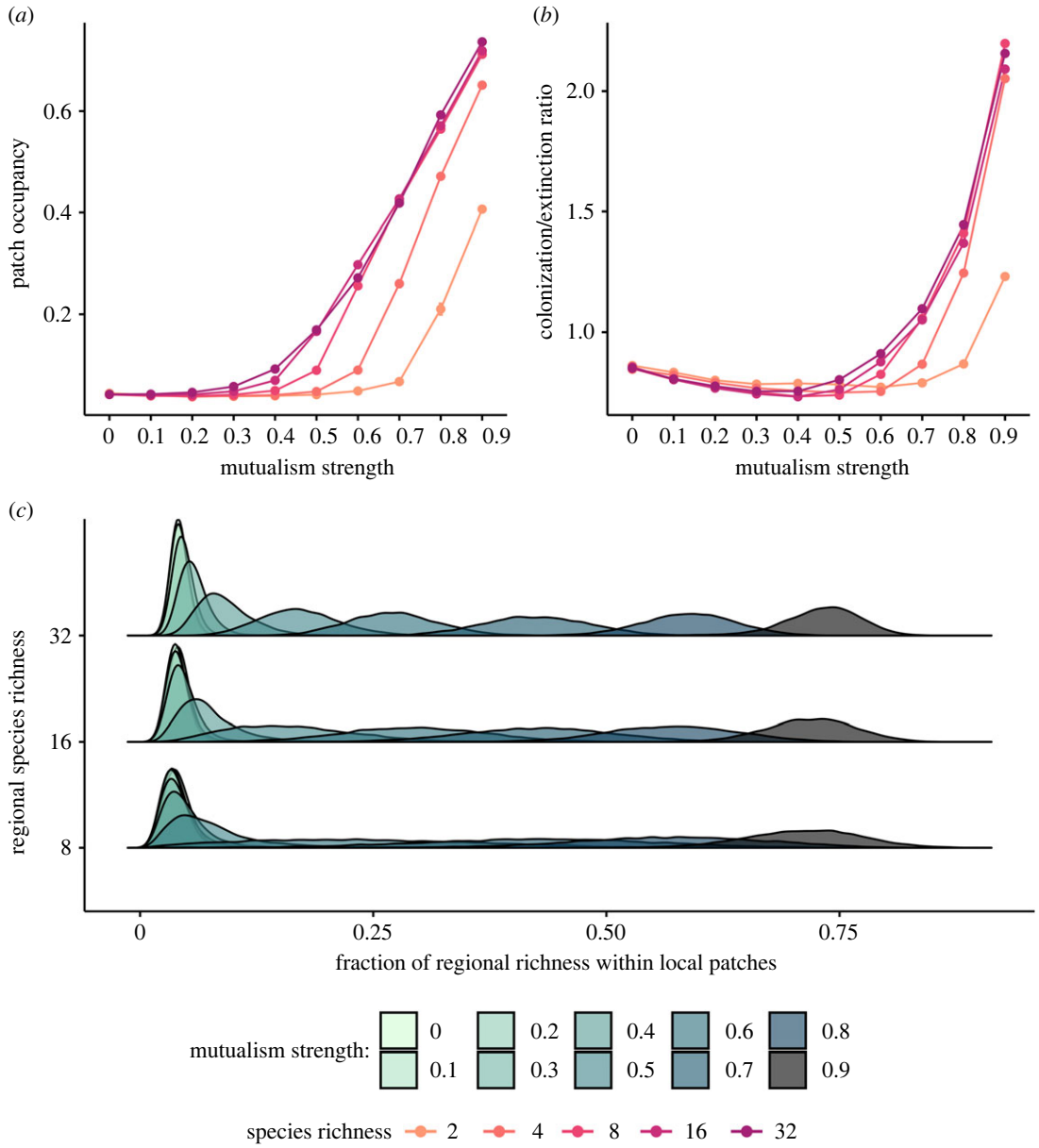

Figure 3. Mutualistic coevolution shapes patterns of (*a*) occupancy, by altering the (*b*) balance between colonization and extinction (calculated as the ratio of population colonization/extinction), thus affecting local patterns in species richness (*c*) in metacommunities under environmental changes ($\theta_{ik} + 0.25$ per generation). In (*a*, *b*) points and lines represent the mean value for 100 simulations. In panel (*c*), curves correspond to the distribution of the fraction of regional richness within local patches (averaged over time) across 100 simulations. Parameter values are as follows: $m_{ik} = 0.0 - 0.9$, $\sigma^2_{Gz_{ik}} = 1.0$, $\varrho_{ik} = 0.1$, $\alpha = 0.1$.

species richness within patches also increases (figure 3*c*). Thus, under environmental changes coevolution favours the persistence of species across the entire landscape, not only on a few patches.

This buffering effect occurs because, by favouring regional trait matching, coevolution and gene flow make species more likely to find suitable patches even when they are maladapted to the environment. Sensitivity analyses showed that these results hold for multiple combinations of parameter values (electronic supplementary material, Information). Furthermore, our sensitivity analysis showed that even without gene flow, mutualistic coevolution can buffer the negative effects of environmental change, but gene flow amplifies the buffering effect. Simulations under an alternative model assuming species interact but do not coevolve cannot reproduce the observed patterns of occupancy, resulting in very low occupancy and complete extinction of the metacommunity regardless of the value of mutualism strength (electronic supplementary material, Information). Therefore, the observed patterns in patch occupancy and richness for varying m, cannot be interpreted only as the effect of decreasing the contribution of the environment as a selective pressure (see the electronic supplementary material, Information for a more detailed discussion).

(c) Coevolution prevents the collapse of metacommunities

Simultaneous extinctions of local populations can result in the regional extinction of a species. According to our simulations, species extinctions, and the eventual collapse of metacommunities in a changing environment can be prevented by mutualistic coevolution (figure 4*a*). Whenever the strength of mutualisms was weak ($m_{ik} = 0.0 - 0.3$) the metacommunity collapsed. However, further increasing the strength of mutualistic interactions prevented the collapse of the metacommunity and increased the fraction of surviving species. Again, the extent of this buffering effect over persistence was modulated by

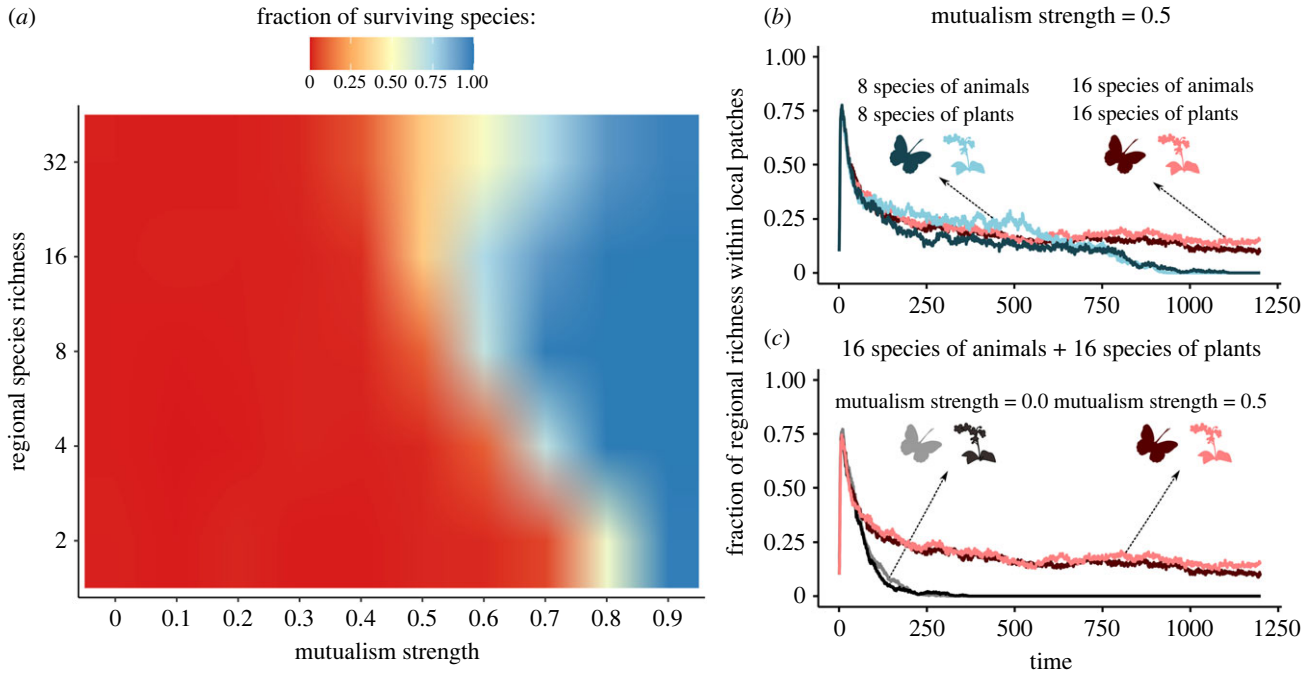

Figure 4. Mutualistic coevolution prevents the collapse of metacommunities under environmental changes ($\theta_{ik} + 0.25$ per generation). (*a*) Relationship between the strength of mutualisms, specie richness and the average fraction of surviving species at the end of simulations. Colours are interpolated to improve visualization. (*b*) Example of a simulation showing how increasing the regional species richness (from a total of 16 to 32 species) can prevent the collapse of the community for the same value of strength of mutualisms ($m_{ik} = 0.5$). (*c*) Example of a simulation with 16 animal and 16 plant species, showing how increasing the strength of mutualisms (from 0.0 to 0.5) can prevent the collapse of the metacommunity. On panels (*b*) and (*c*) each line represents the average for all plants or animal species. Other parameter values are as follows: $m_{ik} = 0.0 - 0.9$, $\sigma^2_{Gz_{ik}} = 1.0$, $\varrho_{ik} = 0.1$, $\alpha = 0.1$.

diversity, such that extinctions were only prevented in species-poor metacommunities at higher levels of mutualism strength. For instance, in an example of a simulated scenario with $m_{ik} = 0.5$, the metacommunity with 16 species collapsed, while in the one with 32 species nearly 25% of both plant and animal species persisted (figure 4*b*). However, without any coevolution ($m_{ik} = 0.0$) all 32 species went extinct (figure 4*c*). This effect of species richness occurred because in species-rich metacommunities, species have potential partners in most patches, which grants a certain baseline suitability even as the environmental conditions deteriorate. Sensitivity analyses showed that the buffering effects of coevolution and species richness against environmental changes held for different parameter values (electronic supplementary material, Information). We also obtained similar results when allowing the strength of coevolution to vary uniformly or in hotspots and coldspots across the landscape, implying that even a few coevolutionary hotspots can prevent the collapse of metacommunities under environmental changes (electronic supplementary material, figure S17).

4. Discussion

In the past decades, evolution has been recognized to occur at timescales that are fast enough to influence contemporary trait distribution patterns and, consequently, the persistence and distribution of ecological populations, thus affecting their response to environmental change [3,59–62]. However, we are only starting to understand how the interplay between local evolution and coevolution scale up and shape ecological patterns across landscapes [10,63]. Here, we integrate coevolution, networks and metacommunity dynamics to show that evolution and mutualistic coevolution acting within local patches may scale up to an entire metacommunity and affect the spatial distribution of populations, patterns of adaptation, and the response of species to environmental changes [63]. Together, our results suggest three main mechanisms whereby local mutualistic coevolution can affect the trait distribution and persistence of species in metacommunities.

First, mutualistic coevolution can shape patterns of local and regional trait matching of populations, increasing connectivity across the landscape. Because colonization success and persistence are highly determined by species traits, varying patterns of trait matching can affect the rates of colonization and extinction of populations in metacommunities. In our model, the conflicting selective pressures of mutualistic partners decreases the trait matching of local populations with the environment and increases the rate of extinction of populations. By contrast, at the regional scale, coevolution increases the trait matching with mutualistic partners across the entire metacommunity and increases the rate of colonization. Previous theoretical work showed that trait convergence in mutualisms can emerge from coevolution in species-rich communities [7,11,27,28,39,42,45]. This trait convergence is driven by how mutualistic interactions form complex networks whose pathways propagate indirect evolutionary effects [51]. Similarly, in our model, colonization of local patches by coevolving populations forms its own spatial network. This spatial network also creates paths through which indirect effects propagate across the landscape. Taken together with previous work [45], our results further indicate that indirect effects that propagate through dispersal across the landscape may contribute to shape not only patterns of regional trait matching among mutualists, but also rates of local extinctions and colonization. Thus, the disruption of indirect pathways across space because of habitat fragmentation, for instance, besides its impacts on metacommunity

dynamics through dispersal limitation may also affect coevolutionary dynamics at the landscape level, an overlooked question that deserves further attention [47,48,64,65].

Second, coevolution with mutualists facilitates colonization of otherwise unsuitable patches and effectively expand the realized niche of species [6,66,67]. By facilitating colonization, increased trait matching at the regional scale may allow species to expand their spatial distributions, even when certain local populations are maladapted to the local environment. In natural populations, local adaptation may counteract environmental gradients and even out ecological patterns in space, reducing variation in mean fitness and in the local abundance of populations across the landscape [63]. Our simulations show that by favouring trait matching among multiple mutualists across the landscape, coevolution may minimize the negative effects of mismatches with the environment. This mechanism is further amplified by increased metacommunity diversity. Therefore, our results suggest that mutualistic coevolution in species-rich metacommunities can be an important force that allow species to expand and maintain their distribution ranges in a heterogeneous landscape.

Third, metacommunity diversity and coevolution can synergistically counteract the effects of environmental changes. When multiple interacting species exert evolutionary pressures in the same direction, trait matching among mutualists increases across the entire landscape. This increased trait matching sustains higher rates of colonization and allow populations to track environmental changes more efficiently. In species-rich mutualisms, greater complexity overcompensates the strength of mutualism so that populations can track environmental changes and species tolerate greater levels of environmental changes even if the strength of coevolution is relatively weak. The less rich the community, the stronger mutualisms need to be to prevent the extinction of species and the collapse of the metacommunity. Thus, our results highlight that any factor that decreases the strength of mutualistic interactions, hinders coevolution or decreases species richness in mutualistic systems, may reduce the likelihood of biodiversity persistence in a changing environment [68,69]. As the environment rapidly changes globally, understanding the mechanisms that allow populations and species to track and colonize suitable environments is a major concern for biodiversity conservation [17,18,70–73]. Locally, species-rich communities have been shown to buffer the effects of environmental changes, because increased trait convergence allows mutualists to rewire interactions in a way that compensate for the extinctions of their partners [31]. Here, we show that mutualistic coevolution can counteract environmental changes at larger spatial scales by maintaining the connectivity of spatial networks. Multispecific coevolution favours trait convergence at larger scales so that any species may have potential partners in several sites, allowing species to persist and colonize novel sites even as the environment changes. This increases the effective connectivity among sites and may help explain how mutualisms facilitate persistence and range expansions under environmental changes and maintain species richness across landscapes [2,74].

There is plenty of empirical evidence that mutualistic interactions and partner diversity allows populations to persist in a wide range of environments and is associated with range expansion of populations [75]. However, we still do not fully understand the mechanisms through which mutualistic interactions drive these range expansions and how coevolution affects spatial patterns. We present a testable mechanism for how mutualistic interactions can allow species to colonize otherwise unsuitable patches, and increase the distribution range of populations, favouring persistence. Although measuring coevolution in natural systems is challenging, the predictions of our model could be tested by assessing trait matching among interacting species at multiple sites (e.g. [76]) and investigating how variation in trait-matching affects colonization and persistence over time or patterns of patch occupancy (e.g. [77]).

Natural systems are increasingly perturbed by human activities, being subjected to high levels of diversity loss and fragmentation [16,78]. Whereas diversity loss impoverishes and simplifies the structure of communities, fragmentation changes the spatial structure of metacommunities and may reduce the potential of mutualistic coevolution to buffer harmful effects of ongoing environmental changes [79–81]. Our results show that coevolution and high species richness have a favourable impact on colonization success, thus implying that maintaining diversity and landscape connectivity is necessary for species persistence under environmental change. Disrupting connection pathways among natural populations can increase the biodiversity erosion driven by human impacts, threatening essential ecosystem functions related to mutualisms, such as pollination and seed dispersal.

Data accessibility. Code and instructions to perform numerical simulations are available from the Dryad Digital Repository: https://doi.org/10.5061/dryad.r2280gbh5 [82] and from GitHub: https://github.com/lgcosmo/Cosmo_et_al_mutualistic_coevolution_metacommunities.

Data are provided in the electronic supplementary material [83].

Authors' contributions. L.G.C.: conceptualization, formal analysis, investigation, methodology, project administration, writing—original draft, writing—review and editing; L.P.S.: conceptualization, methodology, writing—original draft, writing—review and editing; P.R.G.: supervision, writing—original draft, writing—review and editing; M.M.P.: conceptualization, supervision, writing—original draft, writing—review and editing.

All authors gave final approval for publication and agreed to be held accountable for the work performed therein.

Conflict of interest declaration. The authors declare no competing interests.

Funding. This study was financed in part by the Coordenação de Aperfeiçoamento de Pessoal de Nível Superior – Brasil (CAPES) – finance code 001. L.G.C. thanks FAPESP for a PhD scholarship (São Paulo Research Foundation; grant no. 2019/22146-3). L.P.S. receives a Banting Postdoctoral Fellowship from the Government of Canada (Natural Sciences and Engineering Research Council; agreement # 01353). P.R.G. is funded by CNPq (grant no. 307134/2017-2), FAPESP (São Paulo Research Foundation; grant no. 2018/14809-0), and the Royal Society, London (grant no. CHL/R1/180156). M.M.P. is funded by FAPESP (São Paulo Research Foundation; grant no. 2019/25478-7).

References

1. Hoffmann AA, Sgró CM. 2011 Climate change and evolutionary adaptation. *Nature* **470**, 479–485. (doi:10.1038/nature09670)

2. Afkhami ME, McIntyre PJ, Strauss SY. 2014 Mutualist-mediated effects on species' range limits

across large geographic scales. *Ecol. Lett.* **17**, 1265–1273. (doi:10.1111/ele.12332)

3. Moran EV, Alexander JM. 2014 Evolutionary responses to global change: lessons from invasive species. *Ecol. Lett.* **17**, 637–649. (doi:10.1111/ele.12262)
4. Lau JA, terHorst CP. 2019 Evolutionary responses to global change in species-rich communities. *Ann. N. Y. Acad. Sci.* **1476**, 43–58. (doi:10.1111/nyas.14221)
5. Sales LP, Kissling WD, Galetti M, Naimi B, Pires M. 2021 Climate change reshapes the eco-evolutionary dynamics of a Neotropical seed dispersal system. *Glob. Ecol. Biogeogr.* **30**, 1129–1138. (doi:10.1111/geb.13271)
6. Peay KG. 2016 The mutualistic niche: mycorrhizal symbiosis and community dynamics. *Annu. Rev. Ecol. Evol. Syst.* **47**, 143–164. (doi:10.1146/annurev-ecolsys-121415-032100)
7. Thompson JN. 2009 The coevolving web of life. *Am. Nat.* **173**, 125–140. (doi:10.1086/595752)
8. Bascompte J, Jordano P. 2007 Plant–animal mutualistic networks: the architecture of biodiversity. *Annu. Rev. Ecol. Evol. Syst.* **38**, 567–593. (doi:10.1146/annurev.ecolsys.38.091206.095818)
9. Bascompte J. 2009 Disentangling the web of life. *Science* **325**, 416–419. (doi:10.1126/science.1170749)
10. Thompson JN. 2005 *The geographic mosaic of coevolution*. Chicago, IL: University of Chicago Press.
11. Birskis-Barros I, Freitas AVL, Guimarães PR. 2021 Habitat generalist species constrain the diversity of mimicry rings in heterogeneous habitats. *Sci. Rep.* **11**, 5072. (doi:10.1038/s41598-021-83867-w)
12. Strauss SY, Whittall JB. 2006 Non-pollinator agents of selection on floral traits. In *Ecology and evolution of flowers* (eds LD Harder, SCH Barrett), pp. 120–138. Oxford, UK: Oxford University Press.
13. Valenta K, Kalbitzer U, Razafimandimby D, Omeja P, Ayasse M, Chapman CA, Nevo O. 2018 The evolution of fruit colour: phylogeny, abiotic factors and the role of mutualists. *Sci. Rep.* **8**, 1–8. (doi:10.1038/s41598-018-32604-x)
14. Schleuning M *et al.* 2020 Trait-based assessments of climate-change impacts on interacting species. *Trends Ecol. Evol.* **35**, 319–328. (doi:10.1016/j.tree.2019.12.010)
15. Bellard C, Bertelsmeier C, Leadley P, Thuiller W, Courchamp F. 2012 Impacts of climate change on the future of biodiversity. *Ecol. Lett.* **15**, 365–377. (doi:10.1111/j.1461-0248.2011.01736.x)
16. Scheffer M, Carpenter S, Foley JA, Folke C, Walker B. 2001 Catastrophic shifts in ecosystems. *Nature* **413**, 591–596. (doi:10.1038/35098000)
17. Burrows MT *et al.* 2011 The pace of shifting climate in marine and terrestrial ecosystems. *Science* **334**, 652–655. (doi:10.1126/science.1210288)
18. Urban MC. 2015 Accelerating extinction risk from climate change. *Science* **348**, 571–573. (doi:10.1126/science.aaa4984)
19. Fricke EC, Svenning JC. 2020 Accelerating homogenization of the global plant–frugivore meta-network. *Nature* **585**, 74–78. (doi:10.1038/s41586-020-2640-y)
20. Norberg J, Urban MC, Vellend M, Klausmeier CA, Loeuille N. 2012 Eco-evolutionary responses of biodiversity to climate change. *Nat. Clim. Change* **2**, 747–751. (doi:10.1038/nclimate1588)
21. Bronstein JL, Alarcón R, Geber M. 2006 The evolution of plant–insect mutualisms. *New Phytol.* **172**, 412–428. (doi:10.1111/j.1469-8137.2006.01864.x)
22. Thompson JN. 2013 *Relentless evolution*. Chicago, IL: University of Chicago Press.
23. Bronstein JL. 1994 Our current understanding of mutualism. *Q. Rev. Biol.* **69**, 31–51. (doi:10.1086/418432)
24. Temple SA. 1977 Plant–animal mutualism: coevolution with dodo leads to near extinction of plant. *Science* **197**, 885–886. (doi:10.1126/science.197.4306.885)
25. Bronstein JL, Dieckmann U, Ferrière R. 2004 Coevolutionary dynamics and the conservation of mutualisms. In *Evolutionary Conservation Biology* (eds R Ferrière, U Dieckmann, D Couvet), pp. 305–326. Cambridge, UK: Cambridge University Press.
26. Miller-Struttmann NE *et al.* 2015 Functional mismatch in a bumble bee pollination mutualism under climate change. *Science* **349**, 1541–1544. (doi:10.1126/science.aab0868)
27. Guimarães Jr GP, Jordano P, Thompson JN. 2011 Evolution and coevolution in mutualistic networks. *Ecol. Lett.* **14**, 877–885. (doi:10.1111/j.1461-0248.2011.01649.x)
28. Nuismer SL, Jordano P, Bascompte J. 2013 Coevolution and the architecture of mutualistic networks. *Evolution* **67**, 338–354. (doi:10.1111/j.1558-5646.2012.01801.x)
29. Elias M, Gompert Z, Jiggins C, Willmott K. 2008 Mutualistic interactions drive ecological niche convergence in a diverse butterfly community. *PLoS Biol.* **6**, e300. (doi:10.1371/journal.pbio.0060300)
30. Fenster CB, Armbruster WS, Wilson P, Dudash MR, Thomson JD. 2004 Pollination syndromes and floral specialization. *Annu. Rev. Ecol. Evol. Syst.* **35**, 375–403. (doi:10.1146/annurev.ecolsys.34.011802.132347)
31. Nuismer SL, Week B, Aizen MA. 2018 Coevolution slows the disassembly of mutualistic networks. *Am. Nat.* **192**, 490–502. (doi:10.1086/699218)
32. Vizentin-Bugoni J, Debastiani VJ, Bastazini VAG, Maruyama PK, Sperry JH. 2020 Including rewiring in the estimation of the robustness of mutualistic networks. *Methods Ecol. Evol.* **11**, 106–116. (doi:10.1111/2041-210X.13306)
33. Leibold MA *et al.* 2004 The metacommunity concept: a framework for multi-scale community ecology. *Ecol. Lett.* **7**, 601–613. (doi:10.1111/j.1461-0248.2004.00608.x)
34. Urban MC, Skelly DK. 2006 Evolving metacommunities: toward an evolutionary perspective on metacommunities. *Ecology* **87**, 1616–1626. (doi:10.1890/0012-9658(2006)87[1616:EMTAEP]2.0.CO;2)
35. Loeuille N, Leibold MA. 2008 Evolution in metacommunities: on the relative importance of species sorting and monopolization in structuring communities. *Am. Nat.* **171**, 788–799. (doi:10.1086/587745)
36. Loeuille N, Leibold MA. 2008 Ecological consequences of evolution in plant defenses in a metacommunity. *Theor. Popul. Biol.* **74**, 34–45. (doi:10.1016/j.tpb.2008.04.004)
37. Urban MC *et al.* 2008 The evolutionary ecology of metacommunities. *Trends Ecol. Evol.* **23**, 311–317. (doi:10.1016/j.tree.2008.02.007)
38. Williams JL, Hufbauer RA, Miller TEX. 2019 How evolution modifies the variability of range expansion. *Trends Ecol. Evol.* **34**, 903–913. (doi:10.1016/j.tree.2019.05.012)
39. Nuismer SL, Thompson JN, Gomulkiewicz R. 1999 Gene flow and geographically structured coevolution. *Proc. R. Soc. Lond. B* **266**, 605–609. (doi:10.1098/rspb.1999.0679)
40. Nuismer SL, Thompson JN. 2006 Coevolutionary alternation in antagonistic interactions. *Evolution* **60**, 2207–2217. (doi:10.1111/j.0014-3820.2006.tb01858.x)
41. Lemos-Costa P, Martins AB, Thompson JN, De Aguiar MAM. 2017 Gene flow and metacommunity arrangement affects coevolutionary dynamics at the mutualism–antagonism interface. *J. R. Soc. Interface* **14**, 20160989. (doi:10.1098/rsif.2016.0989)
42. Fernandes LD, Lemos-Costa P, Guimarães PR, Thompson JN, de Aguiar MAM. 2019 Coevolution creates complex mosaics across large landscapes. *Am. Nat.* **194**, 217–229. (doi:10.1086/704157)
43. Gómez JM, Abdelaziz M, Camacho JPM, Muñoz-Pajares AJ, Perfectti F. 2009 Local adaptation and maladaptation to pollinators in a generalist geographic mosaic. *Ecol. Lett.* **12**, 672–682. (doi:10.1111/j.1461-0248.2009.01324.x)
44. Nuismer SL, Thompson JN, Gomulkiewicz R. 2000 Coevolutionary clines across selection mosaics. *Evolution* **54**, 1102–1115.
45. Medeiros LP, Garcia G, Thompson JN, Guimarães PR. 2018 The geographic mosaic of coevolution in mutualistic networks. *Proc. Natl Acad. Sci. USA* **115**, 12 017–12 022. (doi:10.1073/pnas.1809088115)
46. Gibert JP, Pires MM, Thompson JN, Guimarães PR. 2013 The spatial structure of antagonistic species affects coevolution in predictable ways. *Am. Nat.* **182**, 578–591. (doi:10.1086/673257)
47. Fortuna MA, Bascompte J. 2006 Habitat loss and the structure of plant–animal mutualistic networks. *Ecol. Lett.* **9**, 281–286. (doi:10.1111/j.1461-0248.2005.00868.x)
48. Fortuna MA, Krishna A, Bascompte J. 2013 Habitat loss and the disassembly of mutalistic networks. *Oikos* **122**, 938–942. (doi:10.1111/j.1600-0706.2012.00042.x)
49. Leibold MA, Rudolph FJ, Blanchet FG, De Meester L, Gravel D, Hartig F, Peres-Neto P, Shoemaker L, Chase JM. 2021 The internal structure of

metacommunities. *Oikos* **2022**, e08618. (doi:10.1111/oik.08618)

50. Bronstein JL. 2015 *Mutualism*. Oxford, UK: Oxford University Press.
51. Guimarães PR, Pires MM, Jordano P, Bascompte J, Thompson JN. 2017 Indirect effects drive coevolution in mutualistic networks. *Nature* **550**, 511–514. (doi:10.1038/nature24273)
52. Lande R. 1976 Natural selection and random genetic drift in phenotypic evolution. *Evolution* **30**, 314.
53. Santamaría L, Rodríguez-Gironés MA. 2007 Linkage rules for plant–pollinator networks: trait complementarity or exploitation barriers? *PLoS Biol.* **5**, e31. (doi:10.1371/journal.pbio.0050031)
54. Van Der Gucht K *et al.* 2007 The power of species sorting: local factors drive bacterial community composition over a wide range of spatial scales. *Proc. Natl Acad. Sci. USA* **104**, 20 404–20 409. (doi:10.1073/pnas.0707200104)
55. Questad EJ, Foster BL. 2008 Coexistence through spatio-temporal heterogeneity and species sorting in grassland plant communities. *Ecol. Lett.* **11**, 717–726. (doi:10.1111/j.1461-0248.2008.01186.x)
56. Myers JA, Harms KE. 2011 Seed arrival and ecological filters interact to assemble high-diversity plant communities. *Ecology* **92**, 676–686. (doi:10.1890/10-1001.1)
57. VanDerWal J, Shoo LP, Johnson CN, Williams SE. 2009 Abundance and the environmental niche: environmental suitability estimated from niche models predicts the upper limit of local abundance. *Am. Nat.* **174**, 282–291. (doi:10.1086/600087)
58. Bezanson J, Edelman A, Karpinski S, Shah VB. 2017 Julia: a fresh approach to numerical computing. *SIAM Rev.* **59**, 65–98. (doi:10.1137/141000671)
59. Agrawal AA, Hastings AP, Johnson MTJ, Maron JL, Salminen J-P. 2012 Insect herbivores drive real-time ecological and evolutionary change in plant populations. *Science* **338**, 113–116. (doi:10.1126/science.1225977)
60. Galetti M *et al.* 2013 Functional extinction of birds drives rapid evolutionary changes in seed size. *Science* **340**, 1086–1090. (doi:10.1126/science.1233774)
61. Thompson JN. 1998 Rapid evolution as an ecological process. *Trends Ecol. Evol.* **13**, 329–332. (doi:10.1016/S0169-5347(98)01378-0)
62. Urban MC, De Meester L, Vellend M, Stoks R, Vanoverbeke J. 2012 A crucial step toward realism: responses to climate change from an evolving metacommunity perspective. *Evol. Appl.* **5**, 154–167. (doi:10.1111/j.1752-4571.2011.00208.x)
63. Urban MC *et al.* 2020 Evolutionary origins for ecological patterns in space. *Proc. Natl Acad. Sci. USA* **117**, 17 482–17 490. (doi:10.1073/pnas.1918960117)
64. Gómez JM. 2003 Spatial patterns in long-distance dispersal of *Quercus ilex* acorns by jays in a heterogeneous landscape. *Ecography* **26**, 573–584. (doi:10.1034/j.1600-0587.2003.03586.x)
65. Gómez JM, Bosch J, Perfectti F, Fernández JD, Abdelaziz M, Camacho JPM. 2008 Spatial variation in selection on corolla shape in a generalist plant is promoted by the preference patterns of its local pollinators. *Proc. R. Soc. B* **275**, 2241–2249. (doi:10.1098/rspb.2008.0512)
66. Gerz M, Guillermo Bueno C, Ozinga WA, Zobel M, Moora M. 2018 Niche differentiation and expansion of plant species are associated with mycorrhizal symbiosis. *J. Ecol.* **106**, 254–264. (doi:10.1111/1365-2745.12873)
67. Kazenel MR, Debban CL, Ranelli L, Hendricks WQ, Chung YA, Pendergast TH, Charlton ND, Young CA, Rudgers JA. 2015 A mutualistic endophyte alters the niche dimensions of its host plant. *AoB Plants* **7**, 1–13. (doi:10.1093/aobpla/plv005)
68. Lever JJ, van Nes EH, Scheffer M, Bascompte J. 2014 The sudden collapse of pollinator communities. *Ecol. Lett.* **17**, 350–359. (doi:10.1111/ele.12236)
69. Dakos V, Bascompte J. 2014 Critical slowing down as early warning for the onset of collapse in mutualistic communities. *Proc. Natl Acad. Sci. USA* **111**, 17 546–17 551. (doi:10.1073/pnas.1406326111)
70. Loarie SR, Duffy PB, Hamilton H, Asner GP, Field CB, Ackerly DD. 2009 The velocity of climate change. *Nature* **462**, 1052–1055. (doi:10.1038/nature08649)
71. Corlett RT, Westcott DA. 2013 Will plant movements keep up with climate change? *Trends Ecol. Evol.* **28**, 482–488. (doi:10.1016/j.tree.2013.04.003)
72. Bradshaw CJA *et al.* 2021 Underestimating the challenges of avoiding a ghastly future. *Front. Conserv. Sci.* **1**, 1–10.
73. Thompson PL, Fronhofer EA. 2019 The conflict between adaptation and dispersal for maintaining biodiversity in changing environments. *Proc. Natl Acad. Sci. USA* **116**, 21 061–21 067. (doi:10.1073/pnas.1911796116)
74. Chomicki G, Weber M, Antonelli A, Bascompte J, Kiers ET. 2019 The impact of mutualisms on species richness. *Trends Ecol. Evol.* **34**, 698–711. (doi:10.1016/j.tree.2019.03.003)
75. Fowler JC, Donald ML, Bronstein JL, Miller TEX. 2022 The geographic footprint of mutualism: how mutualists influence species' range limits. *Ecol. Monogr.* e1558. (doi:10.1002/ecm.1558)
76. Thompson JN, Schwind C, Guimarães Jr PR, Friberg M. 2013 Diversification through multitrait evolution in a coevolving interaction. *Proc. Natl Acad. Sci. USA* **110**, 11 487–11 492. (doi:10.1073/pnas.1307451110)
77. Gaiarsa MP, Kremen C, Ponisio LC. 2021 Pollinator interaction flexibility across scales affects patch colonization and occupancy. *Nat. Ecol. Evol.* **5**, 787–793. (doi:10.1038/s41559-021-01434-y)
78. Dirzo R, Young HS, Galetti M, Ceballos G, Isaac NJB, Collen B. 2014 Defaunation in the anthropocene. *Science* **345**, 401–406. (doi:10.1126/science.1251817)
79. Young A, Boyle T, Brown T. 1996 The population genetic consequences of habitat fragmentation for plants. *Trends Ecol. Evol.* **11**, 413–418. (doi:10.1016/0169-5347(96)10045-8)
80. Fletcher RJ, Burrell NS, Reichert BE, Vasudev D, Austin JD. 2016 Divergent perspectives on landscape connectivity reveal consistent effects from genes to communities. *Curr. Landsc. Ecol. Rep.* **1**, 67–79. (doi:10.1007/s40823-016-0009-6)
81. Cushman SA, Shirk A, Landguth EL. 2012 Separating the effects of habitat area, fragmentation and matrix resistance on genetic differentiation in complex landscapes. *Landsc. Ecol.* **27**, 369–380. (doi:10.1007/s10980-011-9693-0)
82. Cosmo LG, Sales LP, Guimarães Jr PR, Pires MM. 2023 Data from: Mutualistic coevolution and community diversity favour persistence in metacommunities under environmental changes. Dryad Digital Repository. (doi:10.5061/dryad.r2280gbh5)
83. Cosmo LG, Sales LP, Guimarães Jr PR, Pires MM. 2023 Mutualistic coevolution and community diversity favour persistence in metacommunities under environmental changes. Figshare. (doi:10.6084/m9.figshare.c.6350191)

Supplementary Information

Mutualistic coevolution and community diversity favor persistence in metacommunities under environmental changes

Leandro G. Cosmo[1], Lilian P. Sales[2,3], Paulo R. Guimarães Jr.[4], Mathias M. Pires[2]

[1]Programa de Pós-Graduação em Ecologia, Departamento de Ecologia, Instituto de Biociências, Universidade de São Paulo - USP, São Paulo, SP, Brazil;

[2]Departamento de Biologia Animal, Instituto de Biologia, Universidade Estadual de Campinas - UNICAMP, Campinas, SP, Brazil;

[3]Biology Department, Faculty of Arts and Science, Concordia University, Montreal, Canada.

[4]Departamento de Ecologia, Instituto de Biociências, Universidade de São Paulo - USP, São Paulo, SP, Brazil

Content

1 Alternative models – partitioning the evolutionary and ecological effects of mutualistic interactions

In our study we evaluated how mutualistic coevolution shapes the distribution and persistence of species in a metacommunity. Here, we simulate two additional scenarios to test how the results reported in the main text changes when: (1) species interact with mutualists, but do not evolve/coevolve and traits changes over time in local patches only as a result of the colonization and extinction dynamics; (2) species interact with mutualists, evolve/coevolve, but gene flow does not occur among patches. For scenario (1) we set the parameter $\sigma^2_{Gz_{ik}}$=0.0, which cancelled all trait changes because of local evolution/coevolution. To simulate scenario (2) we set the fraction of gene flow to 0.0, allowed only empty patches to be colonized, and, when multiple colonization attempts to a given patch were successful at the same time, only the population with the largest suitability colonized the patch. For the two alternative scenarios we ran 50 simulations for each combination of strength of mutualistic interactions and initial species richness with and without environmental changes.

1.1 Results for the metacommunity dynamics without evolutionary change

1.1.1 Without environmental changes

Our simulations show that without coevolution, mutualistic interactions alone do not reproduce the patterns reported in the main text (Figure S1-S2). Assuming no environmental changes, patch occupancy decreases for intermediate values of mutualistic strength, similarly to the patterns reported in the main text. This decrease, however, is sharper and the effects of species richness on the pattern are not consistent across all levels of mutualistic strength. The sharper decrease in occupancy occurs because at intermediate levels of mutualistic strength, the rate of extinction of populations increases

and nearly surpasses the rate of colonization (Figure S1b). Extinction rises because with greater mutualism strength, suitability is more dependent on the interactions, but without coevolution species may not have “compatible” partners locally, which decreases site suitability. As a consequence of the increased rate of extinction, only populations whose traits perfectly matches the environment or the traits of mutualistic partners persist in the metacommunity, increasing both the local and regional trait matching of mutualistic populations due to species sorting (Figure S1c-d). At exceptionally high levels of mutualism strength the match with the environment is less important for suitability and the few persisting species can support their partners, thus explaining the rise in occupancy.

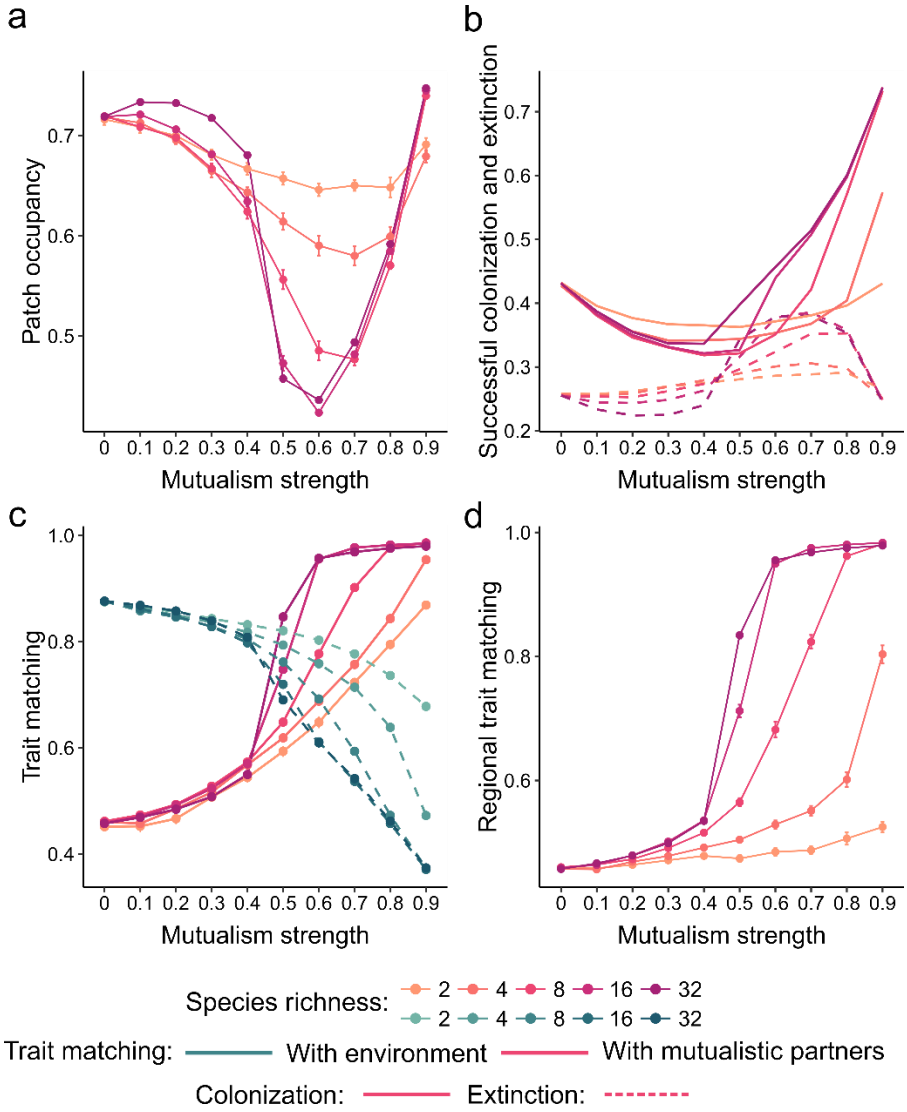

Figure S1 – Results of a model of metacommunity dynamics without evolutionary dynamics for patterns of (a) occupancy, (b) colonization and extinction, and (c-d) trait matching. Points represents the mean value for 50 simulations and bars 95% confidence intervals. Parameter values: m_{ik}= 0.0-0.9, $\sigma^2_{Gz_{ik}} = 0.0$, $\varrho_{ik} = 0.1$, $\alpha = 0.1$.

1.1.2 With environmental changes

With environmental changes but no coevolution, patch occupancy remained very low regardless of the value of strength of mutualisms and whether we allowed or not gene flow among populations (Figure S2a-b). This same pattern held for the extinction of species in the metacommunity, whereas all species went extinct at the end of simulations

regardless of m_{ik} (Figure S2c-d). Therefore, the occurrence of mutualistic interactions alone cannot reproduce the patterns generated by coevolutionary dynamics. Furthermore, these results show that the observed patterns in colonization/extinction dynamics as *m* increases cannot be interpreted only as the effect of decreasing the contribution of the environment as a selective pressure.

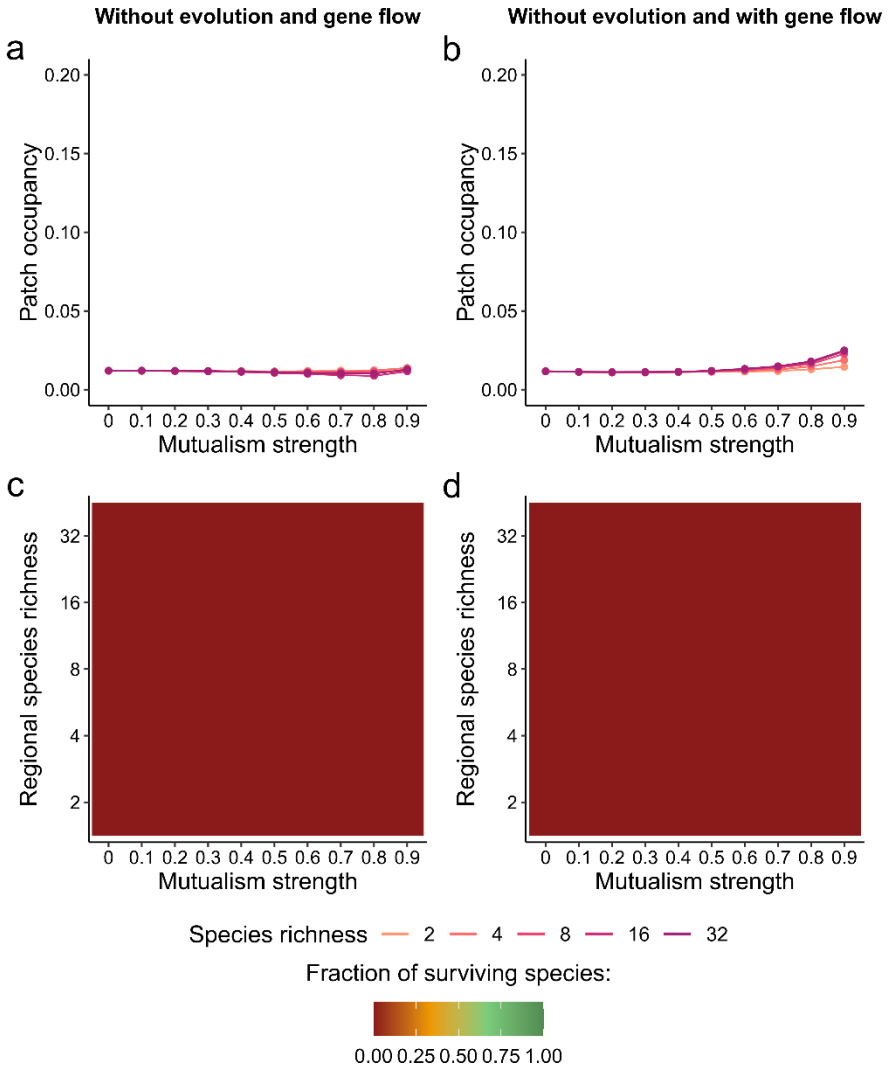

Figure S2 – Results of a model of metacommunity dynamics without evolutionary change for patterns of (a) occupancy, when gene flow is not allowed, (b) occupancy when gene flow is allowed, (c) fraction of surviving species when gene flow is not allowed and (d) fraction of surviving species when gene flow is allowed. In (a-b) points represents the mean value for 50 simulations and bars 95% confidence intervals. Parameter

values: m_{ik}= 0.0-0.9, $\sigma^2_{Gz_{ik}} = 0.0$, $\varrho_{ik} = 0.1$, $\alpha = 0.1$, fraction of gene flow when allowed: 0.05.

1.2 Results for the metacommunity dynamics without gene flow

Our simulations assuming no gene flow generate qualitatively similar patterns to those with gene flow presented in the main text, showing that the outcomes are not only a consequence of gene flow across the landscape, but from coevolution in the metacommunity context (Figure S3-S4). Assuming no gene flow and no changes in the environment over time, mutualistic coevolution had non-linear effects on patch occupancy (Figure S3a), increased the rate of colonization (Figure S3b) and the local/regional trait matching with partners (Figure S3c-d). Furthermore, increasing the species richness in the metacommunity amplified these effects of mutualistic coevolution.

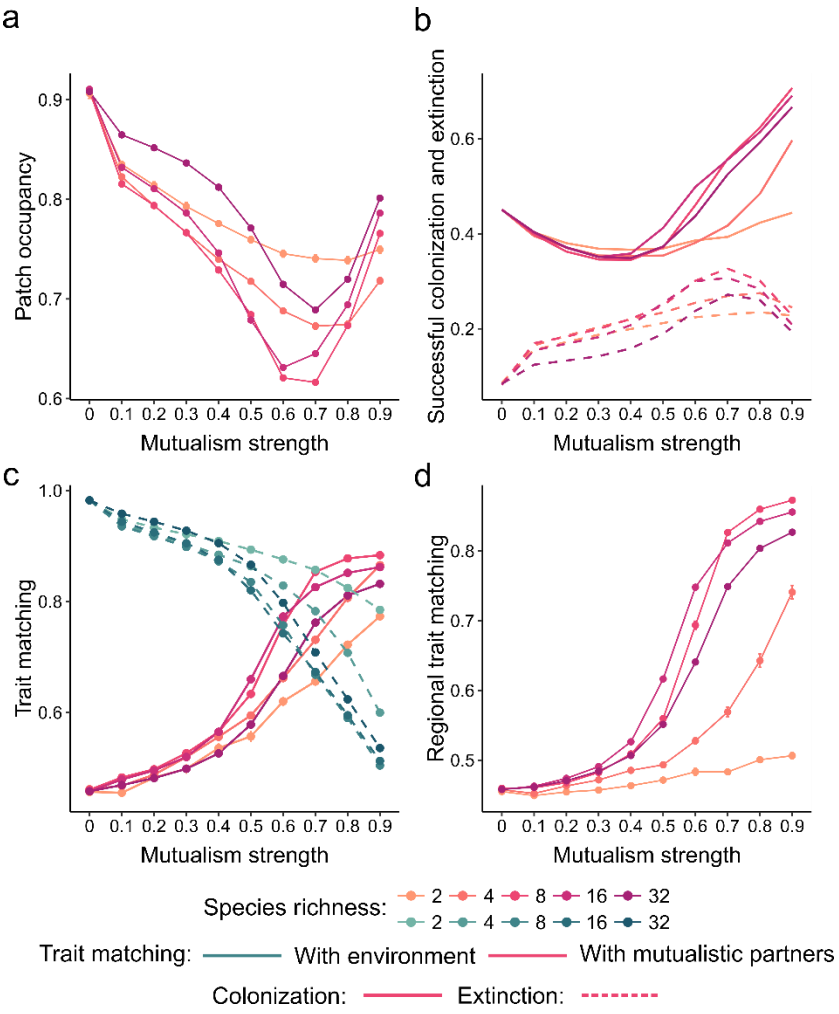

Figure S3 – Results of a model of metacommunity dynamics without gene flow among populations for patterns of (a) occupancy, (b) colonization and extinction, and (c-d) trait matching. Points represents the mean value for 50 simulations and bars 95% confidence intervals. Parameter values: m_{ik}= 0.0-0.9, $\sigma^2_{Gz_{ik}} = 1.0$, $\varrho_{ik} = 0.1$, $\alpha = 0.1$.

When the environment changes, mutualistic coevolution and species richness synergistically increased patch occupancy and buffered the negative effects of environmental change (Figure S4a), even in the absence of gene flow. However, allowing gene flow among populations improved occupancy, highlighting the positive effects of gene flow on the metacommunity under environmental changes (Figure S4b). Furthermore, mutualistic coevolution and species richness were also able to prevent the collapse of the metacommunity without gene flow (Figure S4c). Similar to occupancy patterns, allowing gene flow amplified the buffering effect of coevolution, further increase the fraction of surviving species (Figure S4d).

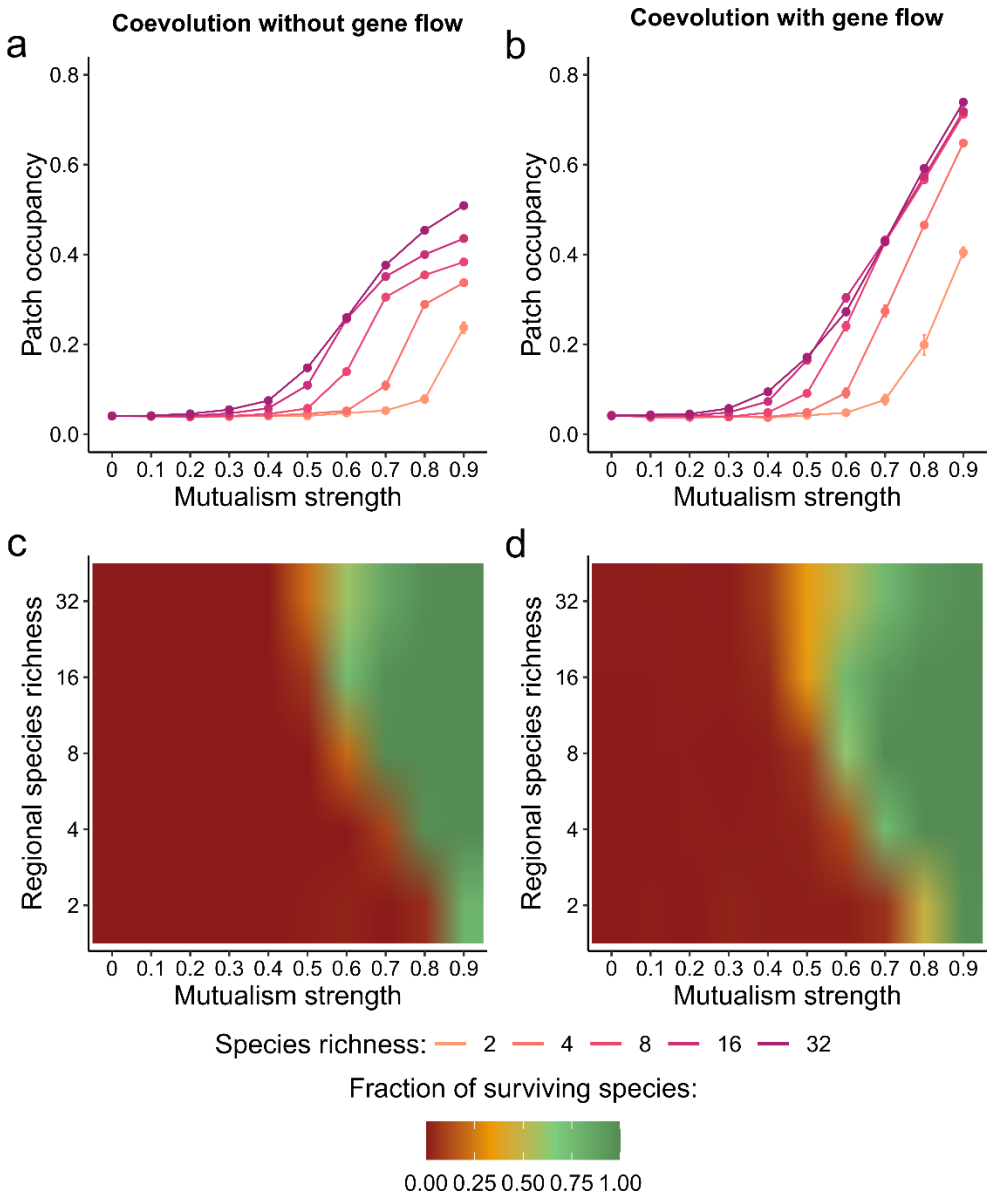

Figure S4 –Results of a model of a coevolving metacommunity for patterns of (a) occupancy when there is no gene flow, (b) occupancy with gene flow, (c) fraction of surviving species without gene flow, and (d) fraction of surviving species with gene flow. In (a-b) points represents the mean value for 50 simulations and bars 95% confidence intervals. On panels (c-d) colors were interpolated to improve visualization. Parameter values: m_{ik}= 0.0-0.9, $\sigma^2_{Gz_{ik}} = 1.0$, $\varrho_{ik} = 0.1$, $\alpha = 0.1$, fraction of gene flow when allowed: 0.05.

2 Sensitivity analyses – simulations with different parameter values

On the main text we present results where we evaluated how coevolution in pairwise and multispecific scenarios affects local and regional patterns in metacommunities with and without environmental changes. Following previous work (Guimarães *et al.* 2017; Medeiros *et al.* 2018), in these simulations we kept most of the model parameters fixed and varied only the strength of mutualistic interactions (m). In our model, coevolution, colonization and extinctions can be affected by two other parameters: (1) ϱ, which high values increase the sensitivity of the adaptive landscape of species and the speed of changes in trait values; and (2) the fraction of gene flow. To test the robustness of our results to different values of these two parameters, we performed a set of sensitivity analyses. In these sensitivity analyses we kept one the parameters fixed (ϱ or the fraction of gene flow) and varied the other. We varied ϱ in 10% steps, up to a 50% increase, from 0.1 to 0.15, and the fraction of gene flow from 0.05 to 0.5. From the results we evaluated how different values of ϱ and fraction of gene flow affected the results reported in the main text.

2.1 Different values of sensitivity of species adaptive landscapes (ϱ)

2.1.1 Without environmental changes

Our simulations show that the patterns reported in the main text qualitatively held when increasing ϱ (Figures S5-S8), with small quantitative changes. Coevolution still had nonlinear effects on patterns of occupancy (Figure S5), increased the rate of colonization (Figure S6) and the local and regional trait matching of species with mutualistic partners (Figure S7-S8).

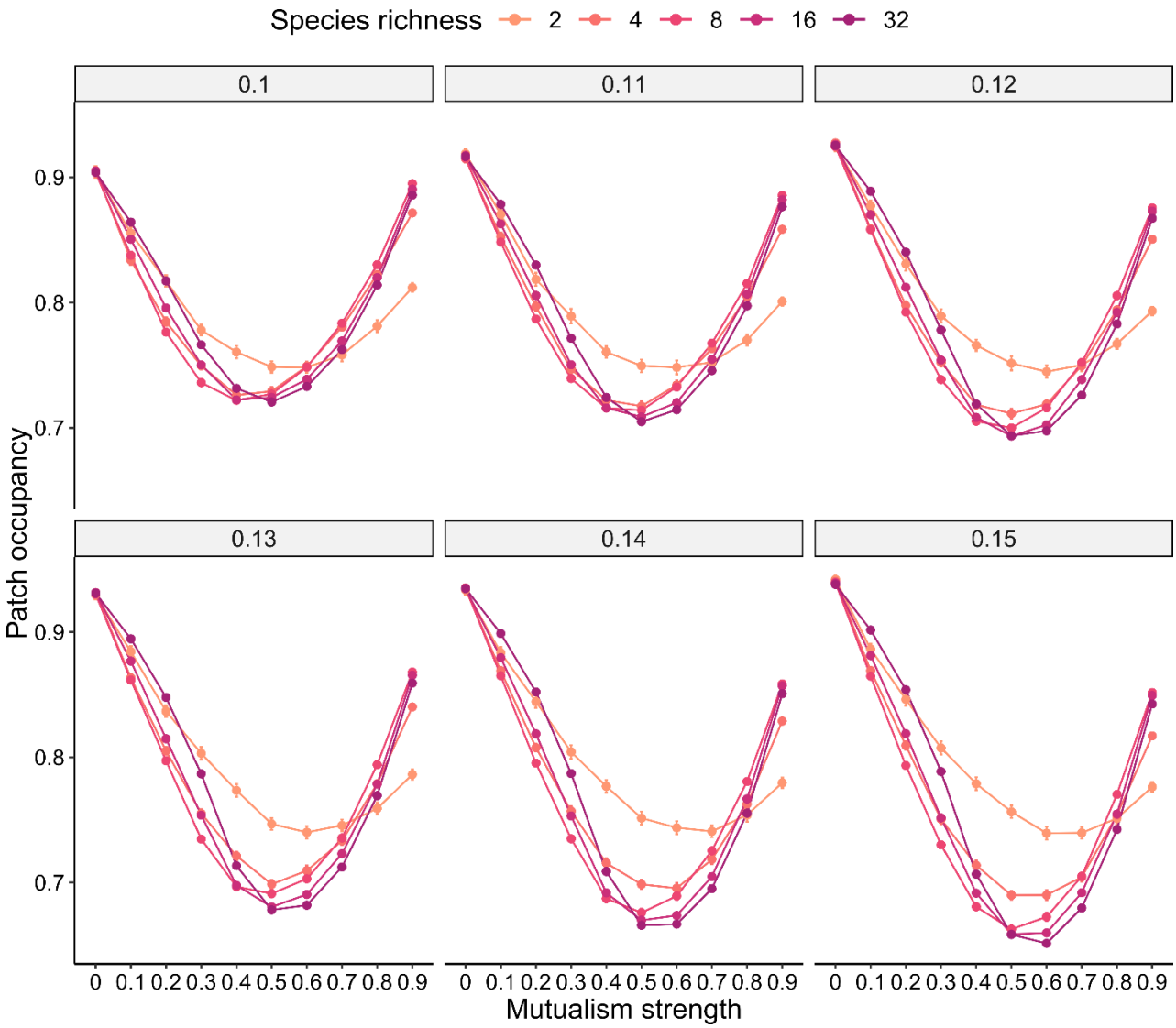

Figure S5 - Effects of different values of the model parameter ϱ (values above each panel) on patterns of patch occupancy. Each point represents the average value of 50 simulations and vertical lines confidence intervals. Points and lines of different colors represents different scenarios of initial species richness in the metacommunity. Other parameter values: m_{ik}= 0.0-0.9, $\sigma^2_{Gz_{ik}} = 1.0$, $\alpha = 0.1$.

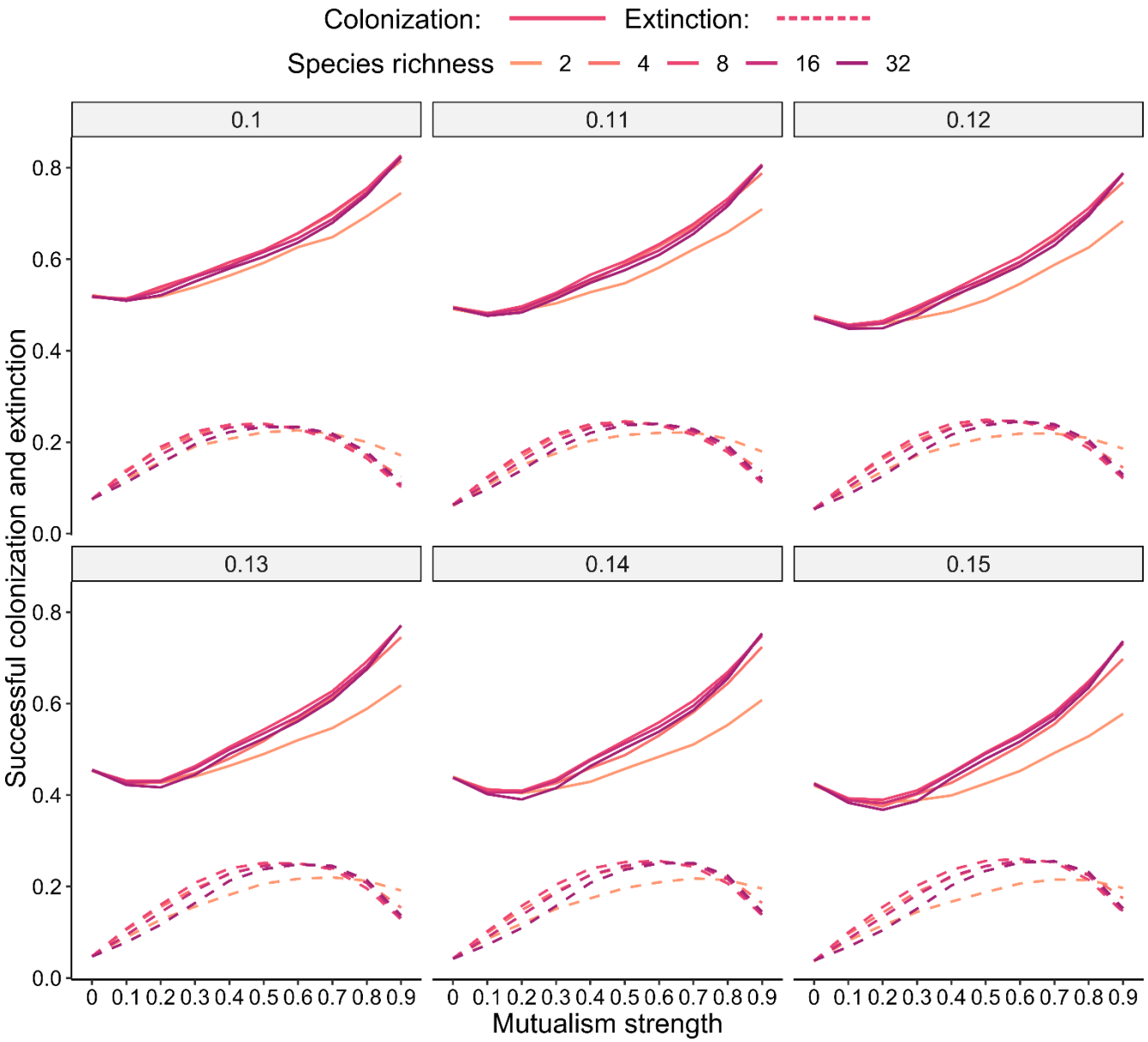

Figure S6 - Effects of different values of the model parameter ϱ (values above each panel) on patterns of colonization (solid lines) and extinction (dashed lines). Each line represents the average value of 50 simulations. Lines of different colors represents different scenarios of initial species richness in the metacommunity. Other parameter values: m_{ik}= 0.0-0.9, $\sigma^2_{Gz_{ik}} = 1.0$, $\alpha = 0.1$.

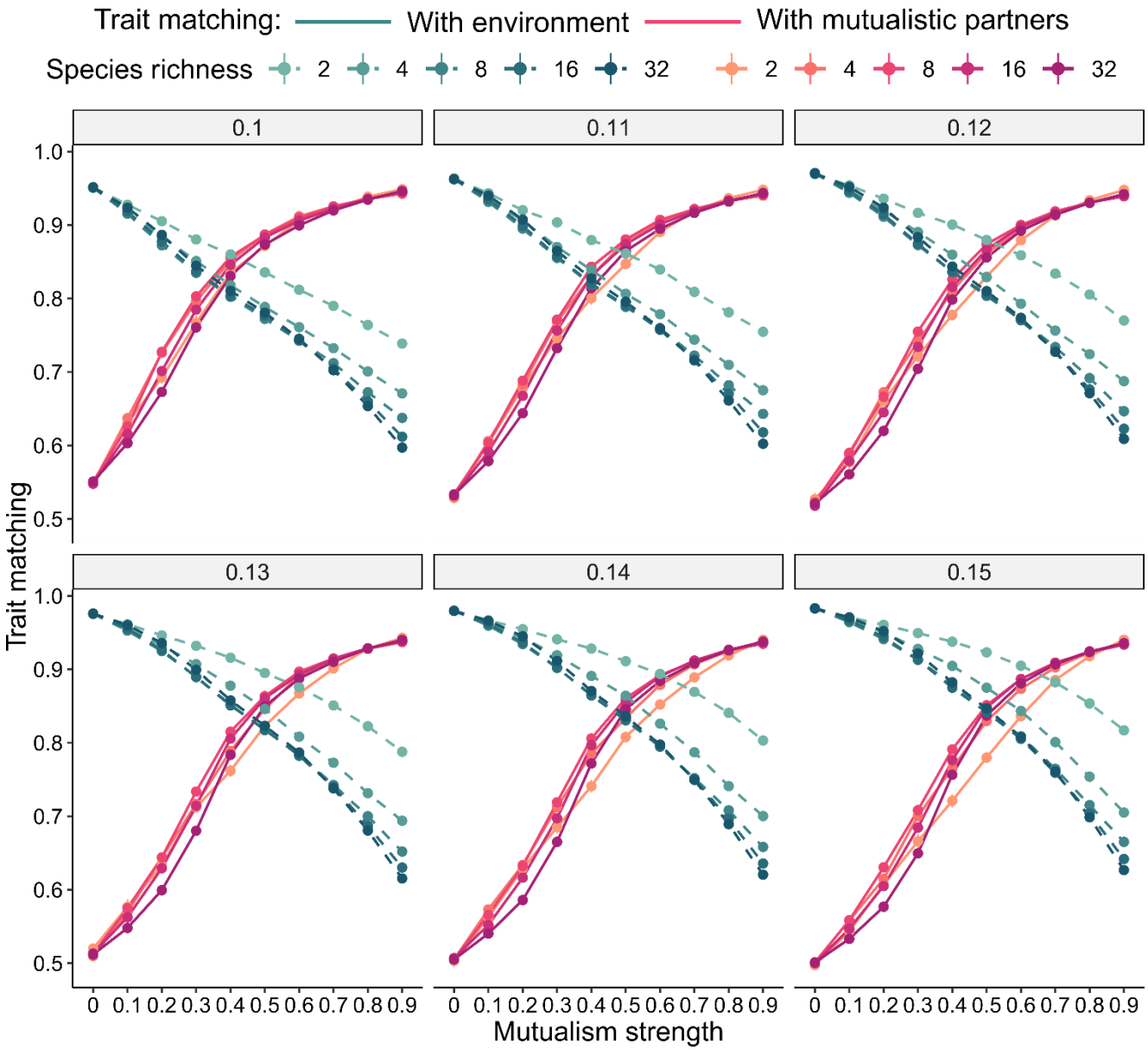

Figure S7 - Effects of different values of the model parameter ϱ (values above each panel) on patterns of local trait matching with the environment (dashed green lines) and mutualistic partners (solid red lines). Each point represents the average value of 50 simulations and vertical lines confidence intervals. Points and lines of different color intensities represents different scenarios of initial species richness in the metacommunity. Other parameter values: m_{ik}= 0.0-0.9, $\sigma^2_{Gz_{ik}} = 1.0$, $\alpha = 0.1$.

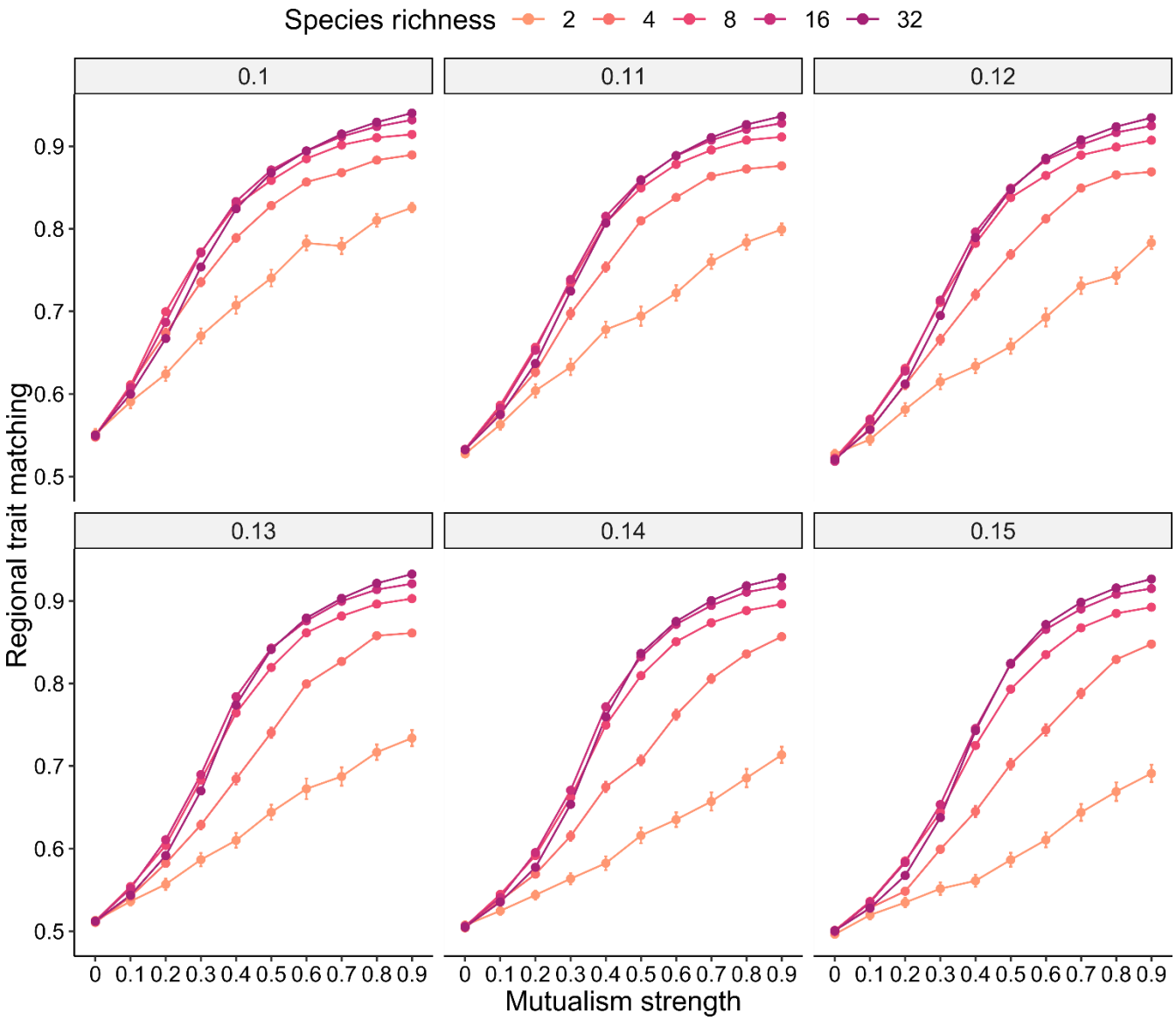

Figure S8 - Effects of different values of the model parameter ϱ (values above each panel) on patterns of regional trait matching with mutualistic partners. Each point represents the average value of 50 simulations and vertical lines confidence intervals. Points and lines of different color intensities represents different scenarios of initial species richness in the metacommunity. Other parameter values: m_{ik}= 0.0-0.9, $\sigma^2_{Gz_{ik}} = 1.0$, $\alpha = 0.1$.

2.1.2 With environmental *changes*

Under environmental changes, our simulations show that the patterns reported in the main text qualitatively still held for the different values of ϱ (Figures S9-S10). Increasing ϱ up to moderate levels still retained the same patterns reported in the main text of the buffering effect of coevolution and species richness against environmental

changes. However, when ϱ increases, species evolve faster and can track environmental changes more efficiently, increasing patch occupancy (Figure S9). Further increasing ϱ reverts patterns of occupancy to similar patterns as if there was no environmental change in the metacommunity. Conversely, increasing ϱ reduced extinctions and allowed more species to survive in the metacommunity, with most the species surviving at high levels of ϱ.

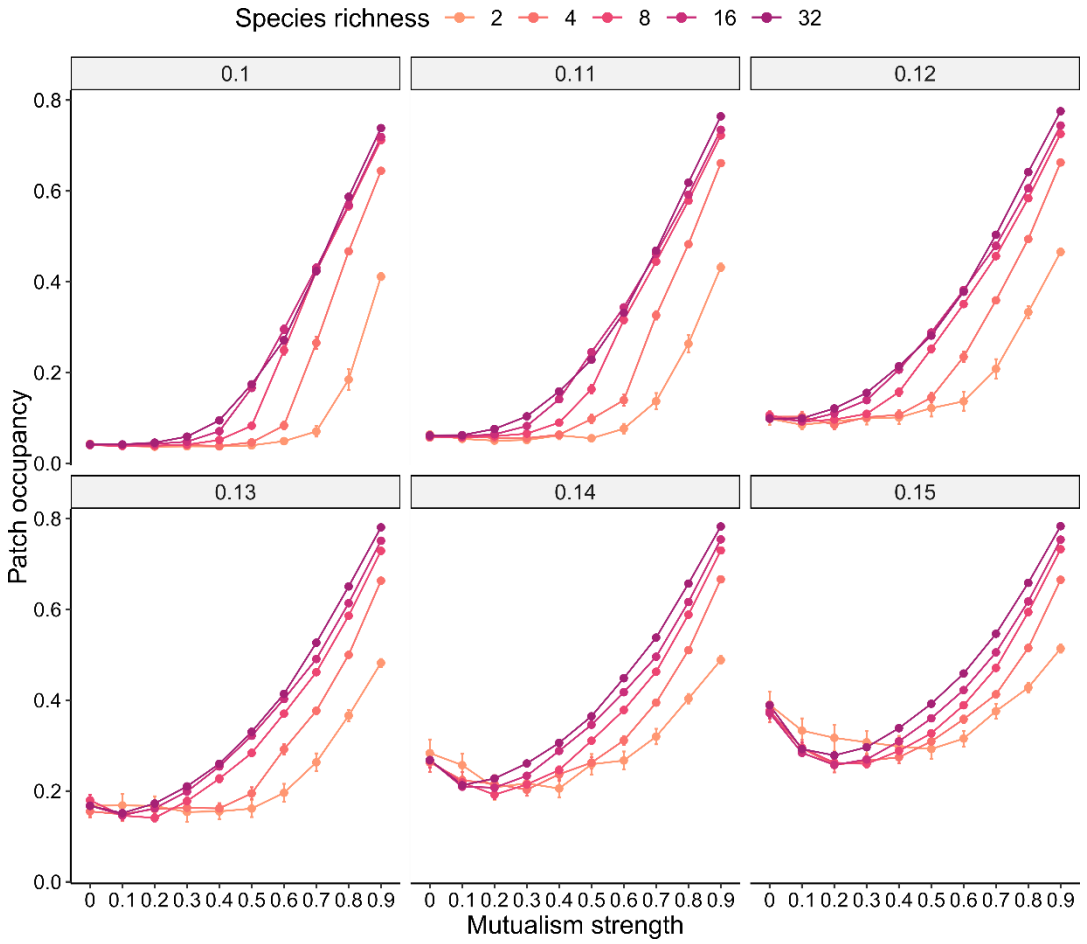

Figure S9 - Effects of different values of the model parameter ϱ (values above each panel) on patterns of occupancy under environmental changes. Each point represents the average value of 50 simulations and vertical lines confidence intervals. Points and lines of different color intensities represents different scenarios of initial species richness in the metacommunity. Other parameter values: m_{ik}= 0.0-0.9, $\sigma^2_{Gz_{ik}} = 1.0$, $\alpha = 0.1$.

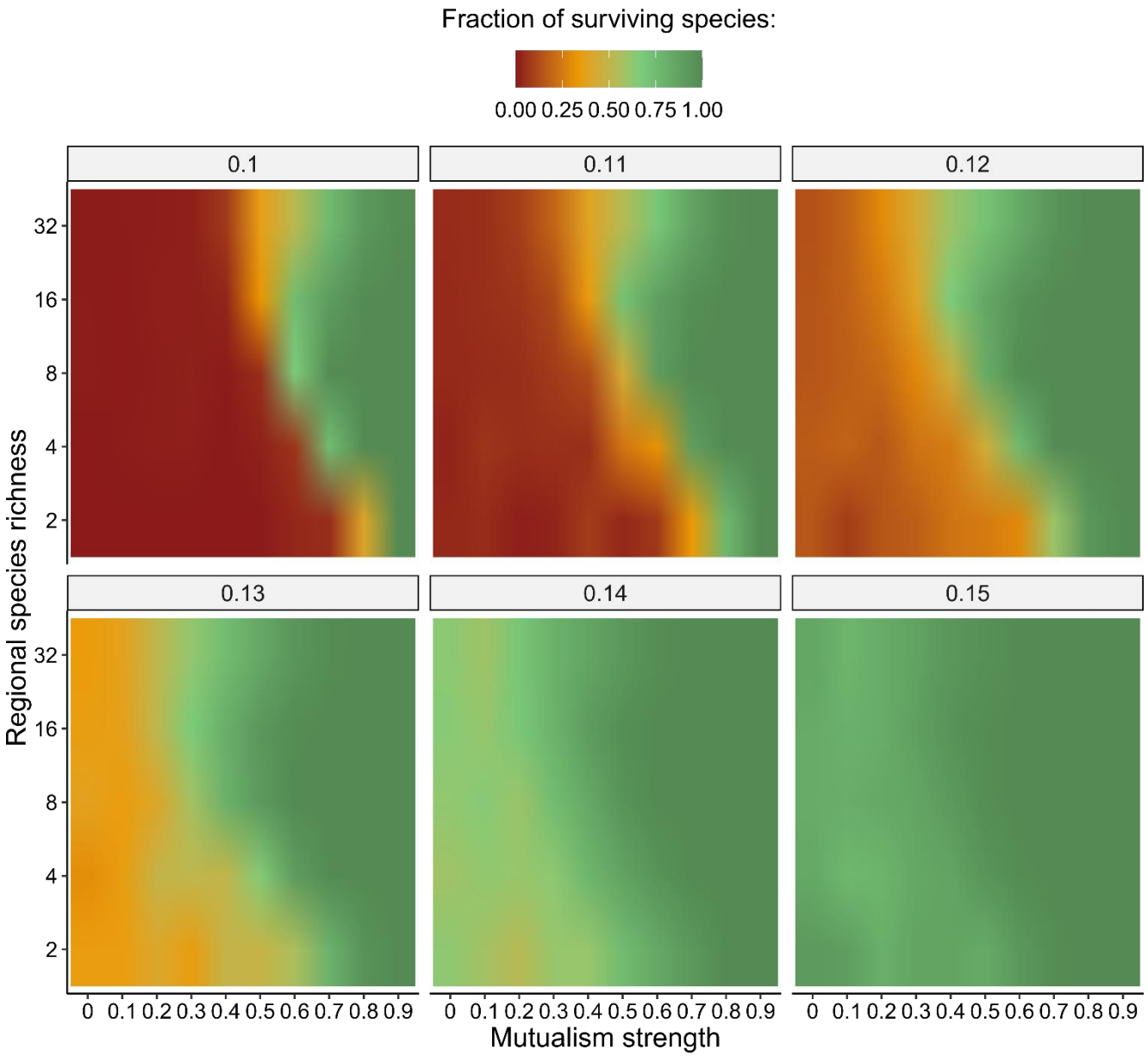

Figure S10 - Effects of different values of the model parameter ϱ (values above each panel) on the fraction of surviving species in the metacommunity under environmental changes. Colors are interpolated to improve visualization. Other parameter values: m_{ik}= 0.0-0.9, $\sigma^2_{Gz_{ik}} = 1.0$, $\alpha = 0.1$.

2.2 Different values of fraction of gene flow

2.2.1 *Without environmental changes*

Our sensitivity analysis shows that increasing the fraction of gene flow among populations in the metacommunity can change the effects of mutualistic coevolution on patterns of patch occupancy for low levels of *m*. When $m < 0.5$, increasing the fraction of gene flow decreases the occupancy of patches (Figure S11) because the rate of extinction of populations increases (Figure S12). The increased rate of extinction for low values of *m* occurs because gene flow decreases the local trait matching with the environment (Figure S13). However, gene flow also increases both the local and regional trait matching with mutualists across all levels of *m* (Figure S14).

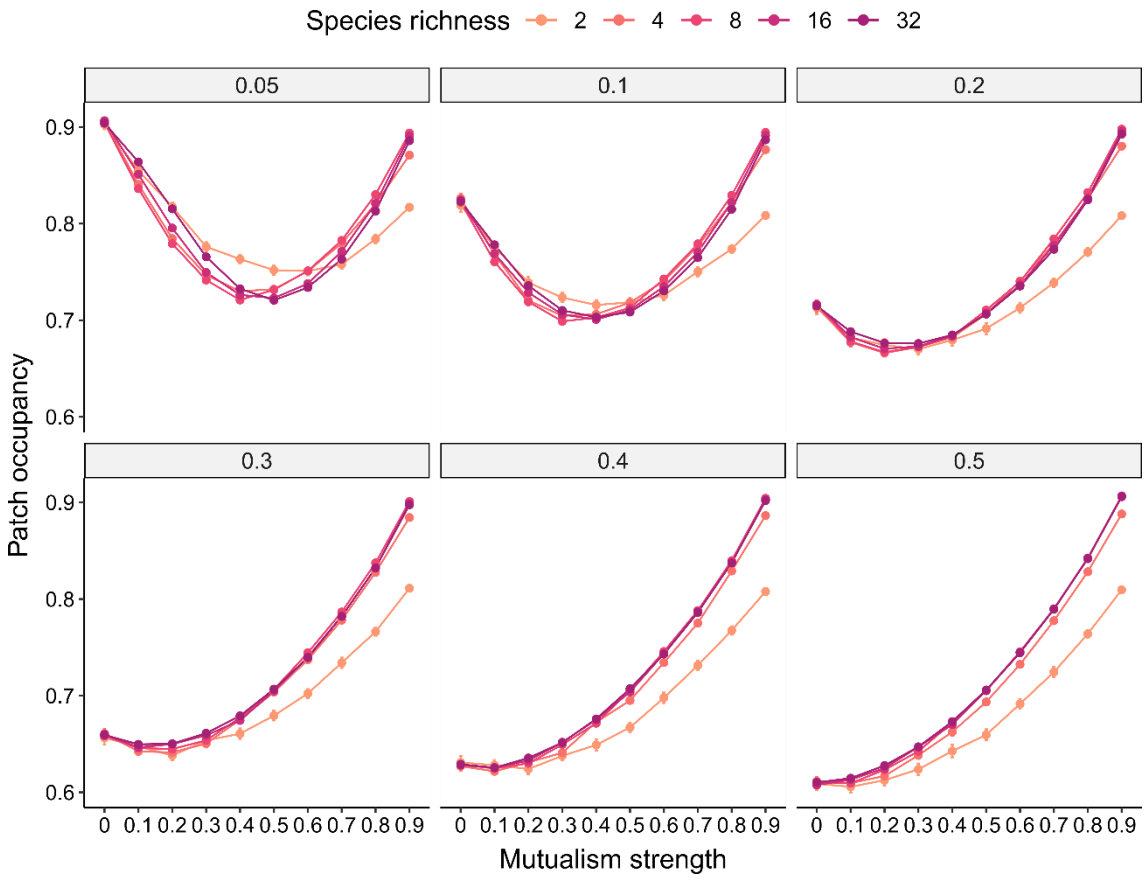

Figure S11 - Effects of different values of fraction of gene flow (values above each panel) on patterns of patch occupancy. Each point represents the average value of 50 simulations and vertical lines confidence intervals. Points and lines of different colors represents

different scenarios of initial species richness in the metacommunity. Other parameter values: m_{ik}= 0.0-0.9, $\sigma^2_{Gz_{ik}} = 1.0$, $\varrho_{ik} = 0.1$, $\alpha = 0.1$.

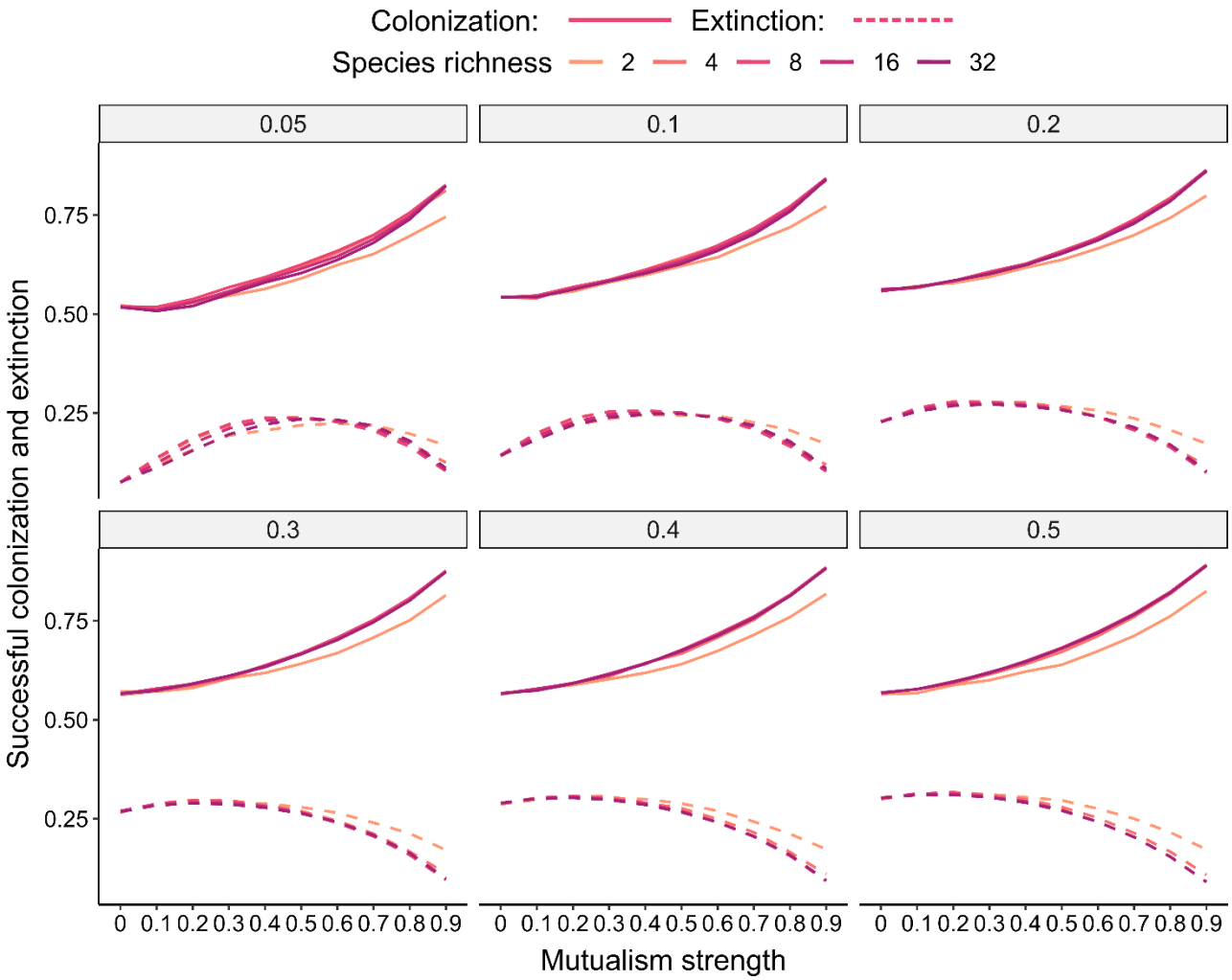

Figure S12 - Effects of different values of fraction of gene flow (values above each panel) on patterns of colonization (solid lines) and extinction (dashed lines). Each line represents the average value of 50 simulations. Lines of different colors represents different scenarios of initial species richness in the metacommunity. Other parameter values: m_{ik}= 0.0-0.9, $\sigma^2_{Gz_{ik}} = 1.0$, $\varrho_{ik} = 0.1$, $\alpha = 0.1$.

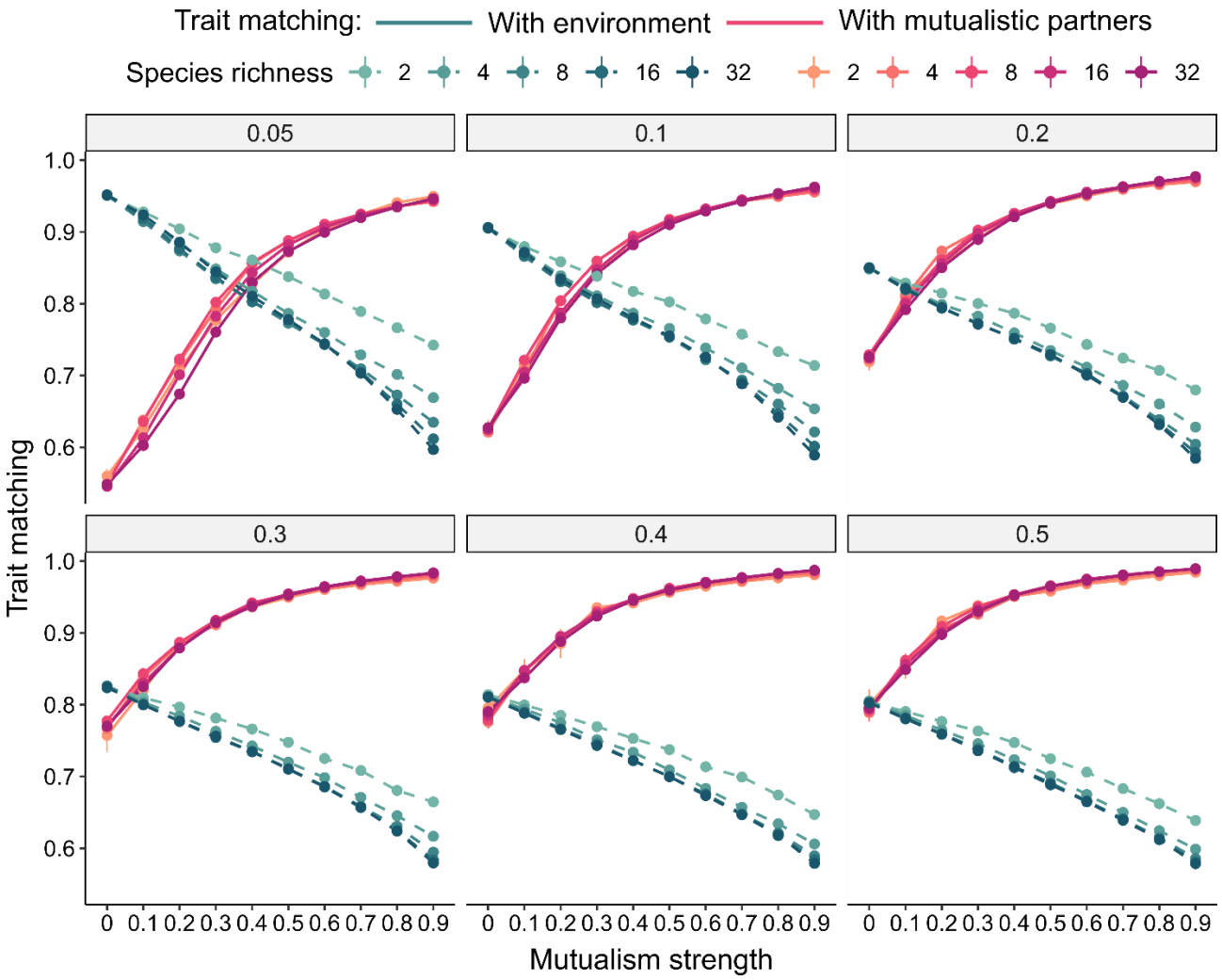

Figure S13 - Effects of different values of fraction of gene flow (values above each panel) on patterns of local trait matching with the environment (dashed green lines) and mutualistic partners (solid red lines). Each point represents the average value of 50 simulations and vertical lines confidence intervals. Points and lines of different color intensities represents different scenarios of initial species richness in the metacommunity. Other parameter values: m_{ik}= 0.0-0.9, $\sigma^2_{Gz_{ik}} = 1.0$, $\varrho_{ik} = 0.1$, $\alpha = 0.1$.

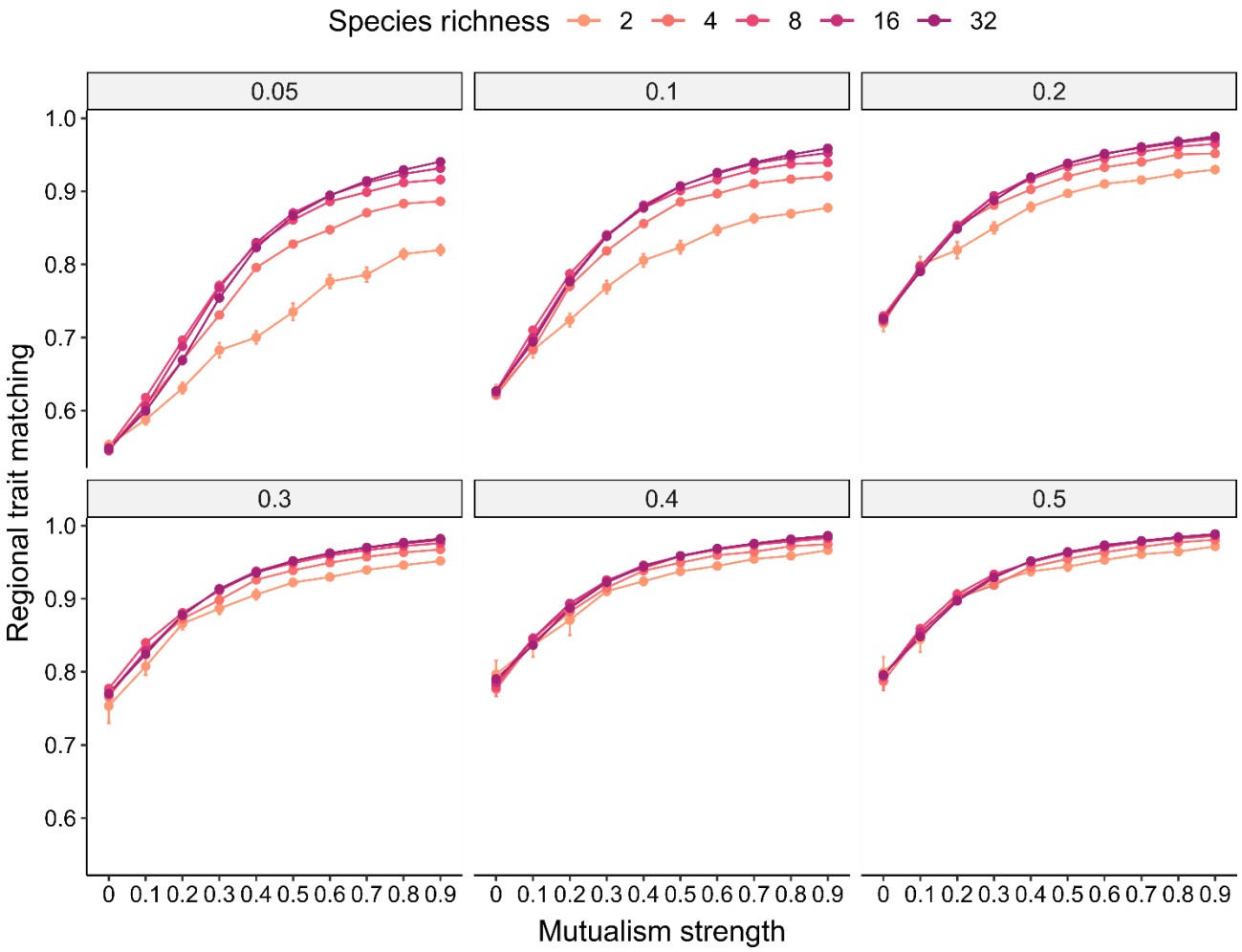

Figure S14 - Effects of different values of fraction of gene flow (values above each panel) on patterns of regional trait matching with mutualistic partners. Each point represents the average value of 50 simulations and vertical lines confidence intervals. Points and lines of different color intensities represents different scenarios of initial species richness in the metacommunity. Other parameter values: m_{ik}= 0.0-0.9, $\sigma^2_{Gz_{ik}} = 1.0$, $\varrho_{ik} = 0.1$, $\alpha = 0.1$.

2.2.2 *With environmental changes*

In the scenario with environmental changes, our sensitivity analysis shows increasing the fraction of gene flow does not qualitatively affect the results reported in the main text. Even for high levels of gene flow (0.5), mutualistic coevolution and species richness increased patch occupancy (Figure S15) and prevented the collapse of the metacommunity (Figure S16).

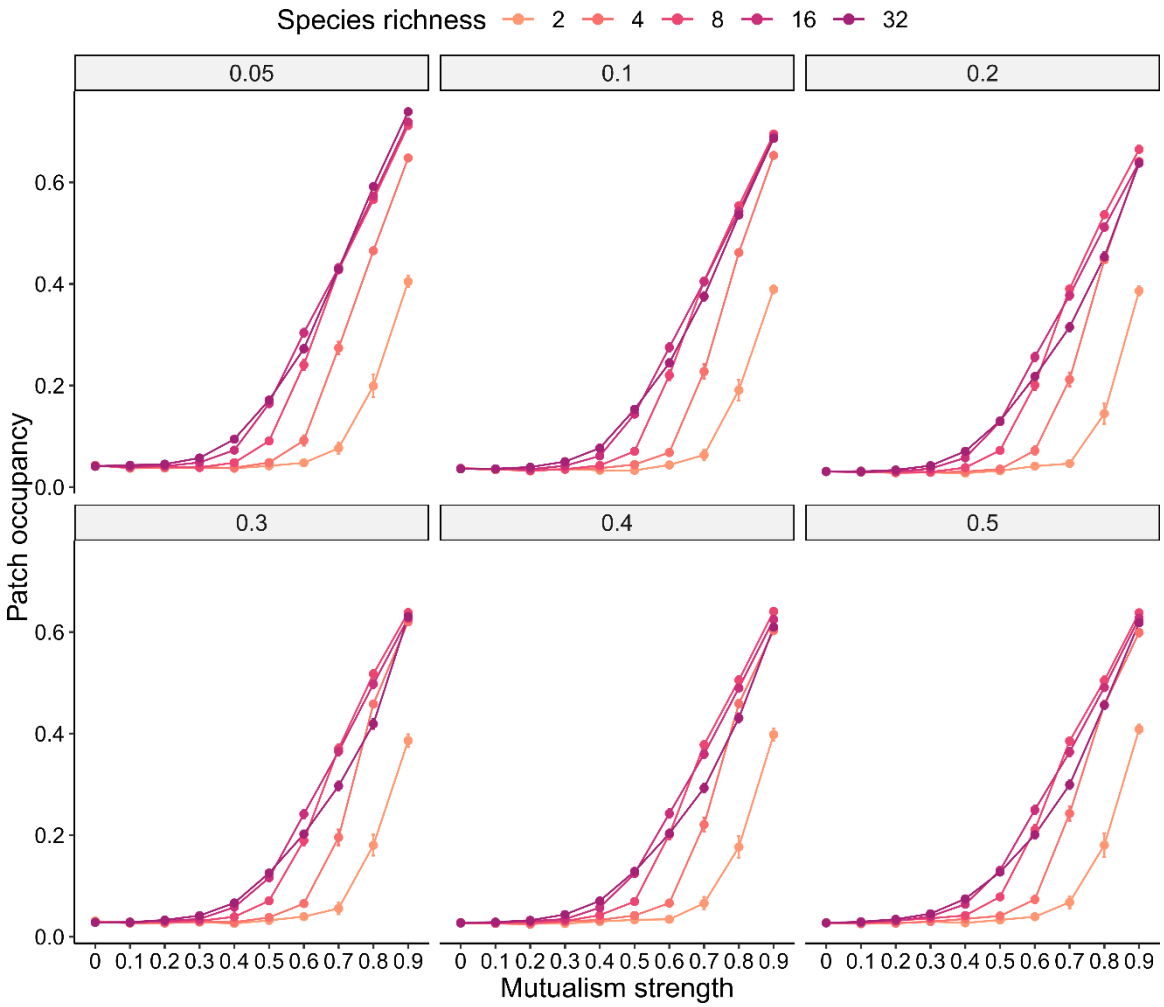

Figure S15 - Effects of different values of fraction of gene flow (values above each panel) on patterns of occupancy under environmental changes. Each point represents the average value of 50 simulations and vertical lines confidence intervals. Points and lines of different color intensities represents different scenarios of initial species richness in the metacommunity. Other parameter values: m_{ik}= 0.0-0.9, $\sigma^2_{Gz_{ik}} = 1.0$, $\varrho_{ik} = 0.1$, $\alpha = 0.1$.

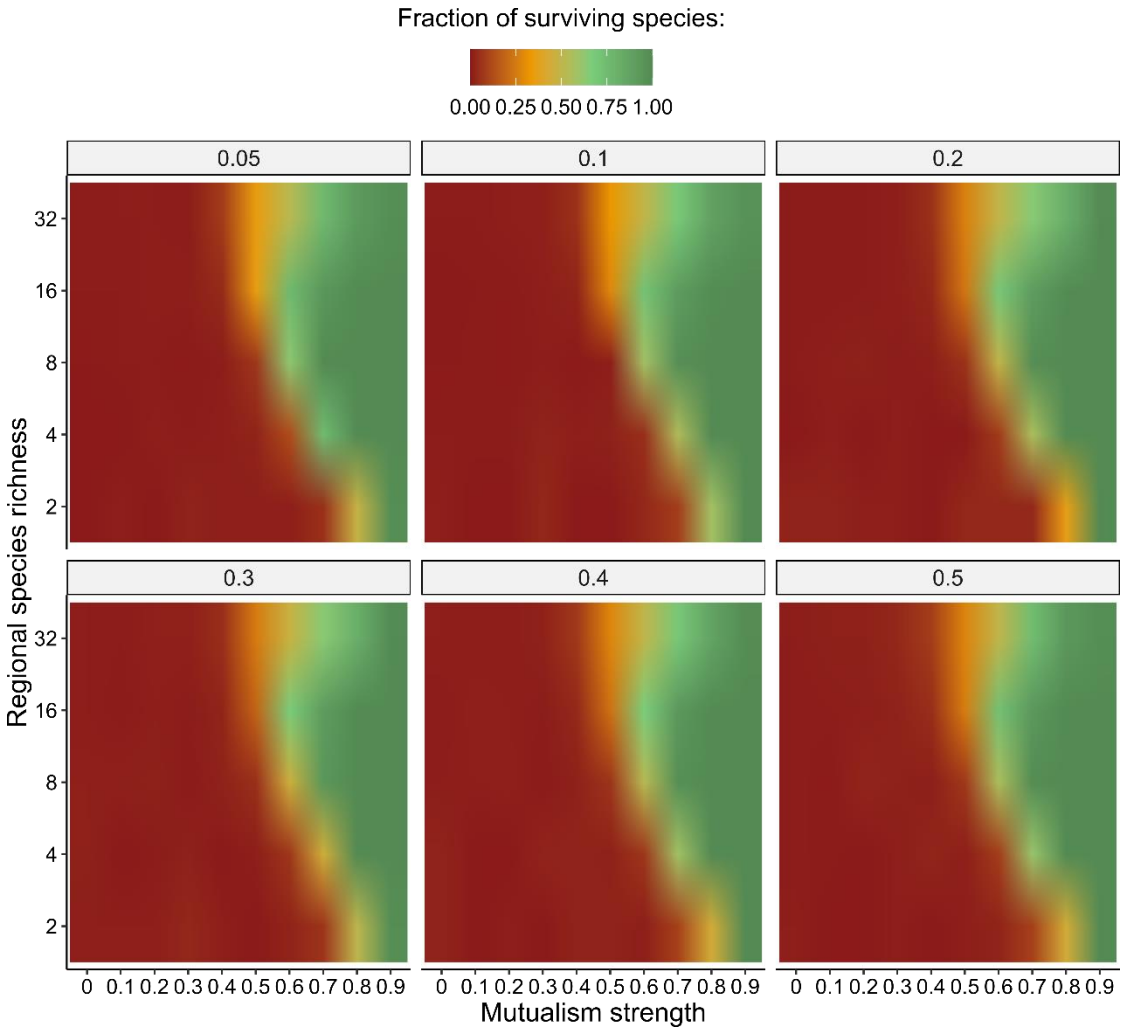

Figure S16 - Effects of different values of fraction of gene flow (values above each panel) on the fraction of surviving species in the metacommunity under environmental changes. Colors are interpolated to improve visualization. Other parameter values: m_{ik}= 0.0-0.9, $\sigma^2_{G z_{ik}} = 1.0$, $\alpha = 0.1$.

2.3 Spatial variation in the strength of mutualisms

The results reported in the main text correspond to a scenario in which the strength of mutualisms (m) does not vary in space. Yet, in natural communities there is spatial variation in the strength of mutualistic interactions and species coevolve in a geographic mosaic of coevolution (Thompson 2005). Thus, we performed an additional set of simulations to understand to what extent our conclusions about the buffering effect of mutualistic coevolution are robust to spatial variation in the strength of mutualisms. We

implemented this additional set of simulations with two complementary approaches. In the first approach we randomly sampled values of *m* for each patch in the metacommunity from a uniform distribution U[0.0, 1.0] and performed 100 simulations for each scenario of initial regional species richness (2 to 16 species) in the metacommunity. For the second one we divided the patches of the metacommunities into hotspots and coldspots (Thompson 2005). We assumed that in the hotspots mutualistic coevolution is strong and for each hotspots we sampled *m* from a uniform distribution U[0.7, 1.0]. In contrast, we assumed that in the coldspots mutualistic coevolution is weak and sampled *m* uniformly U[0.0, 0.3]. For this second approach we performed a set of simulations varying the proportion of hotspots in the metacommunity from 0 to 1 in 0.1 steps (100 simulations per proportion of hotspots and initial regional species richness). In both approaches we simulated environmental change by increasing the value of species θ_{ik} each generation ($\theta_{ik} + 0.25$ per generation).

Our results show that the buffering effect of coevolution in the response of metacommunities to environmental changes is robust to spatial variation in the strength of mutualisms. When *m* varies uniformly across the space, coevolution prevented the collapse of the metacommunities, and the fraction of surviving species increased with the diversity of the metacommunity (Figure S17a). If *m* is distributed into coldspots and hotspots among patches, our results show that for more diverse metacommunities even a small fraction of hotspots prevents the collapse of the metacommunities (S17b). However, as the initial species richness decreases, we need a larger proportion of hotspots in the metacommunity to prevent its collapse. These results are similar to the reported in the main text, in which the more diverse the metacommunity, the weaker *m* needs to be to prevent the complete extinction of species.

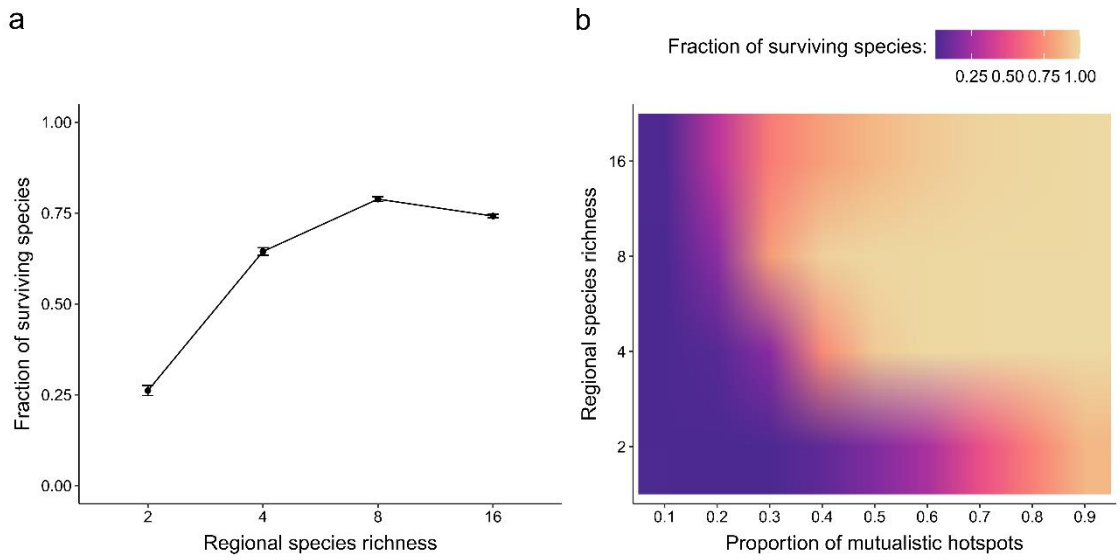

Figure S17 - Mutualistic coevolution prevents the collapse of metacommunities under environmental changes ($\theta_{ik} + 0.25$ per generation) when (a) the strength of mutualisms uniformly varies in space, *m*~U[0.0,1.0]; and (b) the metacommunity is divided into hotspots (*m*~U[0.7,1.0]) and coldspots (*m*~U[0.0,0.3]). On (b) colors are interpolated to improve visualization.

References

Guimarães, P.R., Pires, M.M., Jordano, P., Bascompte, J. & Thompson, J.N. (2017). Indirect effects drive coevolution in mutualistic networks. *Nature*, 550, 511–514.

Medeiros, L.P., Garcia, G., Thompson, J.N. & Guimarães, P.R. (2018). The geographic mosaic of coevolution in mutualistic networks. *Proc. Natl. Acad. Sci.*, 115, 12017–12022.

Thompson, J. N. 2005. *The Geographic Mosaic of Coevolution*. University of Chicago Press.

Considerações Finais

Um dos grandes desafios na ecologia e biologia evolutiva consiste em compreendermos como interações ecológicas sustentam a biodiversidade da Terra. Interações que beneficiam os indivíduos envolvidos – mutualismos – são consideradas uma grande forca que molda a ecologia e evolução de espécies (Thompson 2006; Bascompte & Jordano 2007; Bascompte 2009; Thompson 2009; Bronstein 2015; Bascompte & Scheffer 2022). Porém, apenas estamos começando a compreender os mecanismos pelos quais mutualismos podem influenciar medidas fundamentais da biologia que, em última instancia, determinam a diversidade e funcionamento de ecossistemas naturais. Nesta tese, mostramos que a coevolução em comunidades mutualísticas que formam redes de interação pode ser uma grande força que molda a *aptidão média* e a persistência de espécies por meio de diferentes escalas ecológicas.

Nossos resultados indicam que em uma escala local, a coevolução em redes mutualísticas gera variação na *aptidão média* das espécies. Embora essa variação seja explicada parcialmente pelo número de parceiros, mostramos que o principal determinante da *aptidão média* de espécies que coevoluem em redes mutualísticas são efeitos evolutivos indiretos. Efeitos indiretos dificultam o acoplamento fenotípico entre parceiros diretos, e a adaptação a outras pressões seletivas ambientais. Consequentemente, espécies que são mais influenciadas por efeitos evolutivos indiretos são mais deslocadas de seus picos adaptativos e tem uma menor *aptidão média* após coevoluírem em uma rede mutualística.

Em uma escala regional, essas pressões conflitantes resultantes da coevolução em redes aumentam a extinção local de populações. Os efeitos da dinâmica coevolutiva local, porém, também se manifesta na escala regional: a coevolução aumenta a similaridade entre os atributos de populações de diferentes espécies ao longo do espaço. O aumento de similaridade entre atributos na escala regional, por sua vez, facilita colonizações e expande a distribuição de populações. Com isso, essas populações conseguem colonizar áreas quando não estão adaptadas ao ambiente

abiótico local, o que permite com que espécies persistam regionalmente mesmo diante de mudanças ambientais ao longo do tempo (Cosmo *et al.* 2023).

De modo geral, juntos, nossos resultados mostram que coevolução em redes mutualísticas pode ser um grande determinante da *aptidão média*, persistência e, consequentemente, da biodiversidade e o funcionamento de ecossistemas na natureza.

Referências

Bascompte, J. (2009). Disentangling the web of life. *Science*, 325, 416–419.

Bascompte, J. & Jordano, P. (2007). Plant-animal mutualistic networks: The architecture of biodiversity. *Annu. Rev. Ecol. Evol. Syst.*, 38, 567–593.

Bascompte, J., Jordano, P., Melián, C.J. & Olesen, J.M. (2003). The nested assembly of plant-animal mutualistic networks. *Proc. Natl. Acad. Sci. U. S. A.*, 100, 9383–9387.

Bascompte, J. & Scheffer, M. (2022). The Resilience of Plant-Pollinator Networks. *Annu. Rev. Entomol.*

Bastolla, U., Fortuna, M.A., Pascual-García, A., Ferrera, A., Luque, B. & Bascompte, J. (2009). The architecture of mutualistic networks minimizes competition and increases biodiversity. *Nature*, 458, 1018–1020.

Birskis-Barros, I., Freitas, A.V.L. & Guimarães, P.R. (2021). Habitat generalist species constrain the diversity of mimicry rings in heterogeneous habitats. *Sci. Rep.*, 11, 5072.

Bronstein, J.L. (1994). Our current understanding of mutualism. *Q. Rev. Biol.*, 69, 31–51.

Bronstein, J.L. (2015). *Mutualism*. Oxford University Press, Oxford.

Chave, J. (2013). The problem of pattern and scale in ecology: What have we learned in 20 years? *Ecol. Lett.*

Cosmo, L.G., Assis A.P.A., Pires, M.M., Aguiar, M.A.M., Valido, A., Jordano, P., Thompson, J.N., Bascompte, J. and Guimarães, P.R. Jr. (2023a). Indirect effects shape species fitness in coevolved mutualistic networks. *Nature* (in press).

Cosmo, L.G., Sales, L.P., Guimarães, P.R., Jr & Pires, M.M. (2023b). Mutualistic coevolution and community diversity favour persistence in metacommunities under environmental changes. *Proc. Biol. Sci.*, 290, 20221909.

Estes, L., Elsen, P.R., Treuer, T., Ahmed, L., Caylor, K., Chang, J., *et al.* (2018). The spatial and temporal domains of modern ecology. *Nat Ecol Evol*, 2, 819–826.

Fernandes, L.D., Lemos-Costa, P., Guimarães, P.R., Thompson, J.N. & de Aguiar, M.A.M. (2019). Coevolution creates complex mosaics across large landscapes. *Am. Nat.*, 194, 217–229.

Garibaldi, L.A., Bartomeus, I., Bommarco, R., Klein, A.M., Cunningham, S.A., Aizen, M.A., *et al.* (2015). Trait matching of flower visitors and crops predicts fruit set better than trait diversity. *J. Appl. Ecol.*, 52, 1436–1444.

Gomulkiewicz, R., Thompson, J.N., Holt, R.D., Nuismer, S.L. & Hochberg, M.E. (2000). Hot Spots, Cold Spots, and the Geographic Mosaic Theory of Coevolution. *Am. Nat.*, 156, 156–174.

Guimarães, P.R., Jr, Jordano, P. & Thompson, J.N. (2011). Evolution and coevolution in mutualistic networks. *Ecol. Lett.*, 14, 877–885.

Guimarães, P.R., Jr, Rico-Gray, V., Oliveira, P.S., Izzo, T.J., dos Reis, S.F. & Thompson, J.N. (2007). Interaction intimacy affects structure and coevolutionary dynamics in mutualistic networks. *Curr. Biol.*, 17, 1797–1803.

Guimarães, P.R., Pires, M.M., Jordano, P., Bascompte, J. & Thompson, J.N. (2017). Indirect effects drive coevolution in mutualistic networks. *Nature*, 550, 511–514.

Hay, M.E., Parker, J.D., Burkepile, D.E., Caudill, C.C., Wilson, A.E., Hallinan, Z.P., *et al.* (2004). Mutualisms and Aquatic Community Structure: The Enemy of My Enemy Is My Friend. *Annu. Rev. Ecol. Evol. Syst.*, 35, 175–197.

Hendry, A.P., Schoen, D.J., Wolak, M.E. & Reid, J.M. (2018). The contemporary evolution of fitness. *Annual Review of Ecology, Evolution, and Systematics*.

Janzen, D.H. (1980). When is it Coevolution? *Evolution*, 34, 611–612.

Lande, R. (1976). Natural selection and random genetic drift in phenotypic evolution. *Evolution*, 30, 314.

Lande, R. (1982). A Quantitative Genetic Theory of Life History Evolution. *Ecology*, 63, 607–615.

Lee, S.H. (2016). Network nestedness as generalized core-periphery structures. *Physical Review E*, 93, 1–7.

Lemos-Costa, P., Martins, A.B., Thompson, J.N. & de Aguiar, M.A.M. (2017). Gene flow and metacommunity arrangement affects coevolutionary dynamics at the mutualism–antagonism interface. *J. R. Soc. Interface*, 14, 20160989.

Levin, S.A. (1992). The Problem of Pattern and Scale in Ecology. *Ecology*, 73, 1943–1967.

Medeiros, L.P., Garcia, G., Thompson, J.N. & Guimarães, P.R. (2018). The geographic mosaic of coevolution in mutualistic networks. *Proceedings of the National Academy of Sciences*, 115, 12017–12022.

Nuismer, S. (2017). *Introduction to Coevolutionary Theory*. 1st edn. W. H. Freeman.

Nuismer, S.L., Thompson, J.N. & Gomulkiewicz, R. (1999). Gene flow and geographically structured coevolution. *Proceedings of the Royal Society of London. Series B: Biological Sciences*, 266, 605–609.

Nuismer, S.L., Thompson, J.N. & Gomulkiewicz, R. (2000). Coevolutionary clines across selection mosaics. *Evolution*, 54, 1102–1115.

Olesen, J.M., Bascompte, J., Dupont, Y.L. & Jordano, P. (2007). The modularity of pollination networks. *Proc. Natl. Acad. Sci. U. S. A.*, 104, 19891–19896.

Orr, H.A. (2009). Fitness and its role in evolutionary genetics. *Nat. Rev. Genet.*, 10, 531–539.

Peralta, G., Vázquez, D.P., Chacoff, N.P., Lomáscolo, S.B., Perry, G.L.W. & Tylianakis, J.M. (2020). Trait matching and phenological overlap increase the spatio-temporal stability and functionality of plant-pollinator interactions. *Ecol. Lett.*, 23, 1107–1116.

Poisot, T., Stouffer, D.B. & Kéfi, S. (2016). Describe, understand and predict: why do we need networks in ecology? *Funct. Ecol.*, 30, 1878–1882.

Rice, S. (2005). Evolutionary Theory: Mathematical and Conceptual Foundations. *Systematic Botany*.

Rohr, R.P., Saavedra, S. & Bascompte, J. (2014). Ecological networks. On the structural stability of mutualistic systems. *Science*, 345, 1253497.

Schneider, D.C. (2001). The Rise of the Concept of Scale in Ecology: The concept of scale is evolving from verbal expression to quantitative expression. *Bioscience*, 51, 545–553.

Thompson, J.N. (2005). *The Geographic Mosaic of Coevolution*. University of Chicago Press.

Thompson, J.N. (2006). Mutualistic webs of species. *Science*, 312, 372–373.

Thompson, J.N. (2009). The coevolving web of life. *Am. Nat.*, 173, 125–140.

Wiens, J.A. (1989). Spatial Scaling in Ecology. *Funct. Ecol.*, 3, 385–397.

Wilson, G.W.T., Rice, C.W., Rillig, M.C., Springer, A. & Hartnett, D.C. (2009). Soil aggregation and carbon sequestration are tightly correlated with the abundance of arbuscular mycorrhizal fungi: results from long-term field experiments. *Ecol. Lett.*, 12, 452–461.